

ABSTRACT

Title of Thesis: PHENOLOGY OF ESTUARINE RESPONSE TO
ANTHROPOGENIC AND CLIMATE DRIVERS,
A STUDY OF THE CHESAPEAKE BAY AND
CHESTER RIVER ESTUARIES

Nicole Marie Basenback, Master of Science, 2019

Thesis Directed By: Professor Jeremy Testa
Marine-Estuarine-Environmental Sciences

The effects of nutrient loading on estuaries are well-studied, given the multitude of negative water quality, ecosystem, and economic impacts that have been attributed to the presence of excess nitrogen and phosphorous. A current gap in this knowledge is the consequence of changing climate variability on the seasonal patterns of estuarine processes related to eutrophication, potentially from direct (temperature) and indirect influences (nutrient load timing) of climate warming.

A coupled hydrologic-biogeochemical model (ROMS-RCA) was used to investigate the spatial and temporal changes in the phenology of hypoxia and related biogeochemical processes in the Chesapeake Bay under three different hydrologic regimes. Shifts in nutrient load timing during idealized simulations dampened the overall annual hypoxic volume, resulting from discernable, but relatively small reductions in phytoplankton biomass and both sediment and water-column respiration in three regions of the Bay. Simulated increases in water temperature caused an increase in the spring/early summer hypoxic volume associated with elevated

respirations rates, but this exhaustion of organic matter in the early summer caused a decrease in late summer/fall hypoxic volume due to lowered sediment respiration. Similar simulations in nutrient load timing were conducted using a model of the Chester River estuary, a smaller, shallower sub-estuary system to the Chesapeake Bay. Nutrient load timing and magnitude effects on hypoxia were much smaller in the Chester River as compared to Chesapeake Bay, which is likely due to high concentrations of nitrogen and phosphorus within the system. Therefore, cross-system comparisons are important for understanding the sensitivity of hypoxia to alterations in nutrient load across diverse estuaries. These idealized simulations begin the process of understanding the potential impacts of future climatic changes in the seasonal timing of key biogeochemical processes associated with eutrophication.

PHENOLOGY OF ESTUARINE RESPONSE TO ANTHROPOGENIC AND
CLIMATE DRIVERS, A STUDY OF THE CHESAPEAKE BAY AND
CHESTER RIVER ESTUARIES

By

Nicole Marie Basenback

Thesis submitted to the Faculty of the Graduate School of the
University of Maryland, College Park, in partial fulfillment
of the requirements for the degree of
Master of Science
2019

Advisory Committee:
Professor Jeremy Testa, Chair
Professor Ming Li
Dr. Damian Brady

© Copyright by
Nicole Marie Basenback
2019

Acknowledgements

I would like to express my deepest gratitude to my advisor, Dr. Jeremy Testa, for his support and guidance throughout the completion of this thesis. His enthusiasm and willingness to discuss my work, was always greatly appreciated and motivating. His constructive evaluation of my work has challenged me and I am grateful to have had the opportunity to grow and learn as a scientist while pursuing this project in his lab group.

This research would not have been possible without the generous funding support from the National Science Foundation for my Graduate Research Assistantship, and the Chesapeake Biological Lab (CBL) Graduate Education Committee for promoting my travel to several conferences. I would also like to acknowledge, Dr. Ming Li and Dr. Damian Brady for generously providing insights and inquiries, as my advisory committee, to guide this work.

Many sincere thanks to the members of the Testa Lab during my time at CBL: Casey Hodgkins, Amanda Moore, Chunqi Shen, Drew Hobbs, Kevin Kahover, and Isabel Sanchez. Special thanks to Chunqi Shen and Amanda Moore for sharing your modeling expertise and your willingness to answer questions. It's been a pleasure joining efforts with such a hardworking and generous team. Thank you to the wonderful CBL community for being so welcoming. I have truly enjoyed the friends and colleagues I have met during the last three years at CBL. Thank you to my family for your continuous encouragement. Lastly, to my husband Bryan, for your patience and unconditional support as I pursued this goal.

Table of Contents

Acknowledgements	ii
Table of Contents	iii
List of Figures	v
List of Abbreviations.....	ix
Chapter 1 - Phenology of Estuarine Response to Anthropogenic and Climate Drivers, the Chesapeake Bay as a Case Study	1
Introduction	1
Methods	5
Modeling Tool	5
Nutrient Timing Scenarios.....	6
Summer Water Temperature Increase Scenario	7
Nutrient Shift and Summer Water Temperature Increase Combination Scenarios	8
Year-round Water Temperature Increase Scenario	8
Scenario Analysis	9
Results	9
Nutrient Timing Scenarios.....	9
Water Temperature Increase Scenario	12
Nutrient Shift and Water Temperature Increase Combination Scenarios	13
Year-round Water Temperature Increase Scenario	14
Discussion	15
Nutrient Load Timing	15
Water Temperature Increase.....	17
Conclusion and Future Recommendations	20
References	22
Chapter 2 - Phenology of Estuarine Response to Anthropogenic and Climate Drivers, the Chester River Estuary as a Case Study	44
Introduction	44
Methods	46
Study Site.....	47
Modeling Tool	47
Model Calibration and Validation	48

Nutrient Magnitude Scenarios	49
Nutrient Shift Scenarios.....	49
Dissolved Oxygen at the Chesapeake Bay Boundary Scenario	50
Results	51
Water-column and Sediment Model Validation.....	51
Nitrogen Magnitude Scenarios	52
Phosphorus Magnitude Scenarios.....	53
Nutrient Shift Scenarios.....	54
Dissolved Oxygen at the Chesapeake Bay Boundary Scenario	55
Discussion	55
Conclusion and Future Recommendations	59
References	61

List of Figures

Figure 1.1. (a) RCA model grid (water cells = blue). (b) Map of Chesapeake Bay's major tributaries and Chesapeake Bay Program long-term water quality monitoring stations used in the analysis of model scenarios.	28
Figure 1.2. Conceptual diagram of potential nutrient load shift decoupling. (a) Currently, spring sunlight, temperature and nitrogen load are aligned to initiate a spring phytoplankton bloom. (b) If nutrient loads are shifted earlier in the year, there could be a decoupling of these factors that influence productivity.	29
Figure 1.3. Conceptual diagram for alternative hypothesis of water temperature increase effects on respiration. Conventional hypotheses (a) suggests that warmer water temperature will increase respiration rates throughout the year, while an alternative hypothesis (b) suggests that the increase in temperature will increase respiration and effectively speed up the consumption of labile organic matter earlier in the year, effectively reducing labile organic matter availability and thus respiration in the fall.....	30
Figure 1.4. Comparison of the cumulative flow of all major Chesapeake Bay tributaries (Susquehanna, Patuxent, Patapsco, Potomac, Choptank, Rappahanock, York, and James Rivers) to highlight that the years 2000 (moderately wet), 2002 (dry), and 2004 (wet) are hydrologically different.	31
Figure 1.5. Comparison of base scenario (no changes), predicted hypoxic volume for each year and observed summer hypoxic volume (Testa, Murphy, et al., 2018).....	32
Figure 1.6. Example of how the average NO ₂₃ concentration was used to generate an idealized annual nutrient cycle for each of the major tributaries in the RCA model. The original and idealized concentrations for the Susquehanna River (blue) and Patuxent River (green) for the year 2000 are shown above.....	33
Figure 1.7. (a) An example of the nutrient load shift scenario setup of nitrate and nitrite (NO ₂₃) for one month early (dashed) and two months early (blue) for the Susquehanna River in 2000. This process was repeated for each year and tributary. (b) The resulting cumulative NO ₂₃ load of all tributaries combined, for each year and scenario.....	34
Figure 1.8. Comparison of the hypoxic volume of the nutrient load (NO ₂₃) shift scenarios to the idealized Base scenario at a hypoxia threshold of 2 mg O ₂ /L.	35
Figure 1.9. Comparison of the total change in dissolved oxygen (O ₂) and (a) chlorophyll-a (Chl _a) and (b) total respiration respectively, during the spring (January-May; A-C) and summer (June-August; D-F) seasons.	36

Figure 1.10. Nutrient shift scenario had increased sediment oxygen demand (SOD) in the two upper Chesapeake Bay stations (CB3.3C and CB5.3) and reduced SOD at the lower Bay station (CB6.4).....	37
Figure 1.11. The difference between the nutrient shift scenario and no change scenario in terms of (a) particulate organic nitrogen (PON) and (b) ammonium fluxes (NH ₄).....	38
Figure 1.12. Water temperature increase scenario (TempInc, light blue) in comparison to no change scenario (dark blue), at hypoxia threshold of 2.0 mg O ₂ /L. The water temperature was increased Bay-wide by 1.5 °C from May 1 (start, green line) to July 31 (stop, red line).....	39
Figure 1.13. The difference in sediment organic carbon (SOC, mg C/m ³) between the temperature increase scenario and no change scenario at three stations across the mainstem of the Chesapeake Bay. The water temperature was increased Bay-wide by 1.5°C from May 1 (start, green line) to July 31 (stop, red line).	40
Figure 1.14. The difference in (a) total respiration and (b) sediment oxygen demand (SOD) between the temperature increase scenario and no change scenario at three stations across the mainstem of the Chesapeake Bay. The water temperature was increased Bay-wide by 1.5°C from May 1 (start, green line) to July 31 (stop, red line).....	41
Figure 1.15. Comparison of the hypoxic volumes resulting from combination scenarios of nutrient shift and water temperature increase in comparison to the no change scenario (no changes to nutrients or water temperature), at a hypoxia threshold of 2.0 mg O ₂ /L. The water temperature was increased Bay-wide by 1.5 °C from May 1 (start, green line) to July 31 (stop, red line), and the NO ₂₃ was shifted 1 and 2 months early respectively.	42
Figure 1.16. Comparison of the hypoxic volumes resulting from the water temperature increase scenarios (summer and year-round) in comparison to the no change scenario (no changes to nutrients or water temperature), at a hypoxia threshold of 2.0 mg O/L. For both scenarios the water temperature was increased Bay-wide by 1.5 °C. For the summer scenario this increase occurred from May 1 (start, green line) to July 31 (stop, red line), and for the year-round scenario, from January 1 to December 31.	43
Figure 2.1. Location of Chester River Estuary on the northeastern shore of the Chesapeake Bay.	67
Figure 2.2. (a) Bathymetry (mean water depth, meters) of the Chester River Estuary. (b) Estuary-wide map of modeled bottom-water dissolved oxygen (O ₂) in late June.	68
Figure 2.3. (a) Chester River Estuary model grid (water cells only) with location of freshwater inputs. (b) Sediment-water flux (SONE) stations used in model validation (red, CR01 and CR19) and Chesapeake Bay Program (CBP) long-term water quality monitoring stations (black, ET4.1 and ET4.2) used in the model validation and simulation analysis.....	69

Figure 2.4. Comparison of water column (a) surface and (b) bottom-water observation data at CBP station ET4.1 (Figure 2.3b) and the no change model scenario model output.....	70
Figure 2.5. Comparison of water column (a) surface and (b) bottom-water observation data at CBP station ET4.2 (Figure 2.3b) and the no change scenario model output.....	71
Figure 2.6. Comparison of observed sediment-water fluxes at SONE stations CR01 and CR19 (Figure 2.3b) and the no change scenario model output.	72
Figure 2.7. Example of nitrogen (NO_{23}) concentration increase and decrease scenarios setup for one Chester River estuary tributary. This process was repeated for the phosphorus (PO_4) concentration increase and decrease scenarios.	73
Figure 2.8. (a) Original nitrogen concentration in the 12 boundary rivers in the Chester River estuary. (b) 10-day running average of river NO_{23} inputs used for nutrient shift scenarios. The location of river inputs to model grid can be found in Figure 2.3a.	74
Figure 2.9. Example of shifts in tributary nitrogen concentration by 14 days (top) and 30 days (bottom). Day 150 was used as a reference point (dashed line).	75
Figure 2.10. Example of bottom water layer of Chester model comparison between the (a) Base (no change) scenario and (b) setup of scenario for increased dissolved oxygen in the lower layers of the boundary condition.	76
Figure 2.11. Comparison of the hypoxic volume (top) of NO_{23} nutrient increase and decrease scenarios to the Base (no change) scenario and the difference between them (bottom) at different dissolved oxygen thresholds.	77
Figure 2.12. Difference in sediment-water fluxes between NO_{23} load change (increase/decrease) scenarios and the Base scenario at two CBP stations (ET4.1 and ET4.2).	78
Figure 2.13. Comparison of the hypoxic volume cycle (top) of PO_4 nutrient increase and decrease scenarios to the Base (no change) scenario and the difference between them (bottom) at different dissolved oxygen thresholds.	79
Figure 2.14. Difference in sediment-water fluxes between PO_4 load change (increase/decrease) scenarios and the Base scenario at two CBP stations (ET4.1 and ET4.2).	80
Figure 2.15. Comparison of the hypoxic volume (top) of nutrient load (NO_{23}) shift scenarios to the idealized Base (no change) scenario (bottom) at different dissolved oxygen thresholds.	81
Figure 2.16. Difference in sediment-water fluxes between nutrient shift scenarios and the Base scenario, for both the 14-day (dashed line) and 30-day (solid line) shifts respectively at two CBP stations (ET4.1 and ET4.2).	82

Figure 2.17. Seasonal cycle of differences between bottom water dissolved oxygen at two CBP stations (ET4.1 and ET4.2) between the base simulation and all scenarios.	83
Figure 2.18. Seasonal cycle of differences between bottom water chlorophyll-a at two CBP stations (ET4.1 and ET4.2) between the base simulation and all scenarios.	84
Figure 2.19. Seasonal cycle of differences between bottom water respiration at two CBP stations (ET4.1 and ET4.2) between the base simulation and all scenarios.	85
Figure 2.20. (a) Comparison of model (blue line) versus ConMon station data (green circles) at Sycamore Point (upper Corsica River) (Walter R Boynton et al., 2009). (b) Comparison of modeled, bottom water dissolved oxygen at CBP station ET4.2 (downstream; black line) versus Sycamore Point (SYC; Corsica River; green line).	86
Figure 2.21. Comparison of the hypoxic volume (top) of the increase to Chesapeake Bay boundary dissolved oxygen scenario to the Base (no change) scenario and difference between them (bottom) at different dissolved oxygen thresholds.....	87
Figure 2.22. Comparison of modeled light limitation factors (RLGHT) in RCA at two CBP stations (a) ET4.1 and (b) ET4.2. Note: Light is not limiting when RLGHT > 0.9.	88
Figure 2.23. The ratio of phosphorus, nitrogen and silica concentrations to the half-saturation coefficient (ks) 0.001 mg P/L, 0.010 mg N/L and 0.020 mg Si/L respectively for the Base (no change) scenario. Note: The lower y-axis limit for nitrogen is the ratio of 1.....	89

List of Abbreviations

CBP	Chesapeake Bay Program
CHLA	Chlorophyll-a
ConMon	Continuous Monitoring Program
MDNR	Maryland Department of Natural Resources
NARR	North American Regional Reanalysis
NH ₄	Ammonium
NO ₃	Nitrate
NO ₂₃	Nitrate and Nitrite
PO ₄	Phosphate
PON	Particulate Organic Nitrogen
RCA	Row-Column Aesop
ROMS	Regional Ocean Modeling System
SFM	Sediment Biogeochemical Model
SOC	Sediment Organic Carbon
SOD	Sediment Oxygen Demand
SONE	Sediment Oxygen Nutrient Exchange
TMDL	Total Maximum Daily Load
WQSTM	Water Quality and Sediment Transport Model

Chapter 1 - Phenology of Estuarine Response to Anthropogenic and Climate Drivers, the Chesapeake Bay as a Case Study

Introduction

The impacts of nutrient loading on estuaries have been well-studied over the past several decades, due to the multitude of negative water quality, ecosystem, and economic impacts that have been attributed to excess nitrogen and phosphorus concentrations. High rates of microbial respiration resulting from elevated phytoplankton production, fueled by these excess nutrients, are a strong factor contributing to the seasonal depletion of dissolved oxygen in estuaries (Hagy, Boynton, Keefe, & Wood, 2004). The extent and duration of low dissolved oxygen waters are increasing in frequency and scale worldwide (Diaz & Rosenberg, 2008, Breitburg, 2002). Phytoplankton blooms have been identified as a poor water quality symptom of the inflow of excess nutrients (eutrophication), mainly nitrogen and phosphorus, from the Chesapeake Bay watershed into the estuary. The decomposition of large, spring phytoplankton blooms consumes dissolved oxygen within the water column that then become hypoxic or anoxic (little or no dissolved oxygen present respectively). Low dissolved oxygen conditions are problematic for sessile aquatic organisms and a major stressor for mobile ones. Although reductions in point source nutrient loads and riverine nitrogen and phosphorus have occurred in Chesapeake Bay and other estuaries (Bouraoui & Grizzetti, 2011; Kronvang et al., 2005), there is the continued challenge of increases in non-point source nutrient loads due to population growth and land use changes within the 6100 km² watershed (Goetz et al., 2004).

In the most recent decade, several tools have been used to examine the impacts of climate change and altered nutrient inputs on hypoxia in Chesapeake Bay. Testa et al. (2014) used a suite of sensitivity simulations to highlight the seasonality of dissolved oxygen and identified both

nitrogen and phosphorus loading as important drivers of summer hypoxic volume. Li et al. (2016) used the same model as Testa et al. (2014) and suggested that nutrient loading and related water-column respiration is the main mechanism that determines interannual variability in hypoxia. The timing of hypoxia initiation correlates strongly with winter-spring freshwater flow and the associated accumulation of chlorophyll-a in bottom water (Testa & Kemp, 2014, Testa et al., 2017). Thus, variations in both the volume of water discharging into Chesapeake Bay and the nutrient availability in that water contribute to hypoxia, thus changes in the timing or magnitude of freshwater inputs due to altered climate patterns could highly effect the initiation of hypoxia in the Bay. River flow effects interact with other external forces to control hypoxia, where for example, Scully (2010) used a numerical model to highlight the influence of interannual variability of wind forcing on Chesapeake Bay hypoxic volume. More recently, Irby et al. (2018) displayed the sensitivity of Chesapeake Bay hypoxic volume days to changes in sea level, water temperature, precipitation, and nutrient loading. Restoration efforts to reduce nutrient loads are expected to compete with these climate changes, including increases in temperature that decrease oxygen solubility and elevate respiration, and increased precipitation that leads to elevated nutrient loads (Irby et al., 2018). These past studies, while identifying key external forcing mechanisms that influence annual-scale metrics of hypoxia, did not identify the detailed biogeochemical process that moderate estuarine changes examined on the seasonal, or intra-annual scale.

Planning objectives and tracking restoration success of the Chesapeake Bay has been a long-term goal of the Chesapeake Bay Program since its inception in 1983 (Boesch, 1996). These efforts have continued with the implementation of total maximum daily load (TMDL) nutrient allocations for various pollution sources in 2010 (L C Linker, Batiuk, Shenk, & Cerco, 2013).

Support for adaptive policies to improve climate resiliency and sustainability of the Chesapeake Bay system is one goal of the agreement. The agriculture sector has been identified as a considerable source of nutrient pollution to the Chesapeake Bay estuary (L C Linker et al., 2013) and is also vulnerable to climatic changes. Within the watershed, more than one quarter of the land is devoted to agricultural practices, including growing crops and animal operations (Chesapeake Bay Program, 2011) and in 2012, there were over 2 million acres of farmland in Maryland alone (USDA-NASS, 2012). Climate change is predicted to alter agricultural activities that influence nutrient inputs (irrigation and fertilization), as well as water and soil temperatures that impact crop uptake and nutrient transformations in soils (e.g., denitrification). For example earlier spring temperatures have allowed for agricultural activities across much of the Midwest and Mid-Atlantic regions to begin earlier in recent years. Pennsylvania has seen planting occur 6 days earlier from 1996-2012 compared to 1979-1995 (U.S. Department of Agriculture, 2010). Chang (2019) suggests that farmers may also adjust their practices to future climate change by planting earlier (corn) or later (winter wheat and soy beans) to maximize crop yield. These changes in behavior and climate could lead to an increased and earlier nitrate (NO_3) load (Chang, 2019). Fluctuations in climate can also mediate the seasonality in nutrient inputs because periods of high precipitation events/years, when following several years of dry conditions, has the potential to flush high loads of dissolved nitrogen into the estuary (Lee, Shevliakova, Malyshev, Milly, & Jaffé, 2016).

A current gap in knowledge is the consequence of changing climate factors that influence estuarine phenology, such as changes in the timing of nutrient load inputs. Phenology is a branch of science dealing with the relations between climate and periodic biological phenomena, such as bird migration or plant flowering. Ecosystem phenology is important because changes in the

timing of climate drivers can lead to a mismatch in key biological phenomena. Shifts in nutrient loading to the Bay could also lead to altered biogeochemical cycling within the estuary, such as the timing of the annual spring phytoplankton bloom. Elmore, Nelson, & Craine (2016) showed that increasing air temperatures reduced nitrogen availability in trees during earlier leafout/spring period, which is important when considering the Chesapeake Bay watershed and its connection to estuarine nutrient cycling. Testa et al. (2018) observed a shift in hypoxic volume phenology between the time periods 1985-1999 and 2000-2015, with the latter years experiencing a lower peak volume and slightly earlier cycle. Given the complexity of relevant processes driving phenology and the subtle changes in timing (e.g., days) associated with phenological shifts, there is a clear need to use tools with high spatial and temporal frequency to understand long-term changes to seasonal timing.

The purpose of this chapter is to use a numerical modeling framework to understand the potential changes in Chesapeake Bay associated with altered seasonal timing of nutrient inputs and increased water temperature. The Chesapeake Bay estuary was chosen as the study system for this project, because there is a large, robust collection of datasets available for biogeochemical processes and water quality parameters (Brakebill, Preston, & Martucci, 2004). This estuary is also an economically, and ecologically important system, in which great efforts have been taken in both its study and restoration. I seek to answer the following questions: How do changes in the seasonal timing of nutrient inputs effect the seasonality and spatial response of hypoxia in the Chesapeake Bay? And, how sensitive is the seasonal cycle of hypoxia in Chesapeake Bay to warmer water temperatures?

Methods

To quantify the biogeochemical response of Chesapeake Bay hypoxia to altered timing of nutrient inputs and temperature, I conducted several idealized sensitivity simulations using a coupled, three dimension hydrodynamic-biogeochemical model (ROMS-RCA). Model scenarios included changes in the timing of riverine nutrient concentrations that reflect expected changes in farmer behavior resulting from climate change, as well as seasonally-specific increases in water temperature that are consistent with observed temperature increases over the past 30 years. Phenological response will be quantified by the volume of hypoxic waters, duration of hypoxia from formation to breakup, timing of chlorophyll-a accumulation, and the associated respiratory processes in the water-column and sediments.

Modeling Tool

A coupled hydrologic-biogeochemical model (Regional Ocean Modeling System and Row-Column Aesop, ROMS-RCA) was used to simulate and analyze estuarine biogeochemical responses to simulated changes in temperature and nutrient input timing. ROMS simulations are based on recently published simulations (e.g., Shen et al., 2019) and are run offline to provide salinity, water temperature, advective and diffusive transport for the biogeochemical model, RCA. RCA is a biogeochemical model that simulates water column and sediment (aerobic and anaerobic layers) biogeochemical processes by simulating the cycling of phytoplankton growth (two different groups) using light, temperature, and nutrient availability. Nutrient cycling in RCA involves oxygen, carbon, nitrogen, phosphorus, silica, and sulfur. Nutrient and freshwater inputs for ROMS-RCA are based on gauged inputs measured at the eight major Bay tributaries: including the Susquehanna, Patuxent, Patapsco, Potomac, Choptank, Rappahannock, York, and

James Rivers. ROMS-RCA has a grid resolution of 120x80 (Figure 1.1a) and 20 vertical layers. Detailed descriptions of ROMS-RCA and the sediment biogeochemical model (SFM) can be found in recent publications (Testa et al., 2014, Li et al., 2016, Testa et al., 2013, Shen et al., 2019).

Sensitivity simulations were performed over three years with different hydrologic regimes to allow for the quantification of the impacts of different physical regimes on the estuary's sensitivity to altered temperature and nutrient load timing. I simulated three temporally adjacent years with different overall magnitudes of freshwater inputs, including an above-average river flow year (2004), a below-average river flow year (2002), and a moderate, or average flow year (2000; Figure 1.4). For each of these hydrologic regimes, hypoxic volume observations compare well to model predictions (Figure 1.5).

Nutrient Timing Scenarios

For each of the three hydrologic conditions (2000, 2002, and 2004), the average of all major tributary NO_{23} was used to generate an idealized annual cycle of nitrate concentrations, which was scaled up or down to match the nutrient concentration and load magnitude in each individual tributary (Figure 1.6). This generation of tributary inputs was used as the 'idealized Base' (no change) scenario for comparison of this suite of simulations. For each hydrologic year, two model scenarios were performed that consisted of shifting the nitrogen (NO_{23} , nitrate + nitrite) concentration earlier in the year, for each of the major tributaries modeled. The incoming freshwater flow conditions (i.e., the hydrology of each year) remained constant between model scenarios within the same year, and only the seasonal timing of NO_{23} concentration was altered (Figure 1.7a). NO_{23} timing scenarios consisted of three different model runs: an idealized 'Base'

scenario where no changes in NO_{23} were applied, and two ‘shift’ scenarios where the peak NO_{23} concentration is shifted one and two months early respectively, reflecting hypothesized shifts to earlier NO_{23} concentrations associated with earlier fertilization.

I hypothesize that earlier spring nutrient loading during cooler spring temperatures could lead to a reduced phytoplankton bloom during the warmer months if less nutrients are available during the summer (i.e. a temporal decoupling of load and bloom, Figure 1.2). This would cause a reduction in the amount of available organic matter for respiration and reduce the demand on dissolved oxygen consumption.

Summer Water Temperature Increase Scenario

Given the widespread predictions of elevated temperature in the Chesapeake region over the next 50-80 years, I performed sensitivity simulations to understand the seasonally-specific response of Bay biogeochemistry to elevated temperatures. While climate projections typically predict that water temperature increases will occur across all months of the year (e.g., Chang, 2019), observations made over the past year suggest that last spring and summer temperatures warmed faster than fall or winter (Testa, Kemp, & Boynton, 2018, Testa, Murphy, et al., 2018). Therefore, I applied this scenario to the model by increasing the water temperature passed from ROMS to RCA (uniformly across all model cells) by 1.5 °C during the period spanning May 1 to July 31 for each hydrologic year (2000, 2002, and 2004). The temperature increase scenarios were compared to a Base (no change) scenario that included observed nutrient concentrations in riverine inflows.

I hypothesize that increased summer water temperatures could lead to an increase in hypoxic volume due to warmer temperatures increasing respiration of organic material (Figure

1.3). The factors expected to increase hypoxia in a hot summer, are the decrease in solubility of oxygen in warmer waters, increased respiration rates, and elevated stratification. Although these effects could be offset by a reduction in net primary production due to heat stress, which could limit the amount of organic material available for respiration and potentially generate an earlier breakup of hypoxia. A combination of these factors is likely to influence the scale, location, and timing of hypoxia.

Nutrient Shift and Summer Water Temperature Increase Combination Scenarios

The climate change effects of earlier nutrient load timing and elevated summer water temperatures are likely to occur simultaneously. Therefore, I conducted simulations of summer water temperature increases of 1.5 °C Bay-wide from May 1 to July 31 combined with shifting the NO₂₃ timing 1 and 2 months early respectively for each hydrologic year. These simulations allow for an analysis of interactions between the two climate change-induced alterations of external forcing with reference to the impacts in isolation.

Year-round Water Temperature Increase Scenario

In contrast to the observation of the largest deviations in long-term averages of water temperature occurring in the summer (Testa, Kemp, & Boynton, 2018, Testa, Murphy, et al., 2018), other studies have projected year-round water temperature increases in the Chesapeake Bay region (Ding & Elmore, 2015). To evaluate estuarine sensitivity to potential year-round water temperature increases, I performed a simulation by increasing the water temperature passed from ROMS to RCA (uniformly across all model cells) by 1.5 °C, Bay-wide, for the

entire year. This simulation was repeated for each hydrologic year (i.e., 2000, 2002, and 2004). These year-round temperature increases were directly compared to the early summer increases.

Scenario Analysis

Hourly model outputs from RCA were post-processed using MATLAB to generate timeseries and spatial datasets. The following variables were used to quantify estuarine response: dissolved oxygen criteria (Maryland Department of Environment), denitrification, hypoxic volume, phytoplankton growth/biomass, and hypoxia onset/breakup. Hypoxia variables were evaluated using three dissolved oxygen thresholds 5, 2, and 0.2 mg O₂/L respectively, to represent different ecological thresholds. Each scenario was compared to a respective “no change” Base case. Biogeochemical processes were evaluated at specific stations that spanned the length of the mainstem (Figure 1.1b).

Results

I found Bay-wide and more localized regional changes in hypoxic volume due to earlier nutrient load timing and increased summer water temperatures. The Chesapeake Bay’s phenological response is present, but freshwater inflow remains a strong driver of hypoxic volume.

Nutrient Timing Scenarios

At the Bay-wide scale, idealized simulations of earlier nutrient loads resulted in lower annual hypoxic volumes for all hydrologic regimes (Figure 1.8). The simulated reductions in hypoxic volume were comparable across years, with a maximal reduction between 1.2 and 1.4

km³/day, equating to a 5-10% reduction relative to base conditions (Figure 1.8). For all years, the scenario that shifted NO₂₃ two months earlier saw a larger reduction in annual hypoxic volume than the one month early shift when compared to the Base (no change) scenario. At the hypoxia threshold of 2 mg O₂/L, the two month earlier shift during the moderately wet year (2000) had the largest decrease in annual hypoxic volume with a change of 117.4 km³/day, followed by 106.4 km³/day in 2004 (wet), and 75.4 km³/day in the 2002 (dry) scenario. Although there was no change in the timing of the peak hypoxic volume for any of the scenarios, the reductions were larger in the May-June period in the moderate (2000) and wet (2004) periods, but larger during the July-August period in the dry year (2002; Figure 1.8). The year 2000 (moderate) base, no change, scenario had the latest hypoxia onset day for all regions except two. The timing of hypoxia initiation wasn't heavily influenced by the shift in nutrient timing, and only changed by 1 or 2 days for a region or two in each of the hydrologic years.

The fact that earlier nutrient load timing initiated a decrease in Bay-wide hypoxic volume indicates that there was an increase in bottom-water dissolved oxygen. I computed the difference in modeled total dissolved oxygen, chlorophyll-a, and respiration during the spring (January-May) and summer (June-August) in model cells corresponding to three Chesapeake Bay Program monitoring stations along the Bay mainstem including: CB3.3C (Bay Bridge) in the upper Bay, CB5.3 (Smith Point) mid-Bay, and CB6.4 in the lower Bay. Both the 1- and 2-month shifts in nitrate concentration caused an increase in water column dissolved oxygen that correlated to a decrease in chlorophyll-a (Figure 1.9a) and total respiration (DOC oxidation + sulfide oxidation + phytoplankton respiration) during both the spring and summer seasons (Figure 1.9b). For the moderately wet (2000) and wet (2004) years the middle and lower-Bay stations saw a larger increase in dissolved oxygen in both seasons compared to the upper-Bay station. During the

driest year (2002), the upper-Bay station showed the largest change in dissolved oxygen during the spring season. In general, the two month earlier nutrient shift had a larger effect on the dissolved oxygen linkage with chlorophyll-a and respiration during both seasons than the one month early scenario, by increasing the dissolved oxygen as much as 3 mg O₂/L at the mid-Bay station in the summer. Whereas the one month early nutrient shift scenario generated about a 0.5-1 mg O₂/L at the same station and season.

Remineralization processes in sediments and associated sediment-water fluxes also varied seasonally in response to the simulated shift in nitrate concentration and load. In general, comparisons of the NO₂₃ shift one month early scenario in all regions showed that sediment oxygen demand (SOD), NH₄ flux, and sediment nitrogen all deviated from the 'Base' case beginning in May, continuing through the summer, and then returned to 'Base' case values between October and November (Figure 1.10-1.11). The one month early nutrient shift scenario actually resulted in enhanced sediment oxygen demand (SOD) in the two upper CBP stations (CB3.3C and CB5.3), and slightly reduced SOD at the lower Bay station (CB6.4) (Figure 1.10). The lower Bay station also has the smallest response to the nutrient shift scenario. Sediment particulate organic nitrogen (PON) inputs to the sediment were reduced in the nutrient shift scenarios, as was the sediment-water flux of ammonium (NH₄) (Figure 1.11a and 1.11b). For the upper-Bay stations (CB3.3C and CB5.3), this reduction in PON is initiated around March, but was delayed until May in the lower-Bay station (CB6.4; Figure 1.9a). Ammonium fluxes peaked during late summer through early fall (July to October), and during this time the shift NO₂₃ one month early scenario shows a reduction in NH₄ release from the sediments of 1-5% (Figure 1.11b).

Water Temperature Increase Scenario

The idealized early summer warming scenarios resulted in an altered annual cycle of dissolved oxygen, including lowered hypoxia in the late summer. Hypoxic volume increased during the period of increased water temperature (May-July), but once warming subsided after July 31, model simulations revealed a reduction in hypoxic in all hydrologic years (Figure 1.12). The largest overall (delta) change in annual hypoxic volume occurred during the 2004 scenario at 108.6 km³/day. The wet year (2004) had the largest increase in hypoxia during the temperature increase period and the largest reduction after July 31 time period with a change in volume of 146.3 km³/day and -37.6 km³/day respectively (Figure 1.12). The moderately wet year (2000) had the largest lag after July 31 for hypoxia to decrease below the Base scenario at 10 days, whereas the dry and wet years responded in 7 and 4 days respectively. In this scenario, elevated temperatures increased water column and sediment respiration rates in the lower Bay, driving an elevated and earlier hypoxic volume. When compared to the Base (no change) scenario, both 2000 (moderately wet) and 2004 (wet) had two distinct increases (peaks) during the warmer summer and closer to Base values around the end of June (Figure 1.12).

The seasonal response of hypoxia to temperature increases was driven by changes in water-column and sediment respiration. SOD and water-column respiration increased under warming in the middle and lower Bay, except for the wet year, 2004, when both rates declined with elevated temperature (Figure 1.14). In the upper Bay, SOD and water-column respiration both were reduced or changed minimally under warming. Once warming ended on July 31, sediment respiration (SOD) declined, which corresponded to the reduction in available sediment organic carbon (SOC), which never recovered to levels from the Base case within the remainder of the year (Figure 1.13). The upper-Bay station (CB3.3C) saw the largest reduction in SOC

relative the middle and lower Bay, but SOD reductions were larger in the middle and lower Bay. Comparing the sediment respiration to the water column, we can see that warmer water temperature enhances sediment respiration in the lower-Bay during the summer, but this effect disappears when the warming ends (Figure 1.14a and 1.14b). Increased respiration allows for elevated regeneration of ammonium during the warmer summer, which could stimulate additional phytoplankton production and add additional organic material later in summer to compensate for the material exhausted by warming. Indeed, an increase in water column ammonium (NH_4) in both the surface and bottom waters occurred under warming by approximately 10-20%, providing for the potential to support additional phytoplankton growth. Although this regeneration of nitrogen is relatively strong during the summer temperature increase, the effect doesn't persist very long into the fall, and therefore is unable to sustain further phytoplankton production given that hypoxic volumes and respiration did in fact decline in later summer under warming. In summary, the sediment organic material pool was utilized during the warmer period through July 31, leaving less organic material available to support sediment respiration in the fall, which was consistent with the Bay-wide decrease in fall hypoxic volume.

Nutrient Shift and Water Temperature Increase Combination Scenarios

The combined scenario of earlier nutrient input timing and summer temperature increases resulted in an increase in hypoxic volume (at threshold of 2 mg O_2/L) during the first half of the year (before July 31) and decrease in hypoxic volume in the second half of the year (after July 31) for both scenarios and for all hydrologic years (Figure 1.15). The summer temperature increase only scenario had the largest increase (11-25%) in the first half of the year and smallest

(generally reduced volume) change (- 4-1%) in the second half of the year. The combined nutrient shift + summer temperature increase scenarios had smaller increases (shift 1-month early=8-18%, shift 2-months early=5-13%) than the temperature-only increase, and larger decreases in hypoxic volume in the latter half of the year relative to temperature increases only (shift 1-month early= -3 to -7%, shift 2-months early= -8 to -12%). When looking at the total hypoxic volume for the year, the summer temperature increase overwhelms the timing reduction in hypoxia. The shift NO₂₃ 1-month early scenario had a reduction of 3-6% across all three hydrologic years, whereas the combined temperature and shift scenario had a 2-10% increase. The shift NO₂₃ 2-months early scenario had larger reductions in volume of 5-12% across all three hydrologic years, while the comparable combined scenario had a 3% reduction in 2000, 3% increase in 2002, and negligible change (0.05%) in 2004.

Year-round Water Temperature Increase Scenario

The year-round temperature increase scenario caused elevated hypoxic volumes (at threshold of 2 mg O₂/L) in comparison to the Base (no change) scenario throughout the year. These increases were comparable in 2000 (by 18%) and 2002 (by 17%) and somewhat smaller for 2004 (by 8%) (Figure 1.16). This increase in hypoxic volume was larger than the summer temperature increase scenario, which had a 10, 15, and 5% increase for 2000, 2002, and 2004 respectively. In the year-round increase scenarios, both 2002 and 2004 showed a slight decline in hypoxic volume around October, but it was relatively small in comparison to the overall increase. This late fall decrease is of similar magnitude to the summer temperature increase scenario, but is shifted about a month later. Across all years, the early summer (before July 31) increase in volume was comparable to the summer water temperature increase only scenario.

One difference observed was during 2004, when the increase in hypoxic volume occurred much earlier in the year than all other temperature scenarios (Figure 1.16).

Discussion

The phenological response of Chesapeake Bay to changes in anthropogenic and climate drivers is complex and can be subtle, but model simulations (e.g. ROMS-RCA) are useful for quantifying the effects of seasonal changes to external forcing. I documented responses of Chesapeake Bay hypoxia to two distinct changes in the seasonal timing of physical forcing. Shifts in nutrient load timing had the effect of dampening the overall annual hypoxic volume, generating subtle changes in phytoplankton biomass, sediment and water-column respiration, and hypoxia in three regions across the Bay. The water temperature increase scenario indicated an increase in the spring/early summer hypoxic volume, but a decrease in late summer/fall hypoxic volume after the temperature increase stopped. Each of these idealized simulations represents potential future changes to Chesapeake Bay associated with either a direct (temperature) or indirect (nutrient load timing) response to future climate warming.

Nutrient Load Timing

Previous studies have shown how reductions in nutrient load are linked to improving surface water quality (Eshleman, Sabo, & Kline, 2013), and recovery of submerged aquatic vegetation (Lefcheck et al., 2018), but this study shows that similar reductions in hypoxia can be achieved by a shift in nutrient load timing to earlier in the season (Figure 1.7 and 1.8). This oxygen response may be an overlooked potential effect of changes in farmer behavior and precipitation patterns. A large portion of Chesapeake Bay watershed is occupied by agricultural

landscapes, contributing a large source of estimated nutrient load (42% nitrogen, 55% phosphorus; Chesapeake Bay Program, 2015). Farmer adaptations to changing climate conditions by adjusting agricultural practices to maintain crop yield is important, because it's estimated to lead to earlier nitrate (NO_3) loading (kg/ha) to waterbodies (Chang, 2019). Farmer behaviors in adopting certain agricultural conservation practices (i.e., buffer strips and tile drainage), may also help mitigate the effects of climate change by reducing dissolved phosphorus, and sediment exports (Wagena & Easton, 2018). The shift in nutrient load timing, allows more NO_{23} to be present during a less favorable time of year (e.g., cooler spring/winter) for phytoplankton growth (Figure 1.7a), which means that there is less organic material available for hypoxia generation later in the year.

Freshwater flow is a strong driver of nutrient load and a primary predictor of the magnitude of annual hypoxia (Li et al., 2016). Due to the geographic structure of the Chesapeake Bay, the Susquehanna River is the dominant source of freshwater and nutrients and correlates significantly with summer hypoxic volume (Hagy et al. 2004). Model results highlight this flow effect regardless of the nutrient timing or temperature scenario (Figure 1.8), with the high flow year (2004) having the largest annual hypoxic volume, followed by smaller volumes for the moderate (2000) and low flow years (2002). The nutrient timing scenario had the largest relative reduction on chlorophyll, respiration, and the hypoxic volume during the moderate flow year (2000) for both scenarios. The reduction of ammonium fluxes and sediment nutrients to the timing shifts was stronger during the moderate and low flow years in the upper-Bay, which may indicate that high flow conditions push the spring bloom and associated organic matter deposition seaward (Testa et al., 2014) and thus the upper-Bay had little biogeochemical production in 2004. The Susquehanna River provides 87% of the freshwater to this portion of the

Bay (Schubel & Pritchard, 2006), and is influencing the response of SOD at the upper-Bay station the most during the wet/high flow year.

An unexpected result of the simulations was the apparent stimulation of SOD and water-column respiration with altered nutrient input timing and reduced hypoxia. This feature was especially evident in the upper and middle Bay in the moderate and high flow year and the lower Bay during the wet year. This result reflects the fact that respiration (and associated oxygen uptake) can be limited by oxygen availability (e.g., Sampou & Kemp, 1994). Thus, in the upper and middle-Bay, where oxygen concentrations in bottom waters under the base scenario are anoxic or severely hypoxic, SOD and water-column respiration are oxygen limited. When the nutrient shifts reduced oxygen consumption due to reduction of chlorophyll-a and total respiration (Figure 1.9a and 1.9b), more oxygen uptake within the sediments was allowed in later summer (Figure 1.10).

Water Temperature Increase

Many previous studies have examined long-term changes in hypoxic volume (Hagy et al. 2004, Murphy, Kemp, & Ball 2011) and stimulated responses to future climate change (Irby et al., 2018), but fewer studies have examined detailed metabolic responses associated with changes in hypoxic volume (Li et al., 2016). Murphy, Kemp, & Ball (2011) found that over a 60-year record, significant increases in early summer hypoxia and slight decrease in late summer hypoxia. Other studies have shown how increases in water temperature are likely to increase the annual hypoxic volume in the Bay (Irby et al., 2018), but this study shows that the slight increase in hypoxic volume is seen due an increase in the early summer temperature, but a subsequent decrease in later summer/early fall volume (Figure 1.12). Testa, Murphy, et al., (2018)

hypothesized that warmer early summer temperatures would stimulate the respiration of the spring bloom, exhaust organic matter earlier in the year, and allow for relief from hypoxia due to lower late summer respiration rates. These model simulations are consistent with that hypothesis, where the seasonal temperature change lead to a faster rate of sediment and water-column respiration in the early summer, and when temperature returned to observed levels, there was less sediment organic matter to support respiration and nutrient fluxes (Figure 1.13). Thus, the impacts of future climate changes may not simply lead to higher hypoxia, but rather increase hypoxia in early summer and decrease it in later summer. Such a pattern has emerged in Chesapeake Bay since 1985 consistent with a ~ 1 °C increase in temperature.

These idealized simulations appear to support the hypothesis that temperature increases can have complex and seasonally-dependent effects on hypoxic. Future simulations that include more realistic temperature changes from downscaled model simulations and account for other effects of climate change (e.g., changes in freshwater discharge), will lead to a better understanding of these seasonal alterations. While long-term forecasting efforts of hypoxic volume are needed to understand expected mid-century changes, retrospective analyses of hypoxia changes to temperature are useful to inform those longer-term simulations. At any rate, reductions in late summer/early fall hypoxic volume – a potentially unexpected consequence of warming - could potentially open up access to suitable fish habitat. For example, in the Patuxent River, striped bass habitat has been found to be limited by reduced dissolved oxygen (O₂) levels more than high temperature during summer months (Kraus, Secor, & Wingate, 2015), and improved bottom water oxygen could expand cool-water temperature refuges for fish in late summer.

Improvements in late summer/fall habitat under warming may be lower, however, given that temperature increases in all times of year. The year-round temperature increase scenario generated a larger hypoxic volume, almost double the increase of the summer temperature increase scenario alone (except 2002 with a 15-17% increase). While the late fall hypoxic volume also persisted in the year-round temperature increase scenario, there was a longer lag time before volumes declined in 2002 and 2004, and there was no reduction in hypoxic volume during the second half of 2000. Thus, although temperature increases may indeed lead to a more rapid respiration of labile organic material in the early part of the annual cycle, model simulations suggest that temperature increases across all times of year will extend a larger hypoxic volume into the mid to late fall.

The combined scenarios of earlier nutrient load timing and warmer summer temperature showed that the reduction in hypoxic volume generated by the shift in nutrient load timing is overcome by the increase in summer water temperature. This result indicates that although organic matter reductions through lowered primary production under earlier nutrient inputs will reduce pressure to generate hypoxia, elevated respiration rates of the existing organic material will increase hypoxia. However, the reduction in later summer hypoxia associated with warmer summer temperatures persists with the addition of earlier nutrient inputs, and the reduction in hypoxic volume was larger in the combined nutrient shift + warming scenarios for 2000 and 2002, than the summer temperature increase scenario alone (and was comparable across years; 4-8%). Thus, the combination of these two likely climate change effects on external forcing will likely lead to an altered seasonality of hypoxic volume.

Conclusion and Future Recommendations

TMDL targets are generated on an annual basis, but the results of idealized model simulations presented here indicate that intra-seasonal changes in loading may also impact hypoxia, given the same annual load. Future changes in the timing of agricultural activity – including changes that occur in response to climate changes – will have cascading effects on the estuary if the agricultural changes lead to concentration changes within the riverine loads. These seasonal, idealized simulations and the hypoxia responses displayed in them will be modulated by other future climatic changes, including altered wind patterns, sea level rise, and changes in air and water temperature. The reduction in hypoxic volume due to the decoupling of nutrient load and seasonal water temperature may not remain as strong if water temperatures continue to warm earlier in the spring.

Given that this study evaluated each hydrologic regime independently, future work could include consideration of Lee et al. (2016) findings on the potential for large loads of nutrients to be introduced to the estuary when one or more dry years are followed by a moderate/wet year.

Making future projections with a biogeochemical model can be challenging, because the model kinetic formations are inflexible and are limited by the science available to inform model formulation, parameterization, and the inclusion of all relevant biological and biogeochemical interactions. For example, future climate changes will likely alter phytoplankton species abundance and distribution, but the current biogeochemical model only represents two idealized functional types (a summer group and a winter diatom group). Given that these models do not represent a dynamic and flexible community of different phytoplankton types and metabolic modes, the model will have a limited capability to accurately predict the varied potential outcomes for phytoplankton metabolism. Phytoplankton kinetics, including nutrient uptake and

respiration could play a large role in ecosystem nutrient cycling under climate change. Yvon-Durocher et al. (2010) observed a faster rate of increasing ecosystem respiration than primary production when exposed to increasing water temperatures, which could lead to a shifting metabolic balance. In marine phytoplankton, Toseland et al. (2013) found that high temperatures increases the rate of protein synthesis, and ultimately produce higher organismal nitrogen to phosphorus ratios. Phytoplankton sinking and grazing rates within the model could be improved upon as there isn't much data available to constrain these parameters, especially within the context of climate change.

Overall, this study illustrates the complexity biogeochemistry feedbacks loops in estuarine ecology, and how alterations in the phenology of human behavior, physical forcing and biogeochemistry can potentially be important when studying climate change effects on Chesapeake Bay. Modeling tools, like ROMS-RCA, are valuable for studying complex, large scale systems at a high spatial and temporal resolution, because they provide insight to the cascading effects of phenological changes between activities within the watershed and estuary.

References

- Beegle, D. (2013). Nutrient Management and the Chesapeake Bay. *Journal of Contemporary Water Research & Education*, 151(1), 3–8. <https://doi.org/10.1111/j.1936-704x.2013.03146.x>
- Boesch, D. F. (1996). Science and management in four U.S. coastal ecosystems dominated by land-ocean interactions. *Journal of Coastal Conservation*, 2(2), 103–114. <https://doi.org/10.1007/BF02905196>
- Bouraoui, F., & Grizzetti, B. (2011). Long term change of nutrient concentrations of rivers discharging in European seas. *Science of the Total Environment*, 409(23), 4899–4916. <https://doi.org/10.1016/j.scitotenv.2011.08.015>
- Boynton, W R, Frank, J. M., Rohland, F. M., Stankelis, R. M., Lawrence, J. M., Bean, B., & Pine, H. (2003). Monitoring of sediment oxygen and nutrient exchanges in the Chester River estuary in support of TMDL development. In *UMCES Technical Report Series TS-400-03-CB*.
- Boynton, Walter R, Testa, J. M., & Kemp, W. M. (2009). *An Ecological Assessment of the Corsica River Estuary and Watershed Scientific Advice for Future Water Quality Management*. 1–54.
- Brakebill, J. W., Preston, S. D., & Martucci, S. K. (2004). *Digital Data Used to Relate Nutrient Inputs to Water Quality in the Chesapeake Bay Watershed, Version 2.0*.
- Breitburg, D. (2002). Effects of hypoxia, and the balance between hypoxia and enrichment, on coastal fishes and fisheries. *Estuaries*, 25(4 B), 767–781. <https://doi.org/10.1007/BF02804904>
- Chang, S. (2019). *Effects of seasonal and long-term climate variability on nitrate export in the Chesterville Branch catchment of the Eastern Shore, MD*. Johns Hopkins University.
- Chesapeake Bay Program. (n.d.). No Title. Retrieved from <https://www.chesapeakebay.net/issues/agriculture>
- Chesapeake Bay Program. (2011). Agriculture in the Chesapeake Bay Watershed. *Backgrounder*, 0–1. Retrieved from http://www.chesapeakebay.net/documents/5376/agriculture_backgroundunder-final.pdf
- Cloern, J. E., & Jassby, A. D. (2008). Complex seasonal patterns of primary producers at the land-sea interface. *Ecology Letters*, 11(12), 1294–1303. <https://doi.org/10.1111/j.1461-0248.2008.01244.x>
- Cornwell, J. C., Kemp, W. M., & Kana, T. M. (1999). Denitrification in coastal ecosystems:

- Methods, environmental controls, and ecosystem level controls, a review. *Aquatic Ecology*, 33(1), 41–54. <https://doi.org/10.1023/A:1009921414151>
- Correll, D. L., Jordan, T. E., & Weller, D. E. (1999). Transport of nitrogen and phosphorus from Rhode River watersheds during storm events. *Water Resources Research*, 35(8), 2513–2521. <https://doi.org/10.1029/1999WR900058>
- Diaz, R. J., & Rosenberg, R. (2008). Spreading dead zones and consequences for marine ecosystems. *Science*, 321(5891), 926–929. <https://doi.org/10.1126/science.1156401>
- Ding, H., & Elmore, A. J. (2015). Spatio-temporal patterns in water surface temperature from Landsat time series data in the Chesapeake Bay, U.S.A. *Remote Sensing of Environment*, 168, 335–348. <https://doi.org/10.1016/j.rse.2015.07.009>
- Du, J., & Shen, J. (2014). Decoupling the influence of biological and physical processes on the dissolved oxygen in the Chesapeake Bay. *Journal of Geophysical Research: Oceans*, 119, 2183–2200. <https://doi.org/10.1002/2013JC009443>
- Elmore, A. J., Nelson, D. M., & Craine, J. M. (2016). Earlier springs are causing reduced nitrogen availability in North American eastern deciduous forests. *Nature Plants*, 2(10), 1–5. <https://doi.org/10.1038/nplants.2016.133>
- Eshleman, K. N., Sabo, R. D., & Kline, K. M. (2013). Surface water quality is improving due to declining atmospheric N deposition. *Environmental Science and Technology*, 47(21), 12193–12200. <https://doi.org/10.1021/es4028748>
- Fisher, T. R., Peele, E. R., Ammerman, J. W., & Harding, L. W. (1992). Nutrient limitation of phytoplankton in Chesapeake Bay. *Marine Ecology Progress Series*, 82(1), 51–63. <https://doi.org/10.3354/meps082051>
- Goetz, S. J., Jantz, C. A., Prince, S. D., Smith, A. J., Varlyguin, D., & Wright, R. K. (2004). Integrated analysis of ecosystem interactions with land use change: The Chesapeake bay watershed. *Geophysical Monograph Series*, 153(June 2014), 263–275. <https://doi.org/10.1029/153GM20>
- Hagy, J. D., Boynton, W. R., Keefe, C. W., & Wood, K. V. (2004). Hypoxia in Chesapeake Bay, 1950–2001: Long-term change in relation to nutrient loading and river flow. *Estuaries*, 27(4), 634–658. <https://doi.org/10.1007/BF02907650>
- Huttunen, I., Lehtonen, H., Huttunen, M., Piirainen, V., Korppoo, M., Veijalainen, N., ... Vehviläinen, B. (2015). Effects of climate change and agricultural adaptation on nutrient loading from Finnish catchments to the Baltic Sea. *Science of the Total Environment*, 529, 168–181. <https://doi.org/10.1016/j.scitotenv.2015.05.055>
- Irby, I. D., Friedrichs, M. A. M., Da, F., & Hinson, K. E. (2018). The competing impacts of climate change and nutrient reductions on dissolved oxygen in Chesapeake Bay.

- Biogeosciences*, 15(9), 2649–2668. <https://doi.org/10.5194/bg-15-2649-2018>
- Jordan, T. E., Cornwell, J. C., Boynton, W. R., & Anderson, J. T. (2008). Changes in phosphorus biogeochemistry along an estuarine salinity gradient: The iron conveyor belt. *Limnology and Oceanography*, 53(1), 172–184. <https://doi.org/10.4319/lo.2008.53.1.0172>
- Kleinman, P. J. A. (2017). The Persistent Environmental Relevance of Soil Phosphorus Sorption Saturation. *Current Pollution Reports*, 3(2), 141–150. <https://doi.org/10.1007/s40726-017-0058-4>
- Kraus, R. T., Secor, D. H., & Wingate, R. L. (2015). Testing the thermal-niche oxygen-squeeze hypothesis for estuarine striped bass. *Environmental Biology of Fishes*, 98(10), 2083–2092. <https://doi.org/10.1007/s10641-015-0431-3>
- Kronvang, B., Jeppesen, E., Conley, D. J., Søndergaard, M., Larsen, S. E., Ovesen, N. B., & Carstensen, J. (2005). Nutrient pressures and ecological responses to nutrient loading reductions in Danish streams, lakes and coastal waters. *Journal of Hydrology*, 304(1–4), 274–288. <https://doi.org/10.1016/j.jhydrol.2004.07.035>
- Lee, M., Shevliakova, E., Malyshev, S., Milly, P. C. D., & Jaffé, P. R. (2016). Climate variability and extremes, interacting with nitrogen storage, amplify eutrophication risk. *Geophysical Research Letters*, 43(14), 7520–7528. <https://doi.org/10.1002/2016GL069254>
- Lefcheck, J. S., Orth, R. J., Dennison, W. C., Wilcox, D. J., Murphy, R. R., Keisman, J., ... Batiuk, R. A. (2018). Long-term nutrient reductions lead to the unprecedented recovery of a temperate coastal region. *Proceedings of the National Academy of Sciences of the United States of America*, 115(14), 3658–3662. <https://doi.org/10.1073/pnas.1715798115>
- Li, M., Lee, Y. J., Testa, J. M., Li, Y., Ni, W., Kemp, W. M., & Di Toro, D. M. (2016). What drives interannual variability of hypoxia in Chesapeake Bay: Climate forcing versus nutrient loading? *Geophysical Research Letters*, 43(5), 2127–2134. <https://doi.org/10.1002/2015GL067334>
- Linker, L C, Batiuk, R. A., Shenk, G. W., & Cerco, C. F. (2013). Development of the Chesapeake Bay watershed total maximum daily load allocation. *Journal of the American Water Resources Association*, 49(5), 986–1006. Retrieved from <http://onlinelibrary.wiley.com/doi/10.1111/jawr.12105/abstract>
- Linker, Lewis C., Shenk, G. W., Wang, P., Hopkins, K. J., & Pokharel, S. (2012). a Short History of Chesapeake Bay Modeling and the Next Generation of Watershed and Estuarine Models. *Proceedings of the Water Environment Federation*, 2002(2), 569–582. <https://doi.org/10.2175/193864702785665021>
- Maryland Department of Natural Resources. (2019). Eyes on the Bay. Retrieved from Eyes on the Bay website: www.eyesonthebay.net

- Moore, W. S. (1999). The subterranean estuary: A reaction zone of ground water and sea water. *Marine Chemistry*, 65(1–2), 111–125. [https://doi.org/10.1016/S0304-4203\(99\)00014-6](https://doi.org/10.1016/S0304-4203(99)00014-6)
- Murphy, R. R., Kemp, W. M., & Ball, W. P. (2011). Long-Term Trends in Chesapeake Bay Seasonal Hypoxia, Stratification, and Nutrient Loading. *Estuaries and Coasts*, 34(6), 1293–1309. <https://doi.org/10.1007/s12237-011-9413-7>
- Nixon, S. W., Fulweiler, R. W., Buckley, B. A., Granger, S. L., Nowicki, B. L., & Henry, K. M. (2009). The impact of changing climate on phenology, productivity, and benthic-pelagic coupling in Narragansett Bay. *Estuarine, Coastal and Shelf Science*, 82(1), 1–18. <https://doi.org/10.1016/j.ecss.2008.12.016>
- Palinkas, C. M. (2013). Seasonal and interannual patterns of sedimentation in the corsica river (MD): Evaluating the potential influence of watershed restoration. *Estuarine, Coastal and Shelf Science*, 127, 37–45. <https://doi.org/10.1016/j.ecss.2013.04.015>
- Preusch, P. L., Adler, P. R., Sikora, L. J., & Tworkoski, T. J. (2002). Waste management: Nitrogen and phosphorus availability in composted and uncomposted poultry litter. *Journal of Environmental Quality*, Vol. 31, pp. 2051–2057. <https://doi.org/10.2134/jeq2002.2051>
- Sampou, P., & Kemp, W. M. (1994). Factors regulating plankton community respiration in Chesapeake Bay. *Marine Ecology Progress Series*, 110(2–3), 249–258. <https://doi.org/10.3354/meps110249>
- Sanford, L. P., & Boicourt, W. C. (1990). Wind-forced salt intrusion into a tributary estuary. *Journal of Geophysical Research: Oceans*, 95(C8), 13357–13371. <https://doi.org/10.1029/JC095iC08p13357>
- Sanford, W. E., & Pope, J. P. (2013). Quantifying groundwater’s role in delaying improvements to Chesapeake Bay water quality. *Environmental Science and Technology*, 47(23), 13330–13338. <https://doi.org/10.1021/es401334k>
- Schubel, J. R., & Pritchard, D. W. (2006). Responses of Upper Chesapeake Bay to Variations in Discharge of the Susquehanna River. *Estuaries*, 9(4), 236. <https://doi.org/10.2307/1352096>
- Scully, M. E. (2010). The importance of climate variability to wind-driven modulation of hypoxia in Chesapeake Bay. *Journal of Physical Oceanography*, 40(6), 1435–1440. <https://doi.org/10.1175/2010JPO4321.1>
- Shanks, K. (2001). *Middle Chester River Watershed Characterization*. (April), 90.
- Shen, C., Testa, J. M., Li, M., Cai, W. J., Waldbusser, G. G., Ni, W., ... Su, J. (2019). Controls on Carbonate System Dynamics in a Coastal Plain Estuary: A Modeling Study. *Journal of Geophysical Research: Biogeosciences*, 124(1), 61–78. <https://doi.org/10.1029/2018JG004802>

- Testa, J. M., Brady, D. C., Di Toro, D. M., Boynton, W. R., Cornwell, J. C., & Kemp, W. M. (2013). Sediment flux modeling: Simulating nitrogen, phosphorus, and silica cycles. *Estuarine, Coastal and Shelf Science*, 131(July), 245–263. <https://doi.org/10.1016/j.ecss.2013.06.014>
- Testa, J. M., & Kemp, W. M. (2014). Spatial and Temporal Patterns of Winter–Spring Oxygen Depletion in Chesapeake Bay Bottom Water. *Estuaries and Coasts*, 37(6), 1432–1448. <https://doi.org/10.1007/s12237-014-9775-8>
- Testa, J. M., Kemp, W. M., & Boynton, W. R. (2018). Season-specific trends and linkages of nitrogen and oxygen cycles in Chesapeake Bay. *Limnology and Oceanography*, 63(5), 2045–2064. <https://doi.org/10.1002/lno.10823>
- Testa, J. M., Kemp, W. M., Boynton, W. R., & Hagy, J. D. (2008). Long-term changes in water quality and productivity in the Patuxent River estuary: 1985 to 2003. *Estuaries and Coasts*, 31(6), 1021–1037. <https://doi.org/10.1007/s12237-008-9095-y>
- Testa, J. M., Li, Y., Lee, Y. J., Li, M., Brady, D. C., Di Toro, D. M., ... Fitzpatrick, J. J. (2014). Quantifying the effects of nutrient loading on dissolved O₂ cycling and hypoxia in Chesapeake Bay using a coupled hydrodynamic-biogeochemical model. *Journal of Marine Systems*, 139(2014), 139–158. <https://doi.org/10.1016/j.jmarsys.2014.05.018>
- Testa, J. M., Murphy, R. R., Brady, D. C., & Kemp, W. M. (2018). Nutrient- and Climate-Induced Shifts in the Phenology of Linked Biogeochemical Cycles in a Temperate Estuary. *Frontiers in Marine Science*, 5(April), 1–15. <https://doi.org/10.3389/fmars.2018.00114>
- Tian, R. (2019). Factors controlling saltwater intrusion across multi-time scales in estuaries, Chester River, Chesapeake Bay. *Estuarine, Coastal and Shelf Science*, 223(April), 61–73. <https://doi.org/10.1016/j.ecss.2019.04.041>
- Toseland, A., Daines, S. J., Clark, J. R., Kirkham, A., Strauss, J., Uhlig, C., ... Mock, T. (2013). The impact of temperature on marine phytoplankton resource allocation and metabolism. *Nature Climate Change*, 3(11), 979–984. <https://doi.org/10.1038/nclimate1989>
- Tyler, R. M., Brady, D. C., & Targett, T. E. (2009). Temporal and spatial dynamics of diel-cycling hypoxia in estuarine tributaries. *Estuaries and Coasts*, 32(1), 123–145. <https://doi.org/10.1007/s12237-008-9108-x>
- U.S. Department of Agriculture. (2010). Field Crops Usual Planting and Harvesting Dates. *Agricultural Handbook*, (628), 41. Retrieved from <http://usda01.library.cornell.edu/usda/current/planting/planting-10-29-2010.pdf>
- USDA-NASS. (2012). *2012 Census of Agriculture - State Data*. 464–496.
- Valiela, I., Foreman, K., LaMontagne, M., Hersh, D., Costa, J., Peckol, P., ... Lajtha, K. (1992). Couplings of watersheds and coastal waters: Sources and consequences of nutrient

enrichment in Waquoit Bay, Massachusetts. *Estuaries*, 15(4), 443–457.
<https://doi.org/10.2307/1352389>

Wagena, M. B., & Easton, Z. M. (2018). Agricultural conservation practices can help mitigate the impact of climate change. *Science of the Total Environment*, 635, 132–143.
<https://doi.org/10.1016/j.scitotenv.2018.04.110>

Yvon-Durocher, G., Jones, J. I., Trimmer, M., Woodward, G., & Montoya, J. M. (2010). Warming alters the metabolic balance of ecosystems. *Philosophical Transactions of the Royal Society B: Biological Sciences*, 365(1549), 2117–2126.
<https://doi.org/10.1098/rstb.2010.0038>

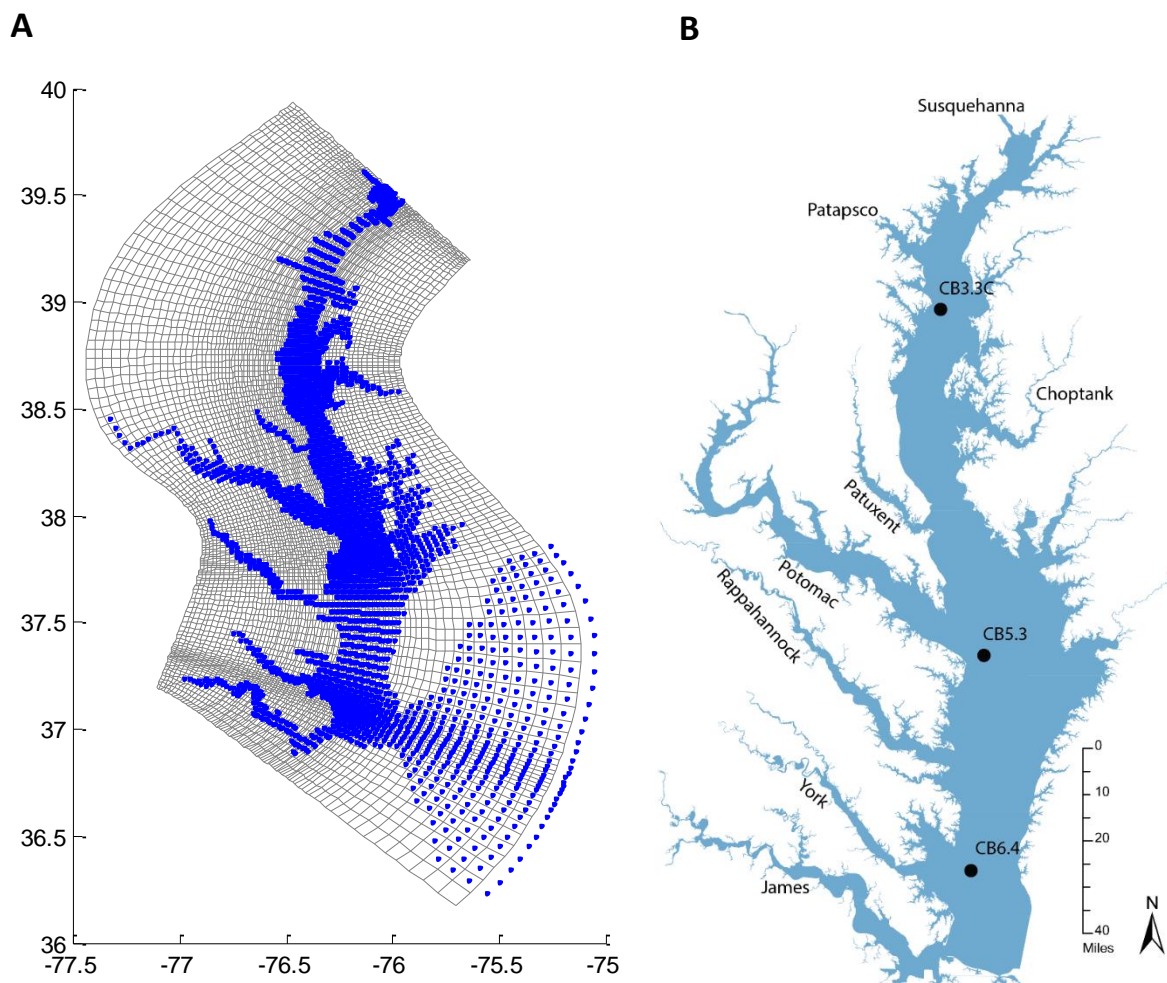


Figure 1.1. (a) RCA model grid (water cells = blue). (b) Map of Chesapeake Bay's major tributaries and Chesapeake Bay Program long-term water quality monitoring stations used in the analysis of model scenarios.

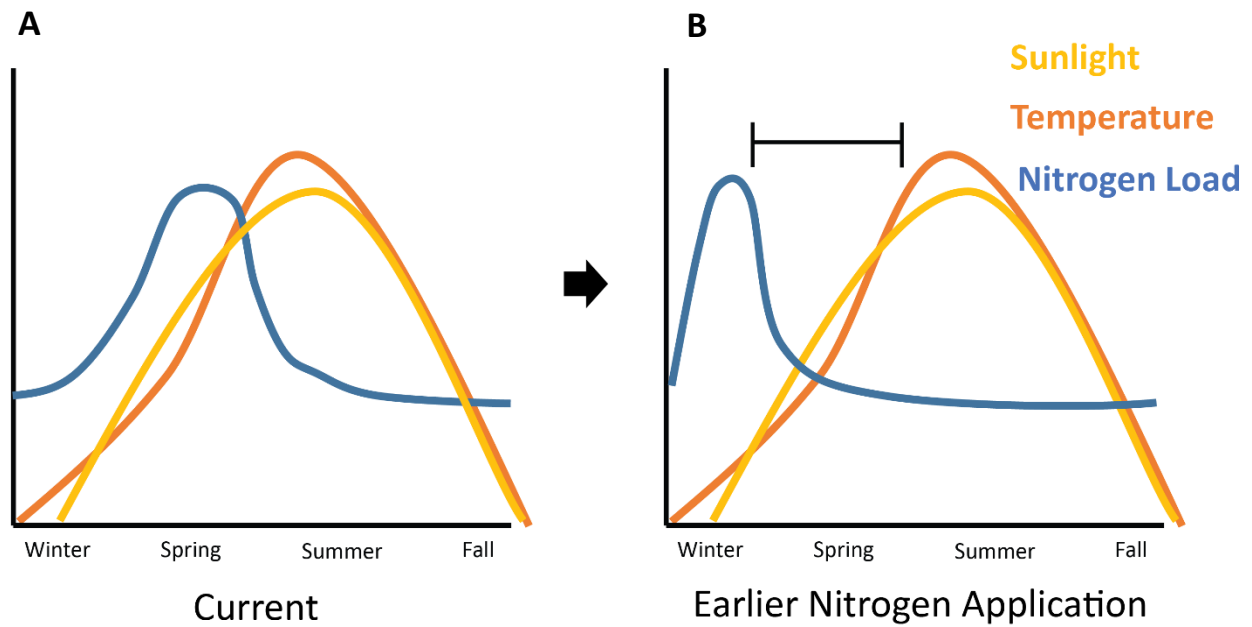


Figure 1.2. Conceptual diagram of potential nutrient load shift decoupling. (a) Currently, spring sunlight, temperature and nitrogen load are aligned to initiate a spring phytoplankton bloom. (b) If nutrient loads are shifted earlier in the year, there could be a decoupling of these factors that influence productivity.

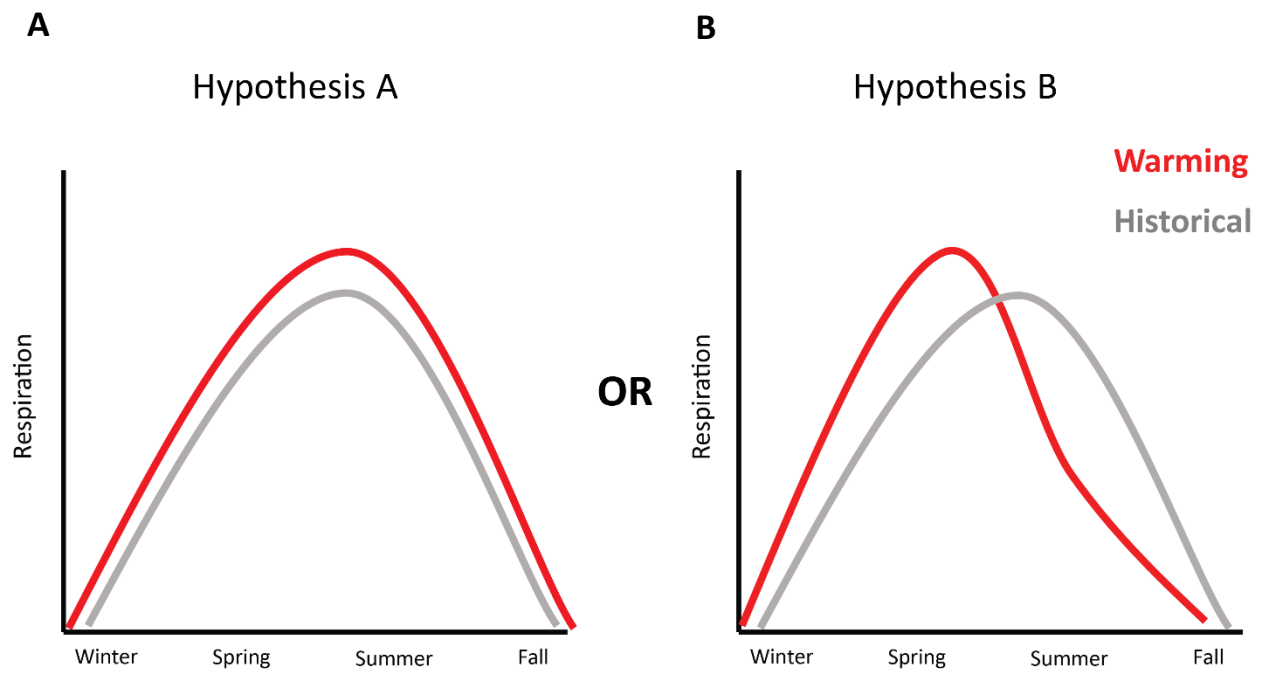


Figure 1.3. Conceptual diagram for alternative hypothesis of water temperature increase effects on respiration. Conventional hypotheses (a) suggests that warmer water temperature will increase respiration rates throughout the year, while an alternative hypothesis (b) suggests that the increase in temperature will increase respiration and effectively speed up the consumption of labile organic matter earlier in the year, effectively reducing labile organic matter availability and thus respiration in the fall.

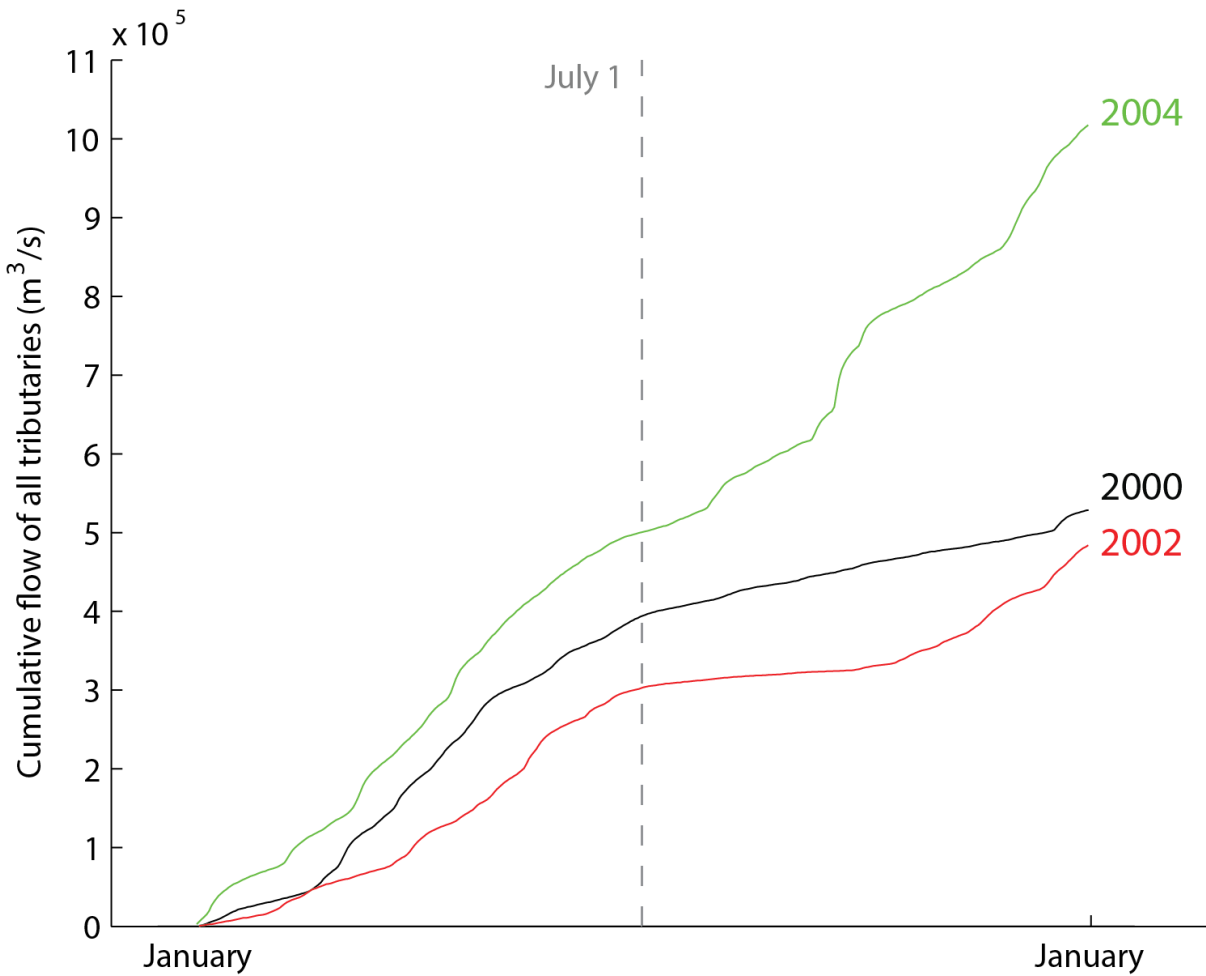


Figure 1.4. Comparison of the cumulative flow of all major Chesapeake Bay tributaries (Susquehanna, Patuxent, Patapsco, Potomac, Choptank, Rappahannock, York, and James Rivers) to highlight that the years 2000 (moderately wet), 2002 (dry), and 2004 (wet) are hydrologically different.

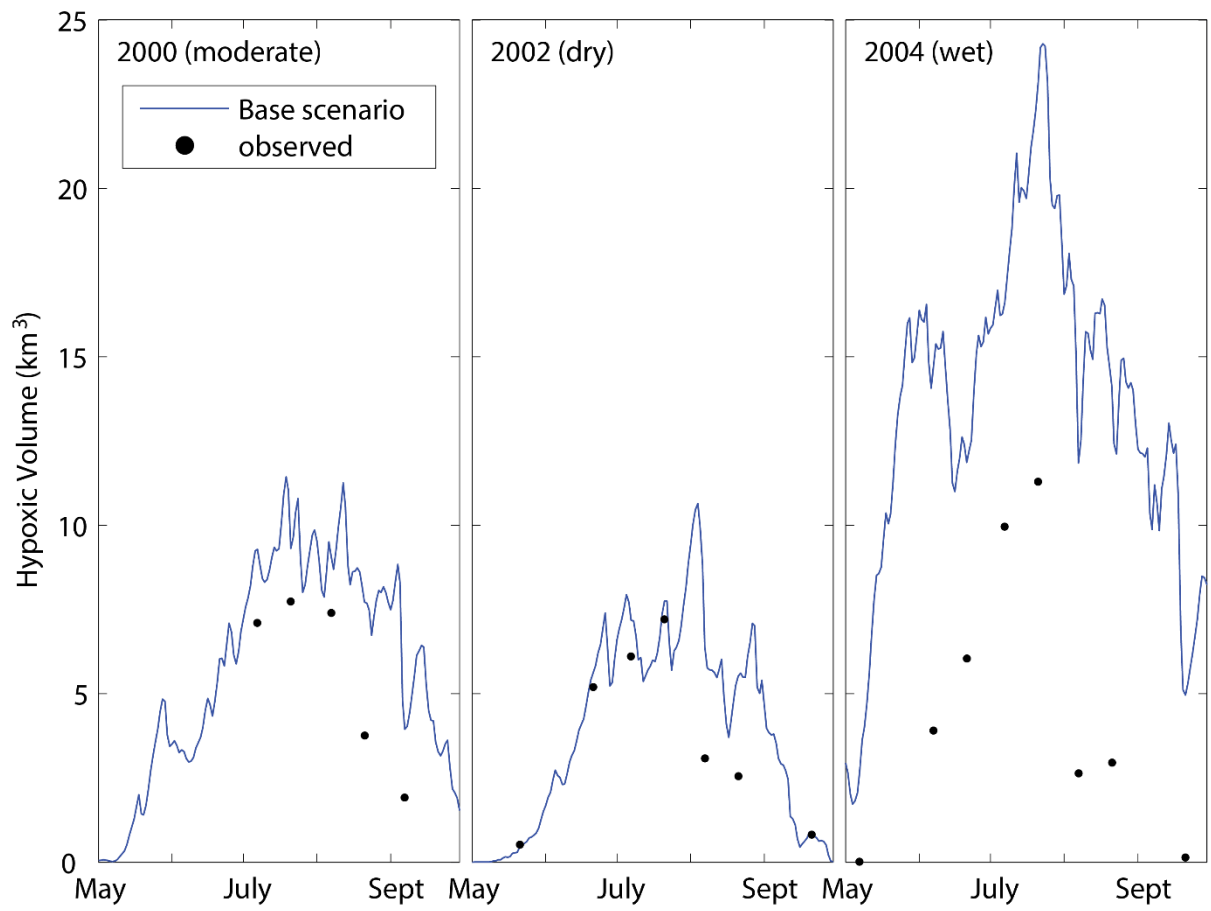


Figure 1.5. Comparison of base scenario (no changes), predicted hypoxic volume for each year and observed summer hypoxic volume (Testa, Murphy, et al., 2018).

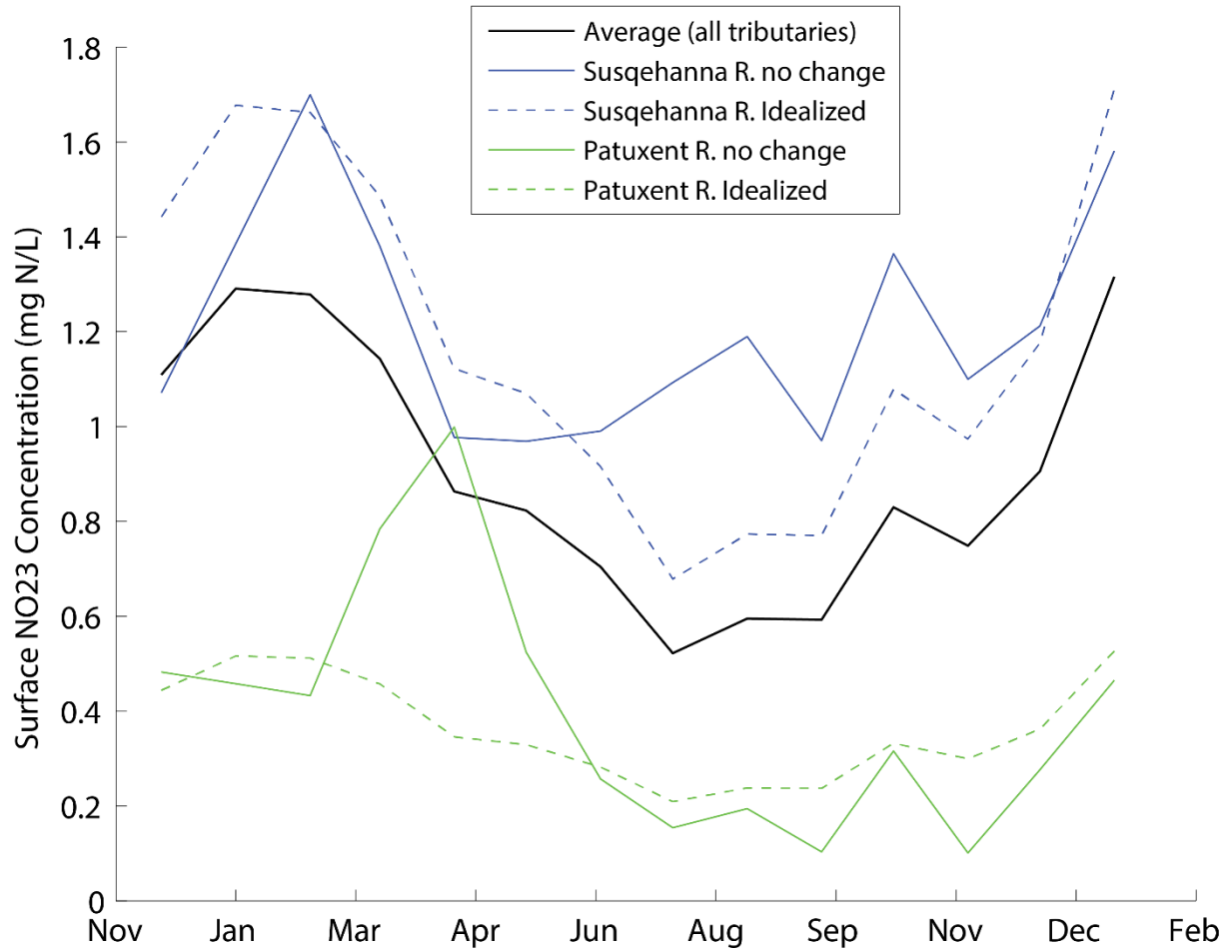


Figure 1.6. Example of how the average NO₂₃ concentration was used to generate an idealized annual nutrient cycle for each of the major tributaries in the RCA model. The original and idealized concentrations for the Susquehanna River (blue) and Patuxent River (green) for the year 2000 are shown above.

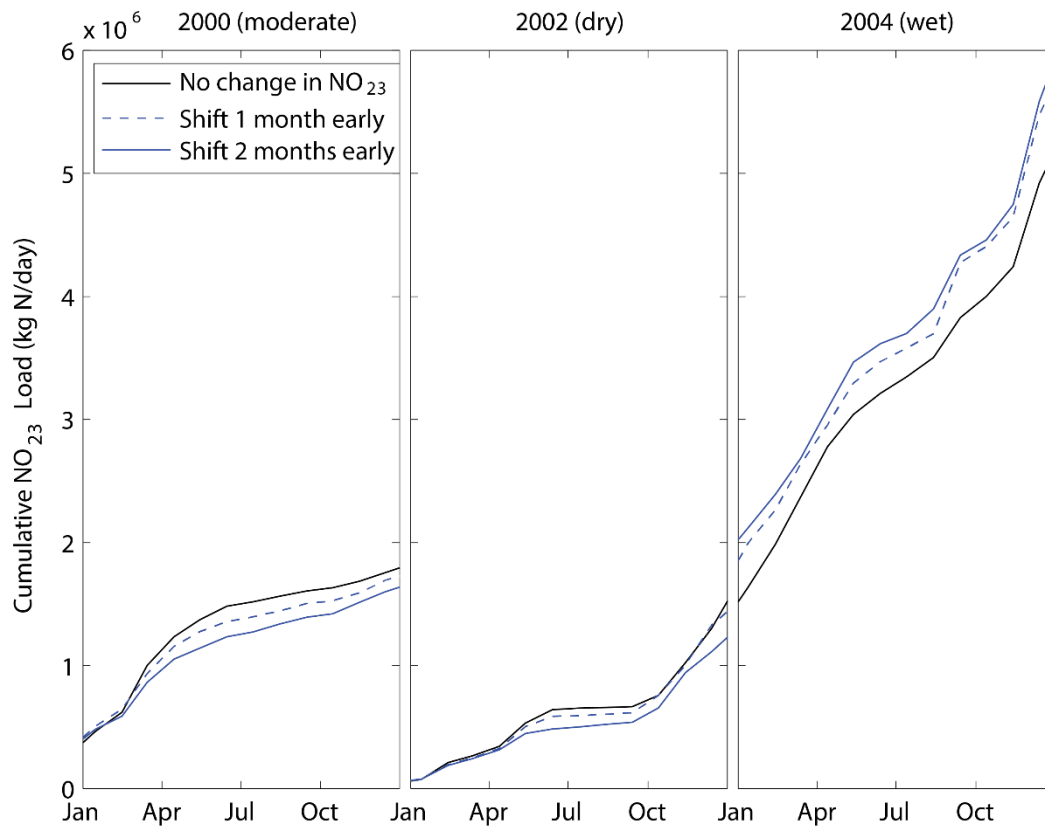
A**B**

Figure 1.7. (a) An example of the nutrient load shift scenario setup of nitrate and nitrite (NO_{23}) for one month early (dashed) and two months early (blue) for the Susquehanna River in 2000. This process was repeated for each year and tributary. (b) The resulting cumulative NO_{23} load of all tributaries combined, for each year and scenario.

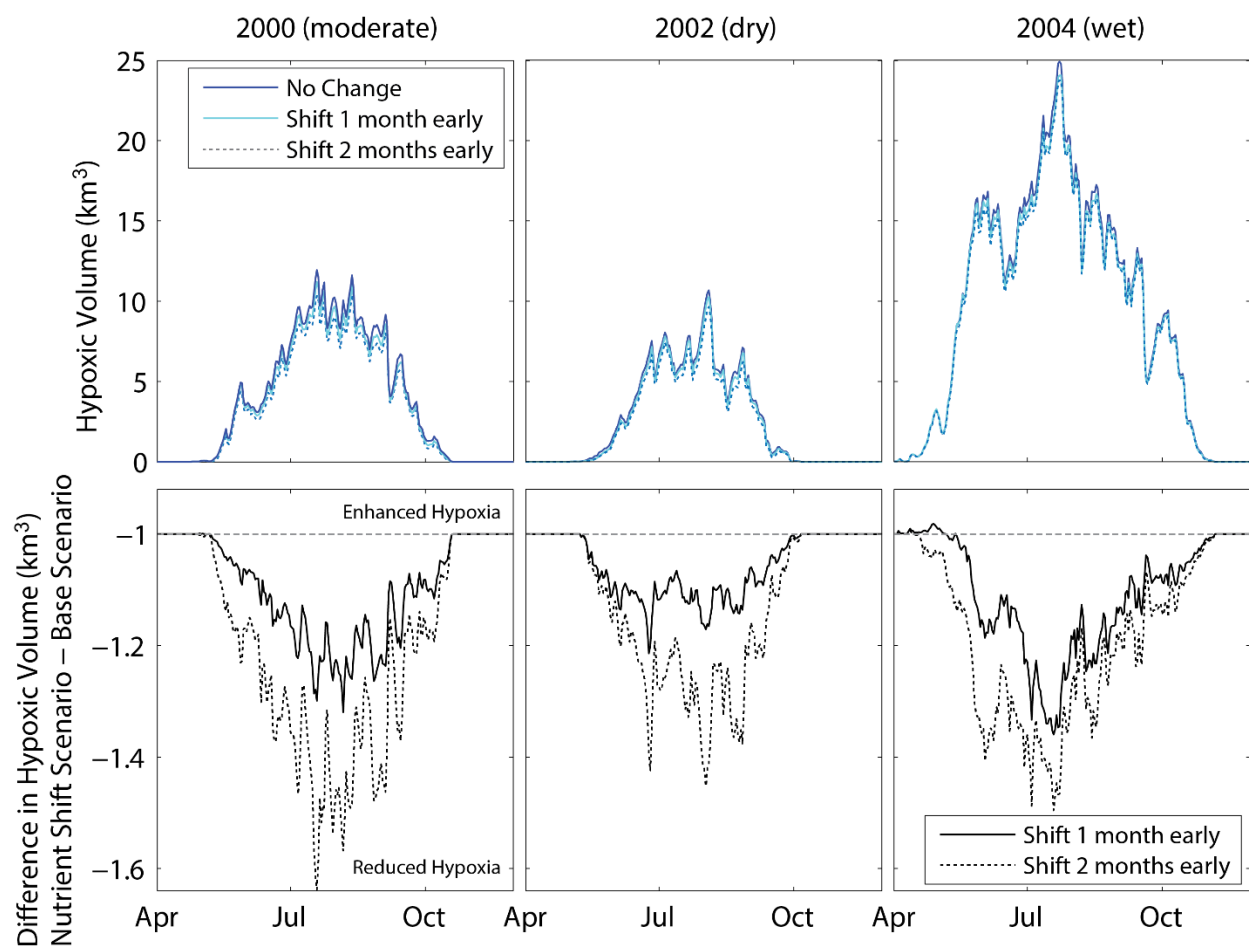


Figure 1.8. Comparison of the hypoxic volume of the nutrient load (NO₂₃) shift scenarios to the idealized Base scenario at a hypoxia threshold of 2 mg O₂/L.

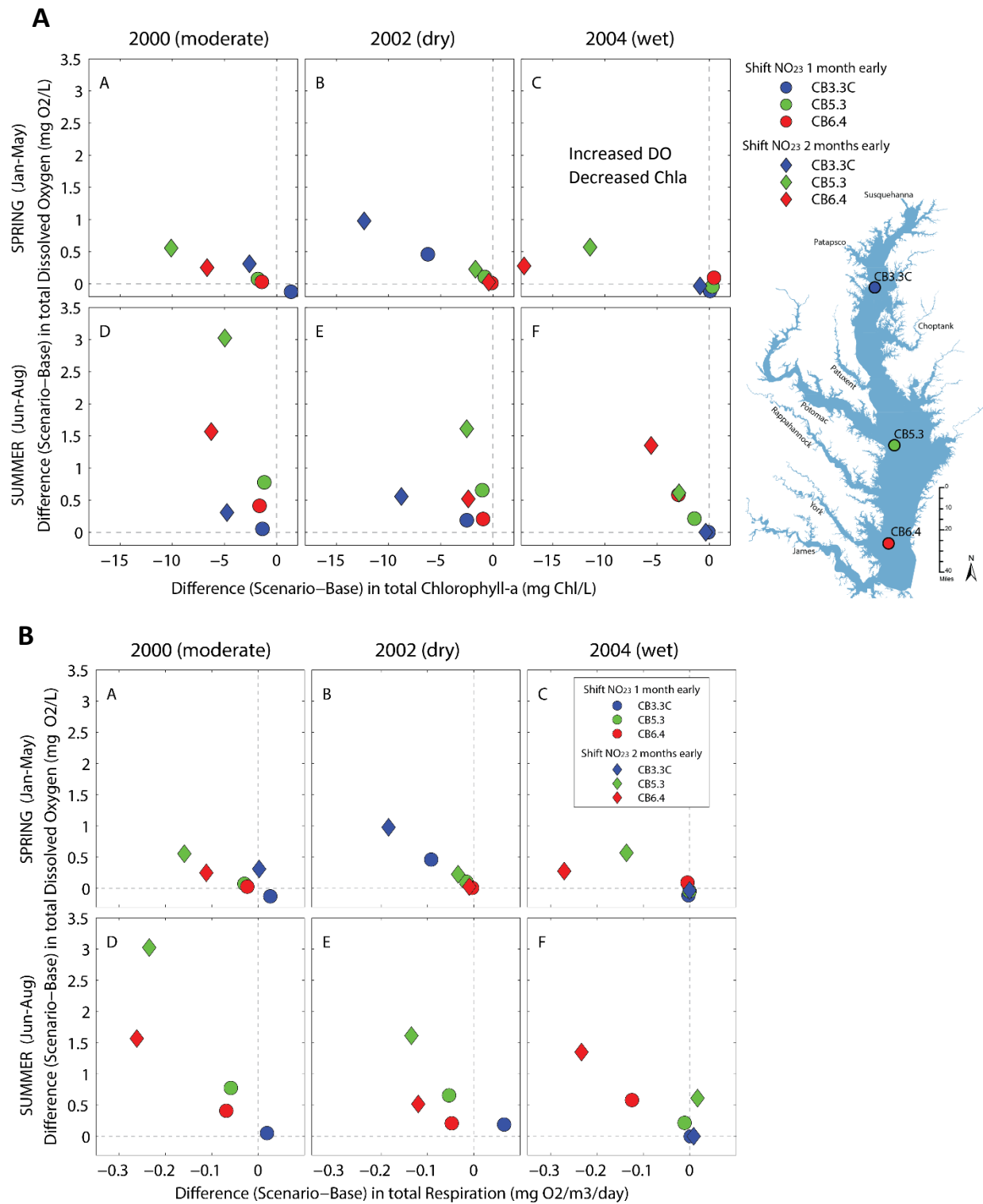


Figure 1.9. Comparison of the total change in dissolved oxygen (O₂) and (a) chlorophyll-a (Chla) and (b) total respiration respectively, during the spring (January-May; A-C) and summer (June-August; D-F) seasons.

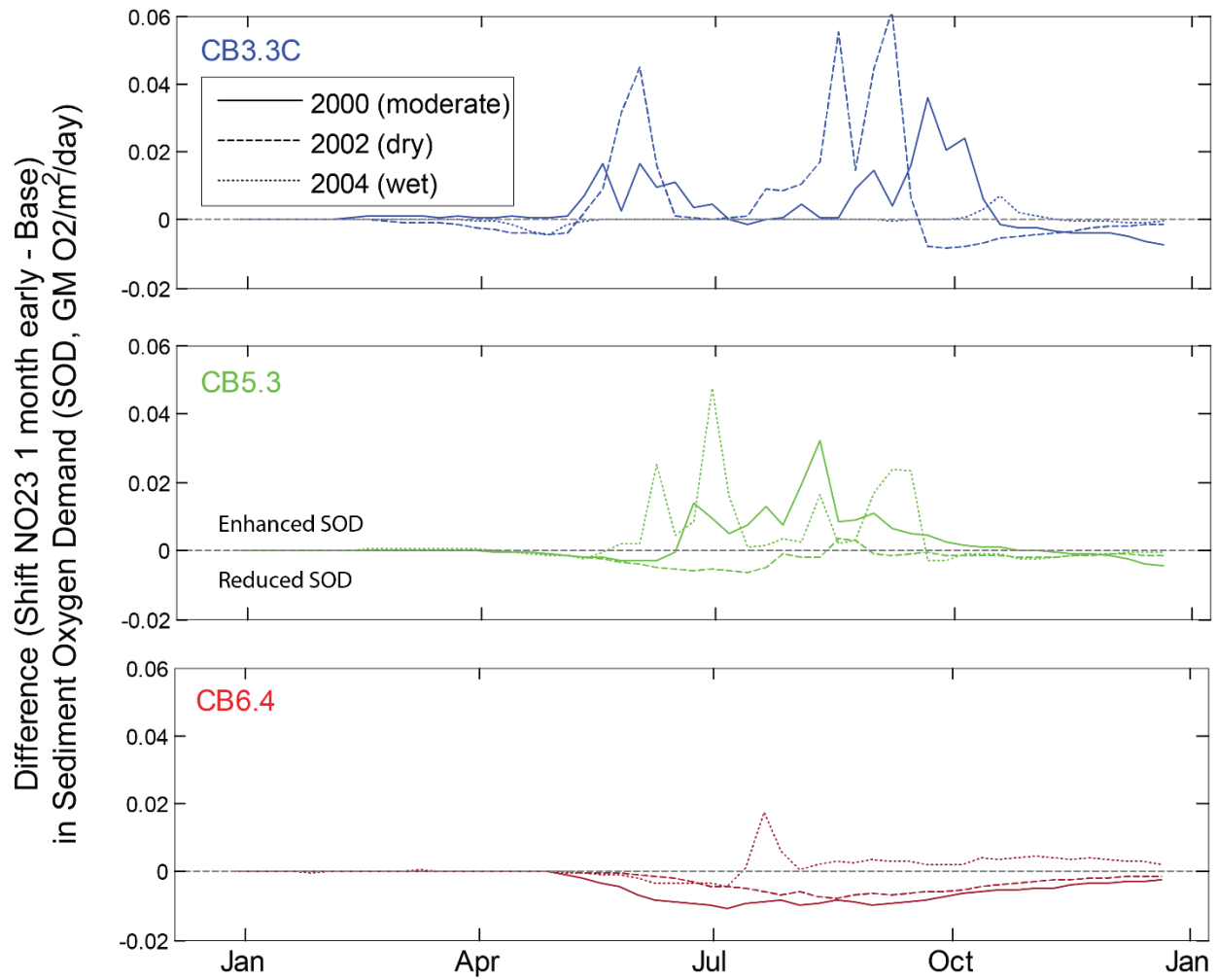


Figure 1.10. Nutrient shift scenario had increased sediment oxygen demand (SOD) in the two upper Chesapeake Bay stations (CB3.3C and CB5.3) and reduced SOD at the lower Bay station (CB6.4).

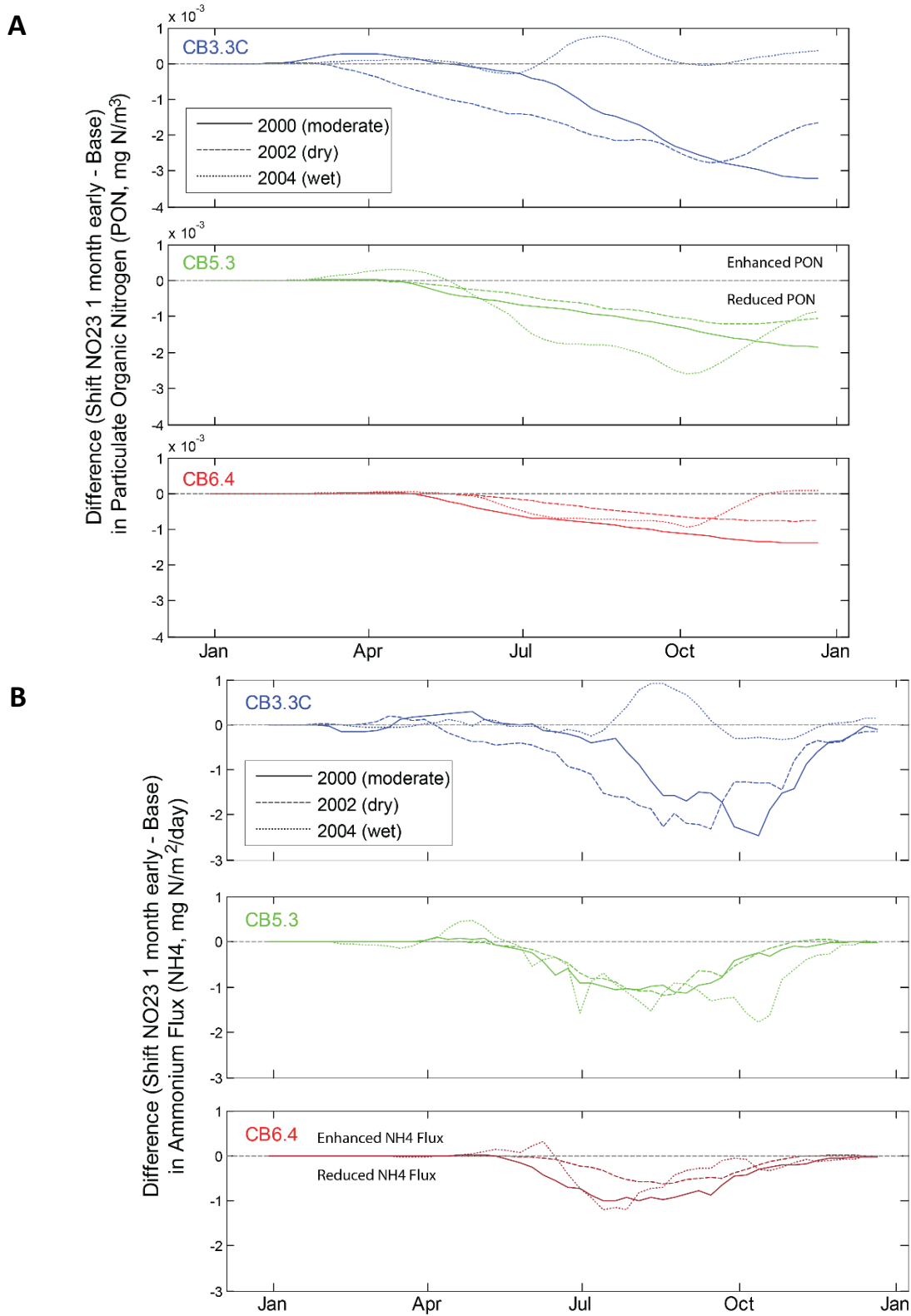


Figure 1.11. The difference between the nutrient shift scenario and no change scenario in terms of (a) particulate organic nitrogen (PON) and (b) ammonium fluxes (NH₄).

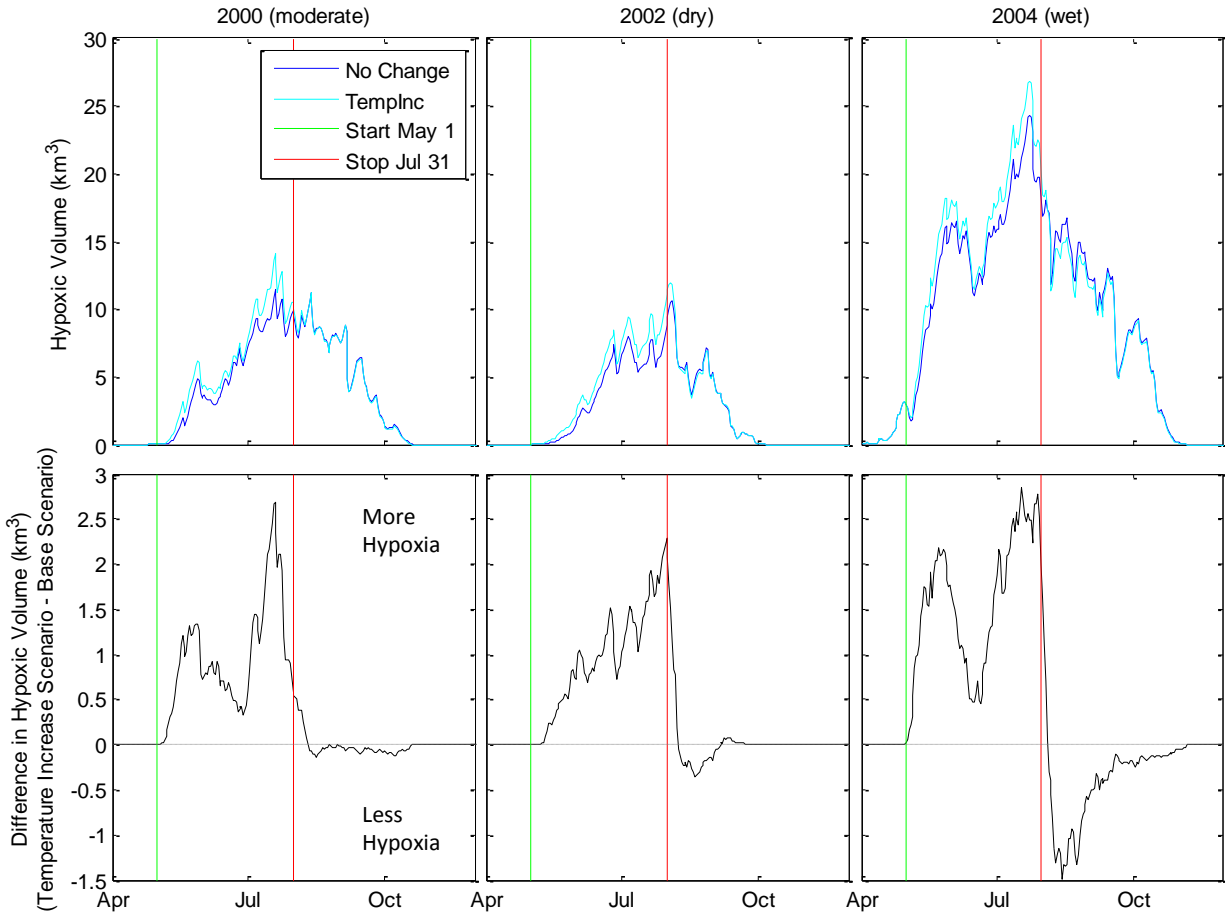


Figure 1.12. Water temperature increase scenario (TempInc, light blue) in comparison to no change scenario (dark blue), at hypoxia threshold of 2.0 mg O₂/L. The water temperature was increased Bay-wide by 1.5 °C from May 1 (start, green line) to July 31 (stop, red line).

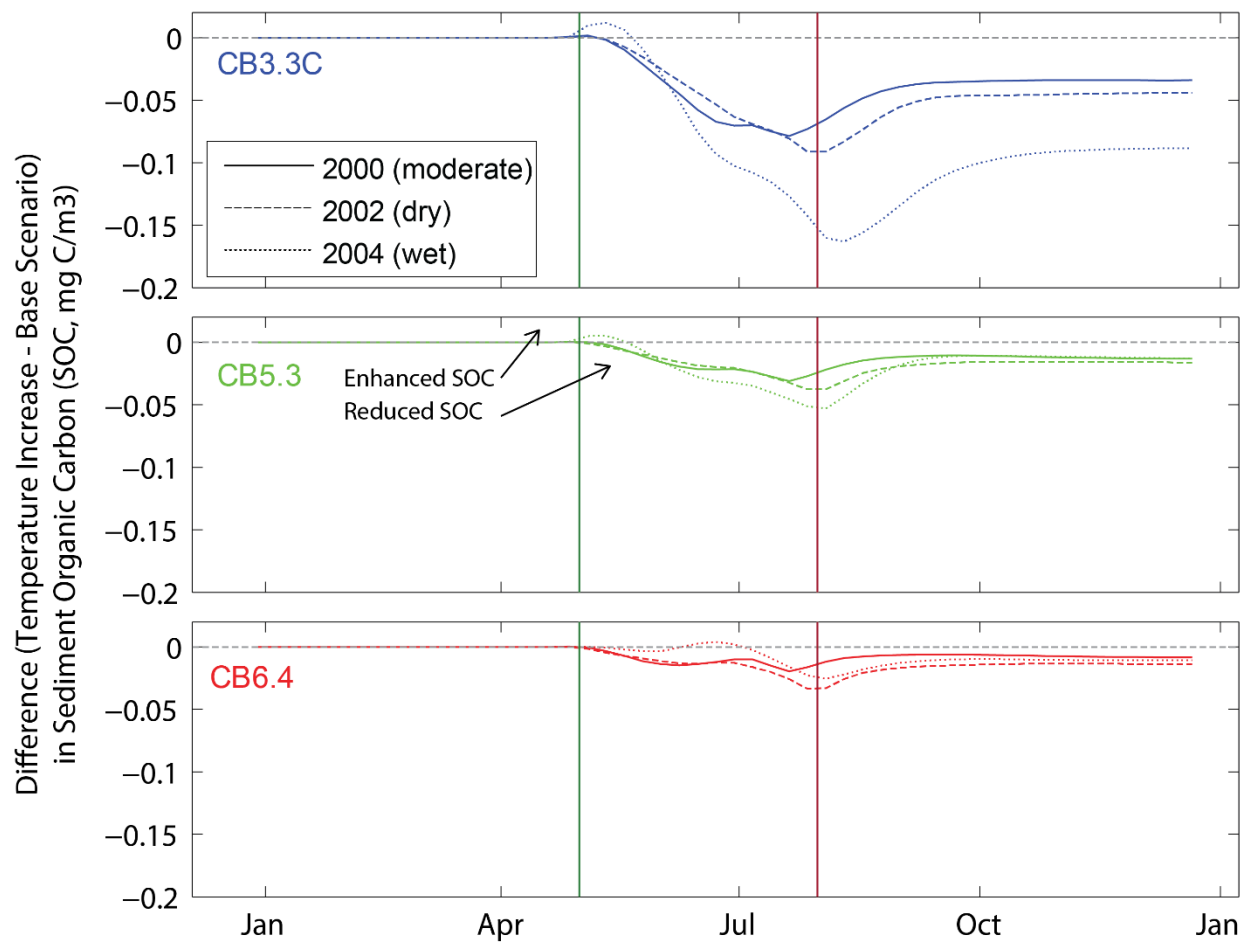


Figure 1.13. The difference in sediment organic carbon (SOC, mg C/m³) between the temperature increase scenario and no change scenario at three stations across the mainstem of the Chesapeake Bay. The water temperature was increased Bay-wide by 1.5°C from May 1 (start, green line) to July 31 (stop, red line).

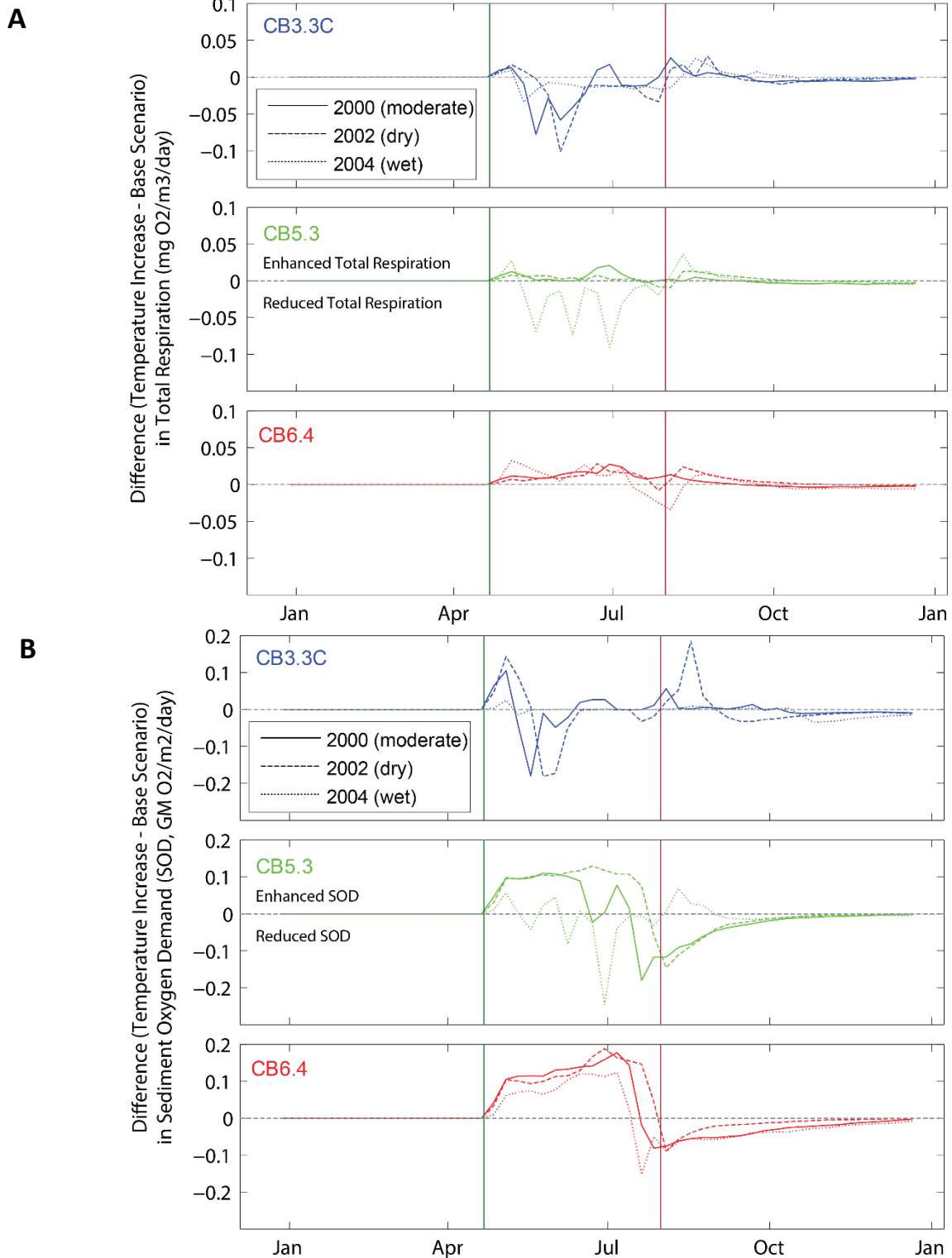


Figure 1.14. The difference in (a) total respiration and (b) sediment oxygen demand (SOD) between the temperature increase scenario and no change scenario at three stations across the mainstem of the Chesapeake Bay. The water temperature was increased Bay-wide by 1.5°C from May 1 (start, green line) to July 31 (stop, red line).

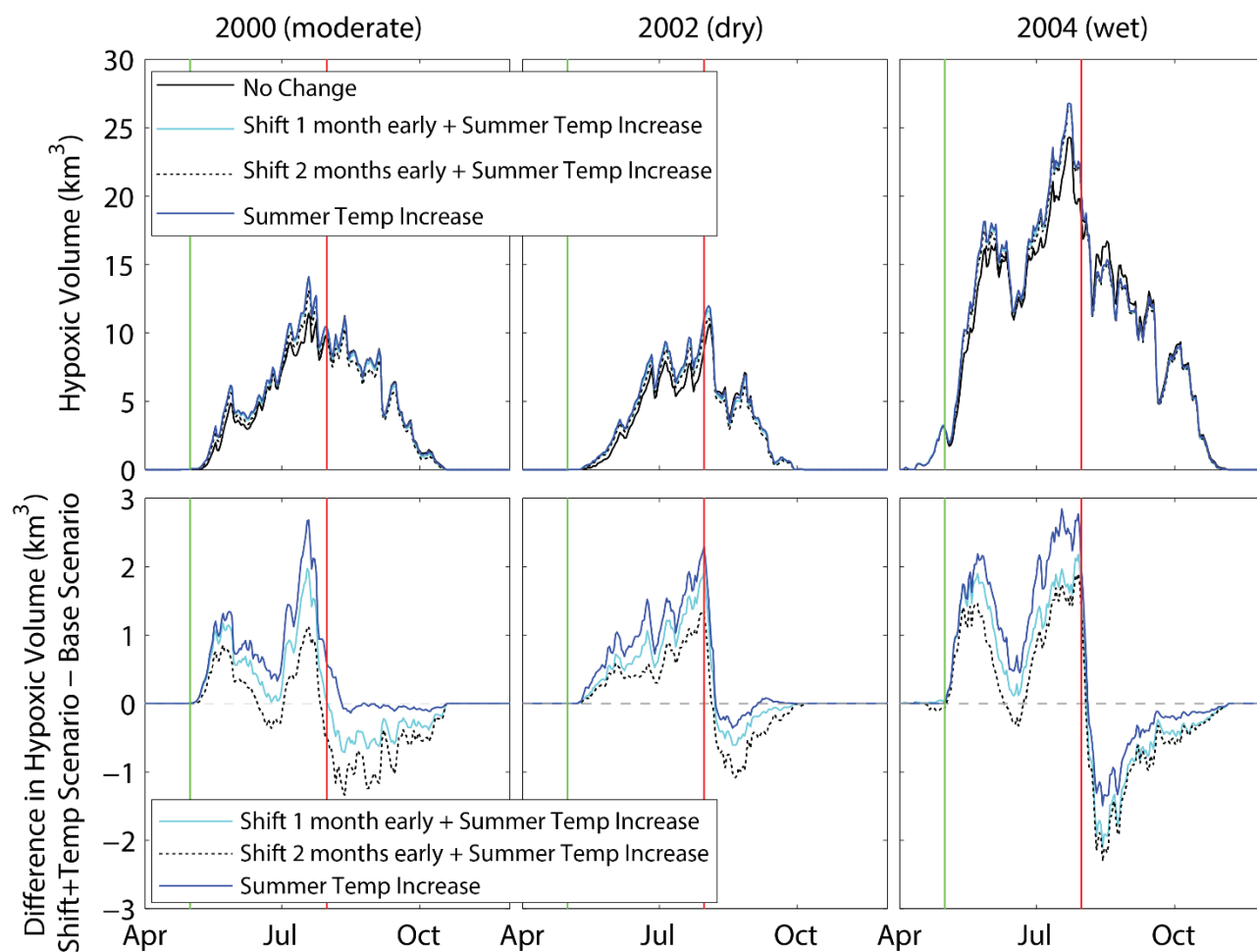


Figure 1.15. Comparison of the hypoxic volumes resulting from combination scenarios of nutrient shift and water temperature increase in comparison to the no change scenario (no changes to nutrients or water temperature), at a hypoxia threshold of 2.0 mg O₂/L. The water temperature was increased Bay-wide by 1.5 °C from May 1 (start, green line) to July 31 (stop, red line), and the NO₂₃ was shifted 1 and 2 months early respectively.

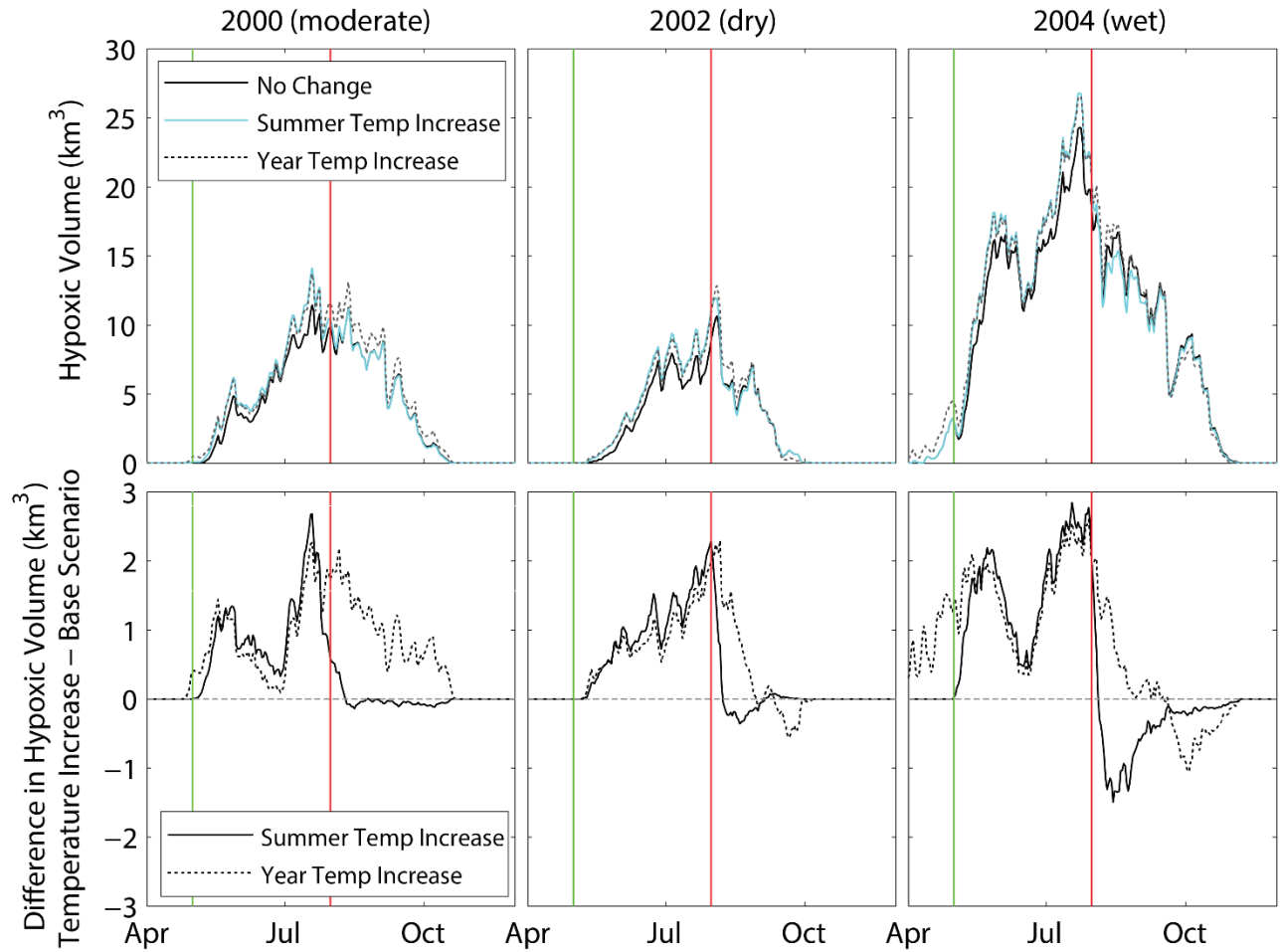


Figure 1.16. Comparison of the hypoxic volumes resulting from the water temperature increase scenarios (summer and year-round) in comparison to the no change scenario (no changes to nutrients or water temperature), at a hypoxia threshold of 2.0 mg O/L. For both scenarios the water temperature was increased Bay-wide by 1.5 °C. For the summer scenario this increase occurred from May 1 (start, green line) to July 31 (stop, red line), and for the year-round scenario, from January 1 to December 31.

Chapter 2 - Phenology of Estuarine Response to Anthropogenic and Climate Drivers, the Chester River Estuary as a Case Study

Introduction

Biogeochemical processes in coastal ecosystems are closely linked to both adjacent land use activities and the internal physical, biological, and chemical features of local water bodies. Due to the nature of their bathymetry, shallow estuarine systems, like many tributaries to the Chesapeake Bay, have several unique characteristics compared to larger, deeper systems that mediate their response to external nutrient inputs. For example, while the mainstem of Chesapeake Bay has a robust seasonal hypoxia cycle over the spatial scale of several kilometers, the Chester River estuary has diel cycling hypoxia, where oxygen is depleted for brief 6-24 hour periods at a limited spatial scale (Boynton et al. 2009; Tyler, Brady, & Targett, 2009). Shallow estuaries are also more consistently vertically mixed (have less stratification) due to both wind and tidal influences that exert stress over the entire water-column. These shallow tributary estuaries are also sensitive to the water quality in the adjacent Chesapeake Bay, where circulation and bathymetry can allow for water exchange into the tributary estuaries, potentially negatively affecting oxygen and nutrient conditions. For example, the Choptank, Chester, and Patuxent estuaries have been shown to import either high-nutrient or low-oxygen water into their lower reaches on seasonal or event-scales, leading to water quality degradation that is independent of local land use (L. P. Sanford & Boicourt, 1990; Testa, Kemp, Boynton, & Hagy, 2008).

Watersheds of the shallow, coastal plain estuaries of the eastern shore of Chesapeake Bay also contrast with those of larger estuaries whose watersheds expand into the Piedmont and other geologic features. For example, the Chester River watershed, unlike the Chesapeake Bay

watershed, has relatively low relief, includes minimal urban land-use, and is dominated by intensive agricultural activities. Agricultural nutrient management is an continuing effort within the Chesapeake Bay watershed (Beegle, 2013) and. one of the challenges with managing agriculture operations on the eastern shore of Maryland is large quantity of poultry litter and the high phosphorus content that it contains (Preusch, Adler, Sikora, & Tworkoski, 2002).

Phosphorus is a difficult nutrient to manage and study, because it ultimately binds to sediment but can become mobilized in hydrologically active soils when binding sites are saturated (Kleinman, 2017). Previous management of poultry litter applications were based on crop nitrogen requirements, which caused an oversaturation of phosphorus to croplands (Preusch et al., 2002). Groundwater movements on the eastern shore of Chesapeake Bay are important, because there is a lag of several decades between nitrogen application on land and its eventual transfer into estuarine waters (W. E. Sanford & Pope, 2013). While these groundwater inputs are poorly quantified, prior studies have highlighted the role of submarine groundwater discharge as a key mode of nitrogen loading to shallow estuaries with more sandy soils (e.g. Moore, 1999; Valiela et al., 1992).

Previous watershed modeling efforts within the Chester River watershed have shown that future changes to climate and farmer behavior could lead to increased and earlier shift in nitrate (NO_3) load (Chang, 2019). Analyses of agricultural activity within large geographical regions (e.g., the mid-Atlantic) have shown a long-term trend of earlier planting dates for corn (e.g., one week earlier), and recent modeling has shown that planting dates for corn are expected to shift 1-3 weeks earlier in the Chesterville Branch Watershed (a sub-estuary of the Chester) by 2050 (mid-century) and by 2100 (Chang, 2019). These shifts in planting dates are associated with earlier fertilizer application and alterations to soil nitrification and remineralization, and when

combined with higher precipitation rates projected for the watershed, would lead to earlier nitrogen inputs to the watershed by 2050 (Chang, 2019). While there is considerable uncertainty in the timing of these additive effects of climate and agricultural practices depending on the climate projection used, the potential changes in nutrient load timing reveal a need to better understand the associated impacts on estuaries.

The purpose of this chapter is to use the same numerical modeling framework as in Chapter 1 to evaluate responses to altered magnitude and timing of nutrient inputs in a shallow, turbid estuary. The Chester River Estuary was chosen as a case study for this project, because of the recent modeling efforts of this estuary (Shanks, 2001, Chang, 2019) and the extensive monitoring and restoration activities undertaken in the Corsica River (Walter R Boynton, Testa, & Kemp, 2009) a major tributary to the Chester River. The following research questions are relevant for Chapter 2: How sensitive is the seasonal cycle of hypoxia in the Chester River to changes in the magnitude of nutrient inputs? And, how do changes in the seasonal timing of nutrient inputs effect the seasonality and spatial response of hypoxia in the Chester River Estuary?

Methods

To evaluate changes in hypoxia seasonality and biogeochemical responses (chlorophyll-a, sediment nutrient and sediment oxygen fluxes, water-column respiration) in the Chester River to altered magnitude and timing of nutrient inputs, I conducted a series of idealized simulations using a coupled, three dimension hydrodynamic-biogeochemical model (ROMS-RCA). Model scenarios included changes in the magnitude of nitrogen and phosphorus loads from 12 major freshwater sources, as well as shifts in the timing of riverine nitrogen concentrations to test the

systems sensitivity to potential indirect seasonal impacts of climate and anthropogenic changes. Phenological responses will again be quantified by the volume of hypoxic waters, duration of hypoxia from formation to breakup, timing of chlorophyll-a accumulation, and the associated respiratory processes in the water-column and sediments.

Study Site

The Chester River Estuary is located on the eastern shore of Maryland of the Chesapeake Bay (Figure 2.1) near the Chesapeake Bay Bridge. The 1,140 km² watershed consists of predominantly agricultural activities (65%; Maryland Department of Planning), specifically large poultry operations. The Chester River has a maximum depth of approximately 14 meters, but a majority of the estuary is less than 6 meters (Figure 2.2a). The watershed area of the basin is approximately 250,000 acres and spans Kent and Queen Anne's counties in Maryland, and New Castle and Kent counties in Delaware.

Modeling Tool

A coupled hydrologic-biogeochemical model (Regional Ocean Modeling System and Row-Column Aesop, ROMS-RCA) was used to simulate and analyze estuarine biogeochemical responses to simulated changes in nutrient input magnitude and timing. This modeling tool was used in Chapter 1 to evaluate altered nutrient load timing and temperature increases in the Chesapeake Bay estuary, and ROMS-RCA has also been configured for the Chester River estuary. The Chester River estuary version of ROMS-RCA has a grid resolution of 174x174, a cell size of approximately 70 m² (Figure 2.3a), and 10 vertical layers. Nutrient and freshwater inputs for Chester ROMS-RCA are based on Chesapeake Bay Program Phase 6 watershed model

inputs aggregated at 12 major tributaries (Figure 2.3a). Atmospheric boundary conditions (air temperature, photosynthetically active radiation, wind speed) were derived from the North American Regional Reanalysis (NARR). The seaward boundary (tides, salinity, nutrients, etc.) was derived from simulations of the Chesapeake Bay Program Water Quality and Sediment Transport Model (WQSTM). All model simulations were performed for the year 2003 as this year is included in the span of years used for the Chesapeake Bay idealized model scenarios in Chapter 1.

Model Calibration and Validation

Model scenario results were validated using bi-monthly to monthly, station-specific measurements of salinity, water temperature, chlorophyll-a, dissolved and particulate nutrient concentrations, and dissolved oxygen from the Chesapeake Bay Program (CBP) monitoring program (www.chesapeakebay.net) for both the tidal and non-tidal portions of the Chester River (Figure 2.4 and 2.5). High-frequency data (15-minute sampling) from the Maryland Department of Natural Resources (MDNR) Continuous Monitoring (ConMon) program (MDNR, 2019) was also used to validate the Chester ROMS-RCA, including salinity, and dissolved oxygen (O_2). The ConMon program consists of placing a YSI (Yellow Springs Incorporated, Inc.) sonde containing multiple sensors one meter off the bottom and attaching it to a structure (i.e., pier). A single sonde and sensor package is deployed for two weeks, sampling water properties (salinity, temperature, and dissolved oxygen) every 15 minutes and is replaced with a calibrated instrument after two weeks to maintain a continuous data stream. I also validated simulated sediment-water fluxes (SONE) of nitrate (NO_3), ammonium (NH_4), phosphate (PO_4), and dissolved oxygen (SOD; sediment oxygen demand) using observations made at several stations

during summer months (June-August) in intact sediment core incubations (W R Boynton et al., 2003, Figure 2.6) in the Chester and Corsica River estuaries.

Nutrient Magnitude Scenarios

I first tested the sensitivity of Chester River hypoxia to changes in the overall magnitude of both nitrate and phosphate loading, where the seasonality of the load was held constant. These model scenarios consisted of increasing and decreasing the nitrogen (NO_{23} , nitrate + nitrite) and phosphorus (PO_4) concentrations in stream discharges for each of the major tributaries modeled (Figure 2.3a). The nitrogen and phosphorus scenarios included multiplying the nutrient concentration by 0.5 and 1.5 times respectively for each of the major tributaries (Figure 2.7), representing a 50% decrease and increase in loading, respectively, for each nutrient. These scenarios were compared to a 'Base' scenario where no changes were made to the nutrient concentrations to assess the impacts of nutrient load on hypoxic volume, chlorophyll-a, and sediment-water nutrient and oxygen fluxes.

I hypothesized that the nutrient load increase will generate a larger hypoxic volume for both the nitrogen and phosphorus scenarios, provided more nutrients are available for phytoplankton growth and subsequent respiration of organic material.

Nutrient Shift Scenarios

I also developed idealized scenarios to represent seasonal shifts in the timing of nutrient concentration within streams to represent potential future changes in the timing of nutrient loading associated with predicted warming, precipitation changes, and agricultural activity (Chang, 2019). Nutrient shift scenarios were applied to the model by shifting the peak nitrogen

(NO₂₃, nitrate + nitrite) concentration earlier in the year for each of the major tributaries modeled. A 10-day running average was applied to the nutrient time-series in each river inflow (Figure 2.8) to smooth the watershed model-derived nutrient concentration data, which were relatively noisy. To avoid generating the artifact of a large pulse in fall nutrients, May 30 (day 150) was used as a reference point and then the NO₂₃ concentration was shifted earlier from that reference point for two scenarios; one with a 14-day earlier shift and one with a 30-day earlier shift (Figure 2.9). The nutrient concentrations after day 150 was held constant within scenarios.

I hypothesized that the nitrogen concentration shift will lead to an earlier peak load, causing a mismatch between highest nutrient concentrations and higher temperature and light periods, thus reducing phytoplankton growth, respiration of organic material, and oxygen depletion.

Dissolved Oxygen at the Chesapeake Bay Boundary Scenario

To test the potential for Chesapeake Bay to force low dissolved oxygen waters into the mouth of the Chester River, I adjusted the dissolved oxygen boundary condition by relieving hypoxic conditions in the lower layers of the water column at the Chesapeake-Chester boundary. This was captured in the model boundary condition file by increasing the dissolved oxygen concentrations in layers 4 through 10 (the deepest layers where hypoxia persisted during the summer) to match those of surface layers. This effectively increased the dissolved oxygen at the Chesapeake Bay boundary of the Chester River model (Figure 2.10).

Results

The hypoxia cycle in the Chester River is characterized by a seasonal volume in deep waters of the central channel that reaches peaks in July, as well as low oxygen conditions in the upper reaches of the larger tributaries (e.g., Corsica River). The most extreme depletions in dissolved oxygen occurred at the mouth of the estuary (i.e. boundary adjacent to Chesapeake Bay), and along the deepest part of the river channel (Figure 2.2a and 2.2b). The phosphorus load scenarios had a larger effect on Chester River hypoxia and organic matter respiration than the nitrogen scenarios. The scenarios that shifted the nitrogen load earlier in the season had the smallest effect on hypoxia, which was nearly undetectable.

Water-column and Sediment Model Validation

Validation of the water column properties generated by the Chester River ROMS-RCA model shows that it represents the salinity and dissolved oxygen patterns well in both the surface and bottom water at CBP stations ET4.1 and ET4.2 (Figure 2.4 and 2.5). The model underestimates some of the seasonal peaks in chlorophyll (by up to 50% in some places) during early spring in surface and bottom waters of the lower estuary (ET4.2) and during mid-summer throughout the water column at the upstream station (ET4.1). Phosphorus concentrations are well-captured by the model at both stations and at all depths, but peak winter inputs of NO_3 were underestimated at both stations throughout the water column. Comparison of modeled sediment-water fluxes at SONE stations CR01 (upstream) and CR19 (downstream) showed that the model was overall more consistent at reproducing SOD (sediment oxygen demand) and PO_4 , NH_4 , and NO_3 fluxes at the downstream station (Figure 2.6). At the upstream station, the model

underrepresented the magnitude of the summer peak in SOD and NH_4 flux, which may be related to the model's underestimation of water column summer chlorophyll-a at this site. Note that sediment-water flux observations were made in the year 2001, while model simulations represent 2003.

Nitrogen Magnitude Scenarios

At the estuary-wide scale, the idealized simulation of increased nitrogen (NO_{23}) concentration and load resulted in a marginally lower annual hypoxic volume ($< 2 \text{ mg O}_2/\text{L}$), while the decrease in nitrogen concentration generated a marginally larger annual hypoxic volume (Figure 2.11). In comparison to the Base (no change) scenario, these changes constituted a decrease of 0.37 km^3 (with NO_{23} increase) and increase of 0.23 km^3 (with NO_{23} decrease) respectively, representing less than a 2% change.

I compared the difference in modeled sediment denitrification (N_2), sediment-water nitrate (NO_3) flux and phosphate (PO_4) flux, and sediment oxygen demand (SOD) at cells representing two CBP stations located in the mainstem of the Chester River: ET4.1 (upstream) and ET4.2 (downstream) (Figure 2.3b). Both stations had similar N_2 and NO_{23} flux responses to changes in NO_{23} concentration, but differed in magnitude. The upstream station (corresponding to ET4.1) had a maximum increase and decrease of approximately $50 \text{ mg N}/\text{m}^2/\text{day}$ during the late summer for the NO_{23} increase and decrease scenarios respectively (Figure 2.12). In contrast, the downstream station (corresponding to ET4.2) had a maximum increase and decrease of approximately $10 \text{ mg N}/\text{m}^2/\text{day}$ during April for the NO_{23} increase and decrease scenarios respectively. The NO_3 flux response is similar in magnitude to the nitrate flux rates at both stations, but the NO_{23} scenarios had the opposite effect, where the decrease in NO_{23} generated an

increase in NO_3 flux (more positive sediment-water NO_{23} fluxes = NO_{23} efflux from sediments), while the NO_{23} load increase generated an increasingly negative NO_{23} flux (i.e., more NO_{23} uptake by sediments). Thus, elevated nitrogen inputs led to higher water column NO_{23} concentrations, higher sediment NO_{23} uptake rates, and higher denitrification. This effect was larger in the upstream, lower salinity regions and the opposite effect occurred in the reduced NO_{23} load simulations.

Phosphorus Magnitude Scenarios

Changes in phosphorus concentration (PO_4) had a larger and opposite effect on hypoxia in comparison to the nitrogen scenarios, where increasing PO_4 lead to an increase in annual hypoxic volume and decreasing PO_4 reduced the annual hypoxic volume at a threshold of 2 mg O_2/L (Figure 2.13). In comparison to the Base (no change) scenario, this was an increase of 0.67 km^3 and decrease of 0.84 km^3 respectively, representing a 5% increase and decrease in hypoxic volume, respectively.

The downstream station (ET4.2) had a smaller response to changes in PO_4 magnitude than the upstream station (ET4.1). Decreasing PO_4 caused an increase in denitrification in the first half of the year (i.e. approximately February to July) before returning to the Base case at both stations (Figure 2.14). The downstream station saw a 1-2% change in PO_4 flux due to the PO_4 increase scenario that was likely due to the increase in phytoplankton growth from more PO_4 available in the water column, and therefore increased deposition of organic phosphorus. Sediment oxygen demand also increased under the elevated PO_4 load scenario.

Nutrient Shift Scenarios

Both nitrogen (NO_{23}) shift scenarios had a small effect on the annual hypoxic volume at all thresholds (5, 2, 0.2 mg O_2/L) in comparison to the idealized Base (no change) scenario. At a threshold of 2 mg O_2/L , the 14-day early scenario generated a slight increase in volume (0.06 km^3) and the 30-day early scenario generated a slightly larger decrease (0.11 km^3) (Figure 2.15).

The 14-day and 30-day early shifts in NO_{23} load had a very similar effects on the biogeochemistry at the downstream station. The denitrification response at the upstream station showed a shift that matched the 14 and 30-day earlier shift in nutrients, where the 30-day early shift occurred before the 14-day shift with an increase in March and subsequent decrease in June (Figure 2.16). The nutrient shift scenarios only affected the upstream station (ET4.1) during the first half of the year, because by July, the denitrification, NO_3 and PO_4 fluxes, and SOD responses returned to the Base case. The downstream station had a relatively smaller response to each of these variables, and a slightly opposite effect in terms of timing for changes in PO_4 flux and SOD response (i.e., remained at Base case until July and then responded to changes in nutrient load timing). At station ET4.1, the PO_4 flux was relatively unchanged, except for a sharp increase of 0.1 and 0.2 mg $\text{P}/\text{m}^2/\text{day}$ in May for the shift 14-day and 30-day early scenarios respectively. This was contrasted by a decrease of 0.2 mg $\text{P}/\text{m}^2/\text{day}$ at the downstream station (ET4.2) in September.

In summary, the responses of seasonal hypoxia in the Chester River estuary to altered nutrient loads (nitrogen and phosphorus) and the timing on nitrogen delivery was apparent, but relatively small compared to the Chesapeake Bay mainstem. Across all dissolved oxygen thresholds there was no change in hypoxia onset day for any scenario (5 mg O_2/L = day 7, 2 mg O_2/L = day 139, 0.2 mg O_2/L = day 161). The estuary appears to be more sensitive to changes in

phosphorus loading than to nitrogen, and it appears that both the upper, low salinity estuary and the lower, more saline estuary appear to respond similarly to changes in nutrient inputs.

Dissolved Oxygen at the Chesapeake Bay Boundary Scenario

Altering the dissolved oxygen at the Chesapeake Bay boundary had a very large effect on the hypoxic volume within the Chester River. By increasing the dissolved oxygen in the sub-surface layers of the boundary domain such that no hypoxic water was externally delivered to the Chester estuary, the total hypoxic volume was decreased by 84% at threshold of 2 mg O₂/L (Figure 2.21). Thus, hypoxia in this estuary appears to be much more sensitive to the Chesapeake Bay boundary condition relative to external inputs of nutrients from the watershed that stimulate internally-generated hypoxia.

Discussion

These idealized model simulations show that the Chester River is sensitive to changes in nutrient inputs, but to a lesser degree than in the Chesapeake Bay and other coastal water bodies. Low sensitivity to nutrient inputs could result from increased turbidity within a shallower, well-mixed system, that is likely light limited for phytoplankton growth and nutrient uptake (Fisher et al., 1992). Total suspended solids (TSS) and Secchi depth indicated more substantial light limited conditions in the upstream station relative to the downstream station, with higher TSS (20-25 mg TSS/L) levels and a smaller Secchi depth (0.2-0.4 m) in the upstream station and TSS of 5-10 mg TSS/L and Secchi depth of 0.5-1.2 m in the lower estuary (www.chesapeakebay.net/data). Modeled light limitation factors (RLGHT) in RCA shows that light is not a limiting factor for either upstream or downstream regions during winter-spring

($RLGHT > 0.9$; Figure 2.22), but that light becomes limiting ($RLGHT < 0.5$) in the upstream, more turbid station (ET4.1, Figure 2.22a) during summer. Light limitation is not a factor limiting phytoplankton growth at the downstream station (ET4.2, Figure 2.22b) during any time of year, consistent with lower TSS and higher Secchi depths. Thus, another factor is likely leading to the insensitivity of phytoplankton growth in response to elevated nutrients.

A second, and more likely cause of low sensitivity to nutrient inputs is the fact that nutrient concentrations are high in the Chester River estuary. The Chester River has high nitrogen and phosphorus concentrations relative to limiting concentrations of 0.07 mg N/L and 0.007 mg P/L used by the Chesapeake Bay Program and higher than the half saturation coefficients in ROMS-RCA (0.01 mg N/L and 0.001 mg P/L). Average NO_{23} and PO_4 concentrations were 0.3 mg N/L and 0.025 mg P/L at CBP stations ET4.1 and ET4.2 (Figure 2.4 and 2.5). Changes in phosphorus were more important in areas where nutrient limitation existed (e.g., station ET4.1, upstream in the estuary). This is consistent with low-salinity waters being more phosphorus limited (Fisher, Peele, Ammerman, & Harding, 1992; Jordan, Cornwell, Boynton, & Anderson, 2008) than more seaward, higher-salinity waters (which do not exist in the Chester estuary). To evaluate the potential for nutrient limitation in the model simulations further, the ratio of phosphorus (PO_4), nitrogen ($NO_{23}+NH_4$), and silica concentrations and their half-saturation coefficients indicated that at both the upstream and downstream stations, none of the above nutrients were limiting within the surface waters, except for phosphorus during a limited period during winter-spring (i.e., values greater than 1, Figure 2.23). This clearly indicates that modest alterations in nutrient loading rates may be expected to have a much more limited impact on phytoplankton growth and hypoxia than the mainstem Chesapeake Bay and other nutrient-limited estuaries.

The altered phosphate (PO_4) loading scenarios had a larger effect on hypoxia in the Chester River estuary than nitrogen (NO_{23}), which is consistent with a more phosphorus limited system. Phosphorus limitation upstream in the Chester River is likely because it is less saline due to the rivers geomorphology (i.e. narrow, shallow, and sinuous), the tidal influence is limited and there is less stratification (Tian, 2019). The relative effect of phosphorus load changes in the Chester River compared to nitrogen is the opposite effect seen in the Bay mainstem (Testa et al., 2014), which could be due to differences in nutrient ratios between the two systems. Higher SOD and PO_4 fluxes under the elevated PO_4 load scenario indicate that additional phosphorus inputs stimulate phytoplankton growth, subsequent decay, and nutrient remineralization in sediments. Denitrification was reduced under the high PO_4 load scenario, which could be due to elevated organic matter (i.e., increased chlorophyll-a, Figure 2.18) causing deoxygenation of sediments (i.e., increased SOD, Figure 2.14) and thus reduced nitrification. Alternatively, this denitrification response could be driven by the increase in phytoplankton growth under elevated PO_4 loading, causing elevated nutrient uptake (i.e., reduction in NO_3 available) in the water column, so less is available for NO_3 flux into sediments to drive denitrification.

Hypoxia was present across the estuary, seasonally in both the deep and shallow waters (i.e., Corsica River). Hypoxic volumes have not been previously computed for the Chester River estuary, and these simulations suggest that volumes of 0.1-1 km^3 are an order of magnitude smaller than mainstem Bay hypoxic volumes (2-15 km^3). Considerable hypoxia was found in the lower Chester River estuary, which indicates that low oxygen waters encroaching from the adjacent Chesapeake Bay can move into the lower portion of the Chester River. While the model also reproduced some hypoxia in shallow areas, it did not fully capture the high frequency, diel-cycling hypoxia that has been observed in, for example, the Corsica River estuary at the

Sycamore Point ConMon station (Figure 2.20a). Clearly, there are high-frequency variations at Sycamore Point in the model that exceed those at ET4.2 (Figure 2.20b), but these variations are not as large as the 10-15 mg O₂/L diurnal variations observed during summer (Walter R Boynton et al., 2009). Future work should more fully address how the model doesn't currently represent diel hypoxia cycling, which may be because the spatial resolution is not large enough to adequately capture the small scale hydrodynamics or because the phytoplankton physiology formulation is insufficient.

While elevated NO₂₃ inputs had a minimal, and perhaps opposite effect than hypothesized on hypoxia, this simulation generated an increase in denitrification which corresponded to the increase of NO₃ flux into the sediment across the estuary. This effect of NO₃ limitation on denitrification has been shown in previous studies, and that by adding more NO₃ supplies fuel for direct denitrification (Cornwell, Kemp, & Kana, 1999). A proportional contrast was seen when NO₂₃ inputs were reduced, as there was a reduction in the NO₂₃ flux into the sediments, and a reduction in denitrification.

Nitrogen load timing had a minimal effect on the phenology of the Chester River. Due to the result of PO₄ magnitude having a more substantial effect, future work could consider looking at the timing of changes in phosphorus. This could be important under a changing climate as larger precipitation events, leading to higher stormflows, would generate changes in phosphorus delivery to the estuary from river inputs. Larger flow volumes and velocities could increase erosion rates and the transportation of larger amounts of sediment, which is a concern for the mobilization of phosphorus that has sorbed to the sediment particles. Correll et al. (1999) showed an increase of up to 3 orders of magnitude in particulate organic nitrogen and phosphorus, and inorganic phosphorus during storm events.

Conclusion and Future Recommendations

While there has been increasing interest in using phenology as a metric for identifying and quantifying changes in complex coastal systems (Cloern & Jassby, 2008; Du & Shen, 2014; Nixon et al., 2009), and some studies have modeled or analyzed through data how interannual variability of climate impacts hypoxia (Li et al., 2016; Testa, Murphy, et al., 2018), this thesis represents a rare application of numerical models to specifically address phenological changes in estuarine biogeochemistry in response to altered seasonality of external forcing. Modeling work in shallow, sub-estuary systems like the Chester River is important because the phenological response is different from that of larger scale systems like the Chesapeake Bay, and ultimately both systems interact to influence the biogeochemical cycling of the other. Applying fine temporal and spatial scale models on the margins of the Chesapeake Bay mainstem is useful for better understanding processes that affect loading of nutrients and organic matter into the larger system.

While the Chester River ROMS-RCA model captures larger seasonal patterns of hypoxia, it didn't capture the diel-cycling of hypoxia seen at monitoring stations in the shallow areas (i.e. Sycamore Point). Future work could begin to address this by looking at phytoplankton physiology and response (chlorophyll-a) in nutrient rich waters, and improving how the model estimates the seasonal cycling of chlorophyll-a across the estuary. Light limitation or other physical drivers may be stronger controlling factors for phytoplankton dynamics in highly eutrophic systems.

This study only considered one year (2003, hydrologically moderately wet), thus to test the interannual effects of systems like the Chester River, future work should include more

hydrologic years (i.e. very wet and dry). This could be especially important in an agriculturally dominated watershed such as this, to understanding phenological shifts in linkages between the watershed-estuary continuum due to expected changes in farmer response (irrigation, fertilization, and crop types) to climate change (Chang, 2019). Simulations showed that changes in PO_4 loading had more influence on Chester River hypoxia, than the NO_{23} scenarios (increase/decrease in load and early shift in load timing), thus future work could include simulations in shifts of the timing of PO_4 load. Such simulations could inform an understanding of how the release of dissolved phosphorus (legacy phosphorus) from oversaturated, hydrologically connected, agricultural soils may be impacting estuary water quality (Kleinman, 2017).

Finally, the idealized simulations presented in this chapter could be built upon by running linked, concurrent simulations of altered watershed discharge, biogeochemistry, and agricultural practices as they impact the magnitude and timing of estuarine biogeochemistry. While the coupling of models has been applied on a larger scale to the Chesapeake Bay region for the purpose of establishing TMDL reduction goals (Lewis C. Linker, Shenk, Wang, Hopkins, & Pokharel, 2012), smaller scale coupled-simulations would be useful for evaluating the sub-watershed effects of agriculture conservation practices (Wagena & Easton, 2018), farmer adaptations to climate change (Chang, 2019; Huttunen et al., 2015), and watershed restoration practices that influence sediment load (Palinkas, 2013).

References

- Beegle, D. (2013). Nutrient Management and the Chesapeake Bay. *Journal of Contemporary Water Research & Education*, 151(1), 3–8. <https://doi.org/10.1111/j.1936-704x.2013.03146.x>
- Boesch, D. F. (1996). Science and management in four U.S. coastal ecosystems dominated by land-ocean interactions. *Journal of Coastal Conservation*, 2(2), 103–114. <https://doi.org/10.1007/BF02905196>
- Bouraoui, F., & Grizzetti, B. (2011). Long term change of nutrient concentrations of rivers discharging in European seas. *Science of the Total Environment*, 409(23), 4899–4916. <https://doi.org/10.1016/j.scitotenv.2011.08.015>
- Boynton, W R, Frank, J. M., Rohland, F. M., Stankelis, R. M., Lawrence, J. M., Bean, B., & Pine, H. (2003). Monitoring of sediment oxygen and nutrient exchanges in the Chester River estuary in support of TMDL development. In *UMCES Technical Report Series TS-400-03-CB*.
- Boynton, Walter R, Testa, J. M., & Kemp, W. M. (2009). *An Ecological Assessment of the Corsica River Estuary and Watershed Scientific Advice for Future Water Quality Management*. 1–54.
- Brakebill, J. W., Preston, S. D., & Martucci, S. K. (2004). *Digital Data Used to Relate Nutrient Inputs to Water Quality in the Chesapeake Bay Watershed, Version 2.0*.
- Breitburg, D. (2002). Effects of hypoxia, and the balance between hypoxia and enrichment, on coastal fishes and fisheries. *Estuaries*, 25(4 B), 767–781. <https://doi.org/10.1007/BF02804904>
- Chang, S. (2019). *Effects of seasonal and long-term climate variability on nitrate export in the Chesterville Branch catchment of the Eastern Shore, MD*. Johns Hopkins University.
- Chesapeake Bay Program. (n.d.). No Title. Retrieved from <https://www.chesapeakebay.net/issues/agriculture>
- Chesapeake Bay Program. (2011). Agriculture in the Chesapeake Bay Watershed. *Backgrounder*, 0–1. Retrieved from http://www.chesapeakebay.net/documents/5376/agriculture_background-er-final.pdf
- Cloern, J. E., & Jassby, A. D. (2008). Complex seasonal patterns of primary producers at the land-sea interface. *Ecology Letters*, 11(12), 1294–1303. <https://doi.org/10.1111/j.1461-0248.2008.01244.x>
- Cornwell, J. C., Kemp, W. M., & Kana, T. M. (1999). Denitrification in coastal ecosystems:

- Methods, environmental controls, and ecosystem level controls, a review. *Aquatic Ecology*, 33(1), 41–54. <https://doi.org/10.1023/A:1009921414151>
- Correll, D. L., Jordan, T. E., & Weller, D. E. (1999). Transport of nitrogen and phosphorus from Rhode River watersheds during storm events. *Water Resources Research*, 35(8), 2513–2521. <https://doi.org/10.1029/1999WR900058>
- Diaz, R. J., & Rosenberg, R. (2008). Spreading dead zones and consequences for marine ecosystems. *Science*, 321(5891), 926–929. <https://doi.org/10.1126/science.1156401>
- Ding, H., & Elmore, A. J. (2015). Spatio-temporal patterns in water surface temperature from Landsat time series data in the Chesapeake Bay, U.S.A. *Remote Sensing of Environment*, 168, 335–348. <https://doi.org/10.1016/j.rse.2015.07.009>
- Du, J., & Shen, J. (2014). Decoupling the influence of biological and physical processes on the dissolved oxygen in the Chesapeake Bay. *Journal of Geophysical Research: Oceans*, 119, 2183–2200. <https://doi.org/10.1002/2013JC009443>
- Elmore, A. J., Nelson, D. M., & Craine, J. M. (2016). Earlier springs are causing reduced nitrogen availability in North American eastern deciduous forests. *Nature Plants*, 2(10), 1–5. <https://doi.org/10.1038/nplants.2016.133>
- Eshleman, K. N., Sabo, R. D., & Kline, K. M. (2013). Surface water quality is improving due to declining atmospheric N deposition. *Environmental Science and Technology*, 47(21), 12193–12200. <https://doi.org/10.1021/es4028748>
- Fisher, T. R., Peele, E. R., Ammerman, J. W., & Harding, L. W. (1992). Nutrient limitation of phytoplankton in Chesapeake Bay. *Marine Ecology Progress Series*, 82(1), 51–63. <https://doi.org/10.3354/meps082051>
- Goetz, S. J., Jantz, C. A., Prince, S. D., Smith, A. J., Varlyguin, D., & Wright, R. K. (2004). Integrated analysis of ecosystem interactions with land use change: The Chesapeake bay watershed. *Geophysical Monograph Series*, 153(June 2014), 263–275. <https://doi.org/10.1029/153GM20>
- Hagy, J. D., Boynton, W. R., Keefe, C. W., & Wood, K. V. (2004). Hypoxia in Chesapeake Bay, 1950–2001: Long-term change in relation to nutrient loading and river flow. *Estuaries*, 27(4), 634–658. <https://doi.org/10.1007/BF02907650>
- Huttunen, I., Lehtonen, H., Huttunen, M., Piirainen, V., Korppoo, M., Veijalainen, N., ... Vehviläinen, B. (2015). Effects of climate change and agricultural adaptation on nutrient loading from Finnish catchments to the Baltic Sea. *Science of the Total Environment*, 529, 168–181. <https://doi.org/10.1016/j.scitotenv.2015.05.055>
- Irby, I. D., Friedrichs, M. A. M., Da, F., & Hinson, K. E. (2018). The competing impacts of climate change and nutrient reductions on dissolved oxygen in Chesapeake Bay.

- Biogeosciences*, 15(9), 2649–2668. <https://doi.org/10.5194/bg-15-2649-2018>
- Jordan, T. E., Cornwell, J. C., Boynton, W. R., & Anderson, J. T. (2008). Changes in phosphorus biogeochemistry along an estuarine salinity gradient: The iron conveyor belt. *Limnology and Oceanography*, 53(1), 172–184. <https://doi.org/10.4319/lo.2008.53.1.0172>
- Kleinman, P. J. A. (2017). The Persistent Environmental Relevance of Soil Phosphorus Sorption Saturation. *Current Pollution Reports*, 3(2), 141–150. <https://doi.org/10.1007/s40726-017-0058-4>
- Kraus, R. T., Secor, D. H., & Wingate, R. L. (2015). Testing the thermal-niche oxygen-squeeze hypothesis for estuarine striped bass. *Environmental Biology of Fishes*, 98(10), 2083–2092. <https://doi.org/10.1007/s10641-015-0431-3>
- Kronvang, B., Jeppesen, E., Conley, D. J., Søndergaard, M., Larsen, S. E., Ovesen, N. B., & Carstensen, J. (2005). Nutrient pressures and ecological responses to nutrient loading reductions in Danish streams, lakes and coastal waters. *Journal of Hydrology*, 304(1–4), 274–288. <https://doi.org/10.1016/j.jhydrol.2004.07.035>
- Lee, M., Shevliakova, E., Malyshev, S., Milly, P. C. D., & Jaffé, P. R. (2016). Climate variability and extremes, interacting with nitrogen storage, amplify eutrophication risk. *Geophysical Research Letters*, 43(14), 7520–7528. <https://doi.org/10.1002/2016GL069254>
- Lefcheck, J. S., Orth, R. J., Dennison, W. C., Wilcox, D. J., Murphy, R. R., Keisman, J., ... Batiuk, R. A. (2018). Long-term nutrient reductions lead to the unprecedented recovery of a temperate coastal region. *Proceedings of the National Academy of Sciences of the United States of America*, 115(14), 3658–3662. <https://doi.org/10.1073/pnas.1715798115>
- Li, M., Lee, Y. J., Testa, J. M., Li, Y., Ni, W., Kemp, W. M., & Di Toro, D. M. (2016). What drives interannual variability of hypoxia in Chesapeake Bay: Climate forcing versus nutrient loading? *Geophysical Research Letters*, 43(5), 2127–2134. <https://doi.org/10.1002/2015GL067334>
- Linker, L C, Batiuk, R. A., Shenk, G. W., & Cerco, C. F. (2013). Development of the Chesapeake Bay watershed total maximum daily load allocation. *Journal of the American Water Resources Association*, 49(5), 986–1006. Retrieved from <http://onlinelibrary.wiley.com/doi/10.1111/jawr.12105/abstract>
- Linker, Lewis C., Shenk, G. W., Wang, P., Hopkins, K. J., & Pokharel, S. (2012). a Short History of Chesapeake Bay Modeling and the Next Generation of Watershed and Estuarine Models. *Proceedings of the Water Environment Federation*, 2002(2), 569–582. <https://doi.org/10.2175/193864702785665021>
- Maryland Department of Natural Resources. (2019). Eyes on the Bay. Retrieved from Eyes on the Bay website: www.eyesonthebay.net

- Moore, W. S. (1999). The subterranean estuary: A reaction zone of ground water and sea water. *Marine Chemistry*, 65(1–2), 111–125. [https://doi.org/10.1016/S0304-4203\(99\)00014-6](https://doi.org/10.1016/S0304-4203(99)00014-6)
- Murphy, R. R., Kemp, W. M., & Ball, W. P. (2011). Long-Term Trends in Chesapeake Bay Seasonal Hypoxia, Stratification, and Nutrient Loading. *Estuaries and Coasts*, 34(6), 1293–1309. <https://doi.org/10.1007/s12237-011-9413-7>
- Nixon, S. W., Fulweiler, R. W., Buckley, B. A., Granger, S. L., Nowicki, B. L., & Henry, K. M. (2009). The impact of changing climate on phenology, productivity, and benthic-pelagic coupling in Narragansett Bay. *Estuarine, Coastal and Shelf Science*, 82(1), 1–18. <https://doi.org/10.1016/j.ecss.2008.12.016>
- Palinkas, C. M. (2013). Seasonal and interannual patterns of sedimentation in the corsica river (MD): Evaluating the potential influence of watershed restoration. *Estuarine, Coastal and Shelf Science*, 127, 37–45. <https://doi.org/10.1016/j.ecss.2013.04.015>
- Preusch, P. L., Adler, P. R., Sikora, L. J., & Tworkoski, T. J. (2002). Waste management: Nitrogen and phosphorus availability in composted and uncomposted poultry litter. *Journal of Environmental Quality*, Vol. 31, pp. 2051–2057. <https://doi.org/10.2134/jeq2002.2051>
- Sampou, P., & Kemp, W. M. (1994). Factors regulating plankton community respiration in Chesapeake Bay. *Marine Ecology Progress Series*, 110(2–3), 249–258. <https://doi.org/10.3354/meps110249>
- Sanford, L. P., & Boicourt, W. C. (1990). Wind-forced salt intrusion into a tributary estuary. *Journal of Geophysical Research: Oceans*, 95(C8), 13357–13371. <https://doi.org/10.1029/JC095iC08p13357>
- Sanford, W. E., & Pope, J. P. (2013). Quantifying groundwater’s role in delaying improvements to Chesapeake Bay water quality. *Environmental Science and Technology*, 47(23), 13330–13338. <https://doi.org/10.1021/es401334k>
- Schubel, J. R., & Pritchard, D. W. (2006). Responses of Upper Chesapeake Bay to Variations in Discharge of the Susquehanna River. *Estuaries*, 9(4), 236. <https://doi.org/10.2307/1352096>
- Scully, M. E. (2010). The importance of climate variability to wind-driven modulation of hypoxia in Chesapeake Bay. *Journal of Physical Oceanography*, 40(6), 1435–1440. <https://doi.org/10.1175/2010JPO4321.1>
- Shanks, K. (2001). *Middle Chester River Watershed Characterization*. (April), 90.
- Shen, C., Testa, J. M., Li, M., Cai, W. J., Waldbusser, G. G., Ni, W., ... Su, J. (2019). Controls on Carbonate System Dynamics in a Coastal Plain Estuary: A Modeling Study. *Journal of Geophysical Research: Biogeosciences*, 124(1), 61–78. <https://doi.org/10.1029/2018JG004802>

- Testa, J. M., Brady, D. C., Di Toro, D. M., Boynton, W. R., Cornwell, J. C., & Kemp, W. M. (2013). Sediment flux modeling: Simulating nitrogen, phosphorus, and silica cycles. *Estuarine, Coastal and Shelf Science*, 131(July), 245–263. <https://doi.org/10.1016/j.ecss.2013.06.014>
- Testa, J. M., & Kemp, W. M. (2014). Spatial and Temporal Patterns of Winter–Spring Oxygen Depletion in Chesapeake Bay Bottom Water. *Estuaries and Coasts*, 37(6), 1432–1448. <https://doi.org/10.1007/s12237-014-9775-8>
- Testa, J. M., Kemp, W. M., & Boynton, W. R. (2018). Season-specific trends and linkages of nitrogen and oxygen cycles in Chesapeake Bay. *Limnology and Oceanography*, 63(5), 2045–2064. <https://doi.org/10.1002/lno.10823>
- Testa, J. M., Kemp, W. M., Boynton, W. R., & Hagy, J. D. (2008). Long-term changes in water quality and productivity in the Patuxent River estuary: 1985 to 2003. *Estuaries and Coasts*, 31(6), 1021–1037. <https://doi.org/10.1007/s12237-008-9095-y>
- Testa, J. M., Li, Y., Lee, Y. J., Li, M., Brady, D. C., Di Toro, D. M., ... Fitzpatrick, J. J. (2014). Quantifying the effects of nutrient loading on dissolved O₂ cycling and hypoxia in Chesapeake Bay using a coupled hydrodynamic-biogeochemical model. *Journal of Marine Systems*, 139(2014), 139–158. <https://doi.org/10.1016/j.jmarsys.2014.05.018>
- Testa, J. M., Murphy, R. R., Brady, D. C., & Kemp, W. M. (2018). Nutrient- and Climate-Induced Shifts in the Phenology of Linked Biogeochemical Cycles in a Temperate Estuary. *Frontiers in Marine Science*, 5(April), 1–15. <https://doi.org/10.3389/fmars.2018.00114>
- Tian, R. (2019). Factors controlling saltwater intrusion across multi-time scales in estuaries, Chester River, Chesapeake Bay. *Estuarine, Coastal and Shelf Science*, 223(April), 61–73. <https://doi.org/10.1016/j.ecss.2019.04.041>
- Toseland, A., Daines, S. J., Clark, J. R., Kirkham, A., Strauss, J., Uhlig, C., ... Mock, T. (2013). The impact of temperature on marine phytoplankton resource allocation and metabolism. *Nature Climate Change*, 3(11), 979–984. <https://doi.org/10.1038/nclimate1989>
- Tyler, R. M., Brady, D. C., & Targett, T. E. (2009). Temporal and spatial dynamics of diel-cycling hypoxia in estuarine tributaries. *Estuaries and Coasts*, 32(1), 123–145. <https://doi.org/10.1007/s12237-008-9108-x>
- U.S. Department of Agriculture. (2010). Field Crops Usual Planting and Harvesting Dates. *Agricultural Handbook*, (628), 41. Retrieved from <http://usda01.library.cornell.edu/usda/current/planting/planting-10-29-2010.pdf>
- USDA-NASS. (2012). *2012 Census of Agriculture - State Data*. 464–496.
- Valiela, I., Foreman, K., LaMontagne, M., Hersh, D., Costa, J., Peckol, P., ... Lajtha, K. (1992). Couplings of watersheds and coastal waters: Sources and consequences of nutrient

enrichment in Waquoit Bay, Massachusetts. *Estuaries*, 15(4), 443–457.
<https://doi.org/10.2307/1352389>

Wagena, M. B., & Easton, Z. M. (2018). Agricultural conservation practices can help mitigate the impact of climate change. *Science of the Total Environment*, 635, 132–143.
<https://doi.org/10.1016/j.scitotenv.2018.04.110>

Yvon-Durocher, G., Jones, J. I., Trimmer, M., Woodward, G., & Montoya, J. M. (2010). Warming alters the metabolic balance of ecosystems. *Philosophical Transactions of the Royal Society B: Biological Sciences*, 365(1549), 2117–2126.
<https://doi.org/10.1098/rstb.2010.0038>

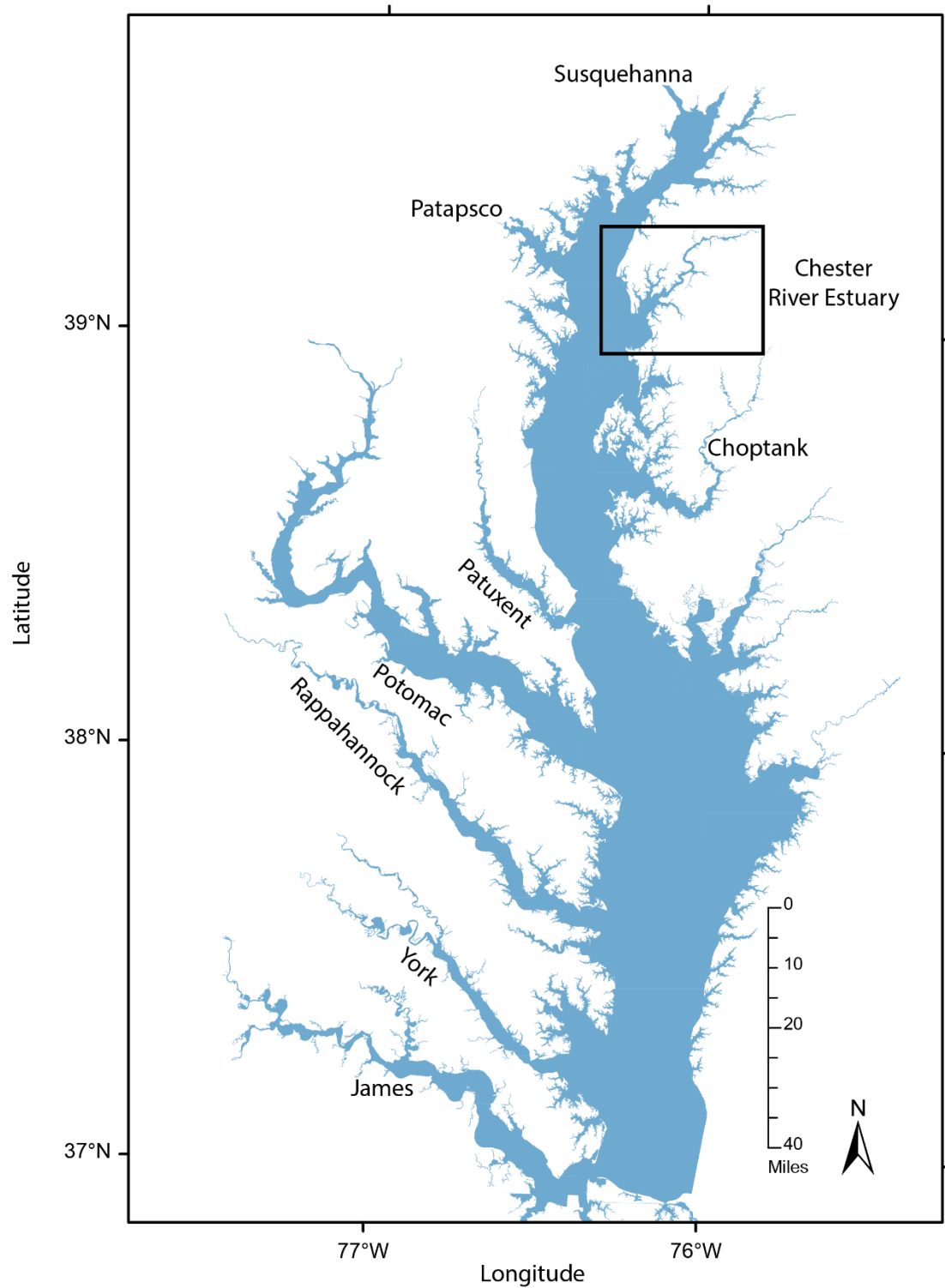


Figure 2.1. Location of Chester River Estuary on the northeastern shore of the Chesapeake Bay.

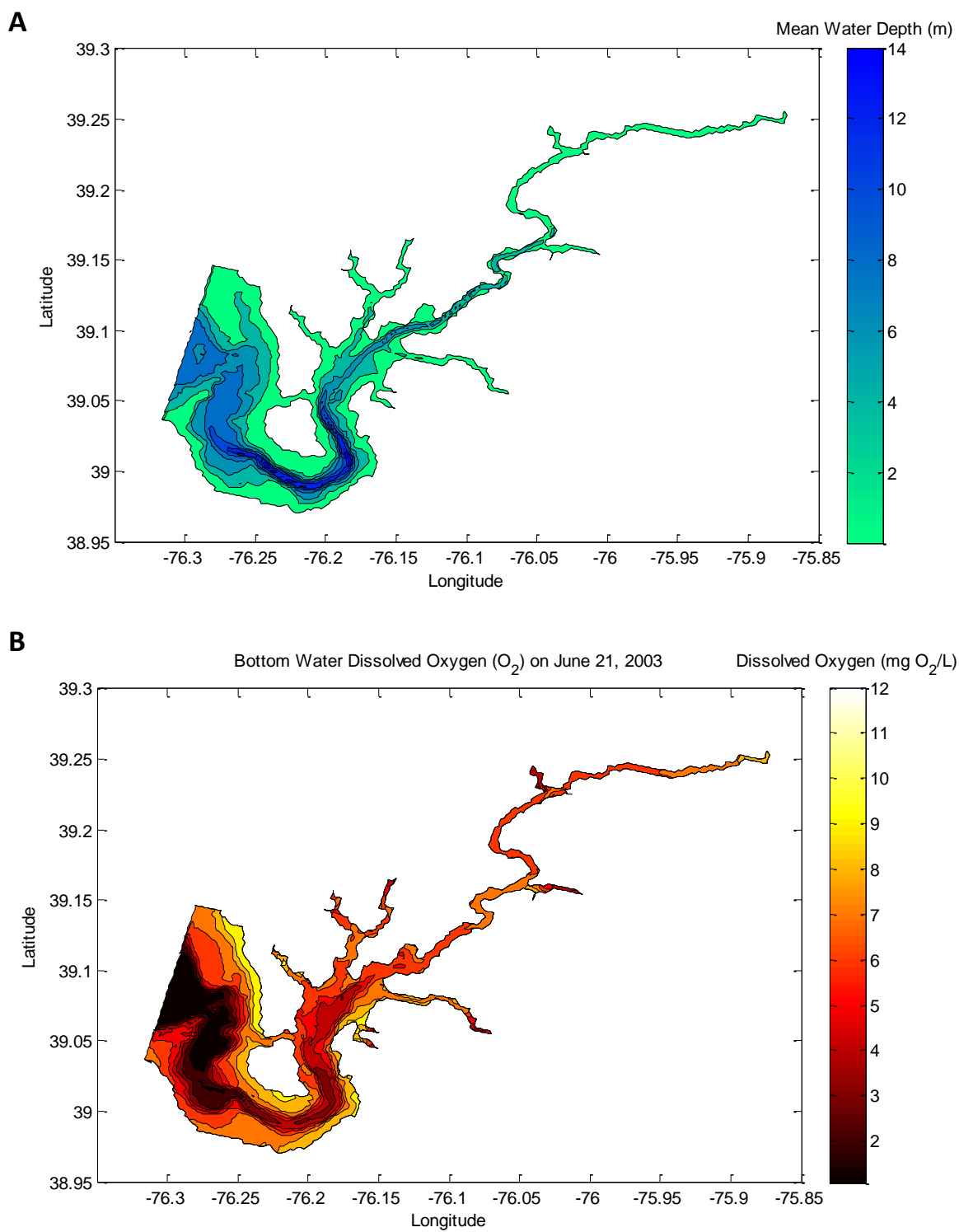


Figure 2.2. (a) Bathymetry (mean water depth, meters) of the Chester River Estuary. (b) Estuary-wide map of modeled bottom-water dissolved oxygen (O_2) in late June.

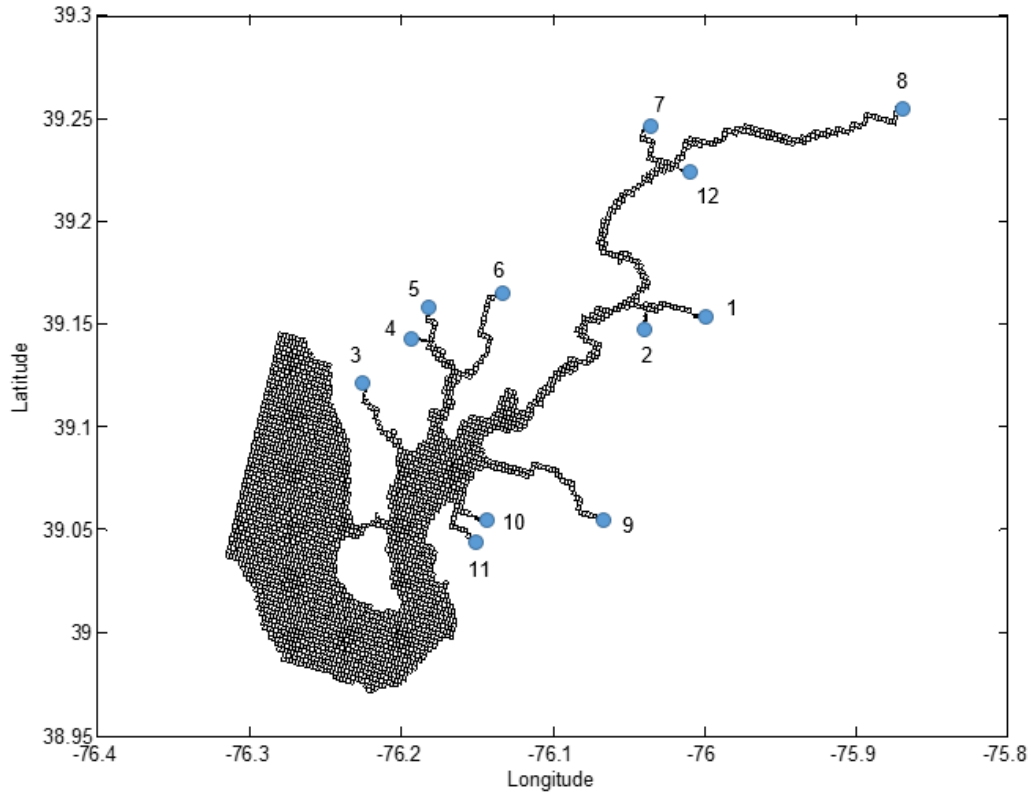
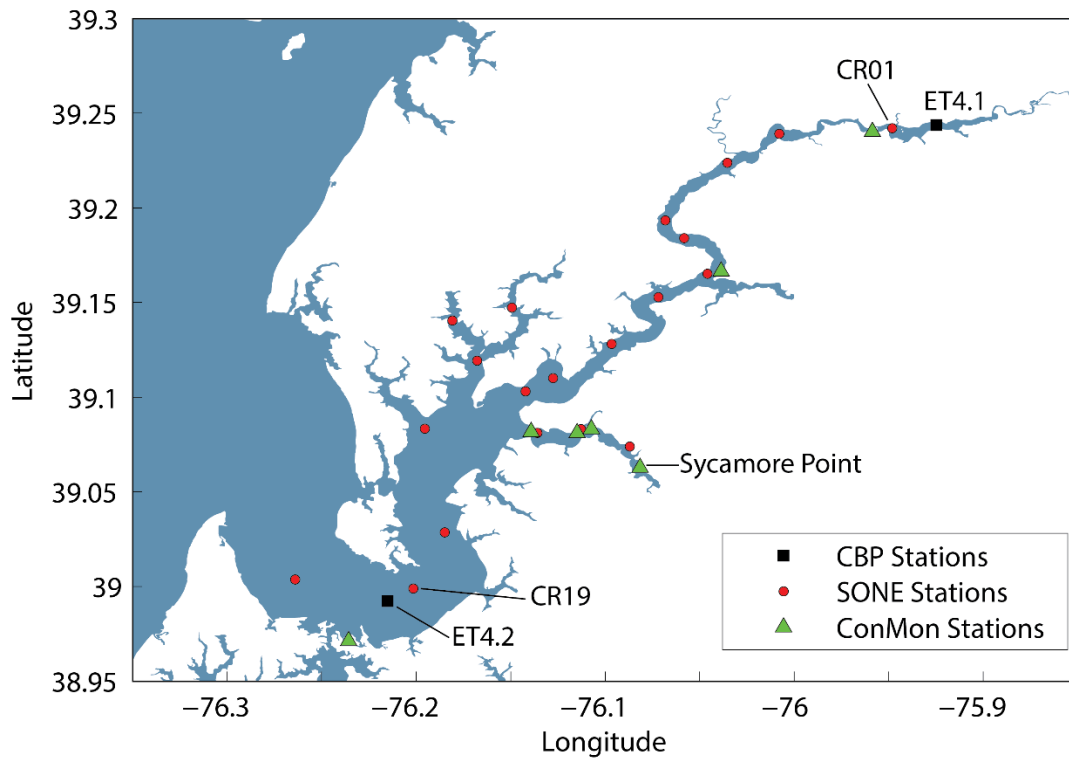
A**B**

Figure 2.3. (a) Chester River Estuary model grid (water cells only) with location of freshwater inputs. (b) Sediment-water flux (SONE) stations used in model validation (red, CR01 and CR19) and Chesapeake Bay Program (CBP) long-term water quality monitoring stations (black, ET4.1 and ET4.2) used in the model validation and simulation analysis.

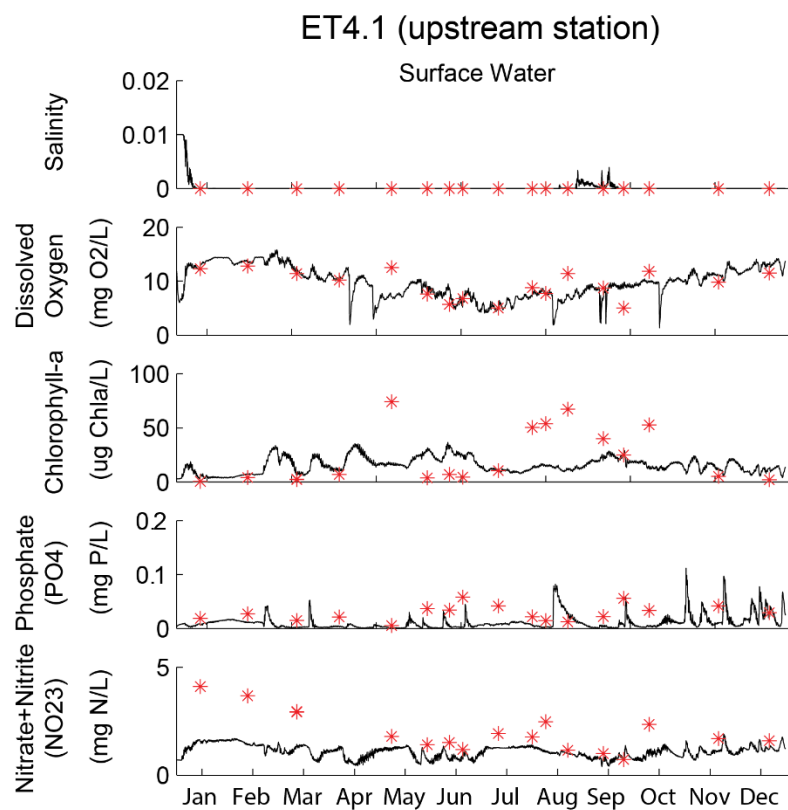
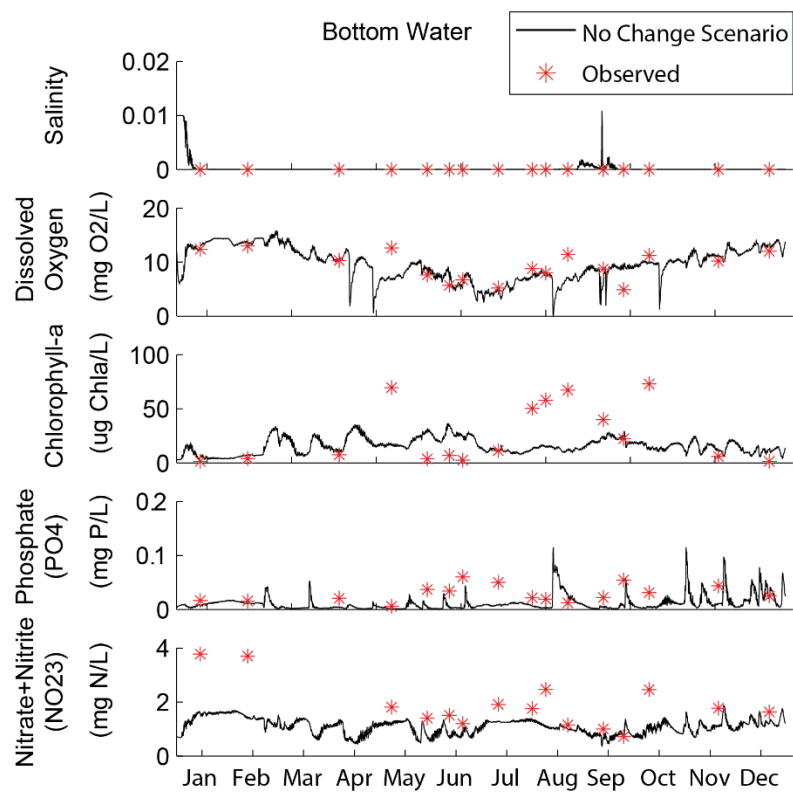
A**B**

Figure 2.4. Comparison of water column (a) surface and (b) bottom-water observation data at CBP station ET4.1 (Figure 2.3b) and the no change model scenario model output.

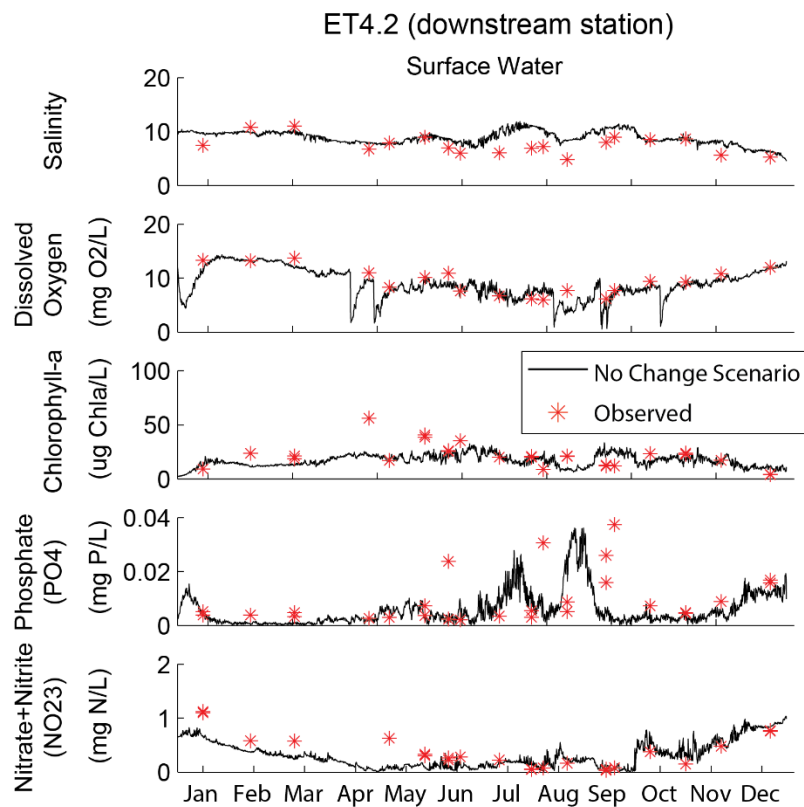
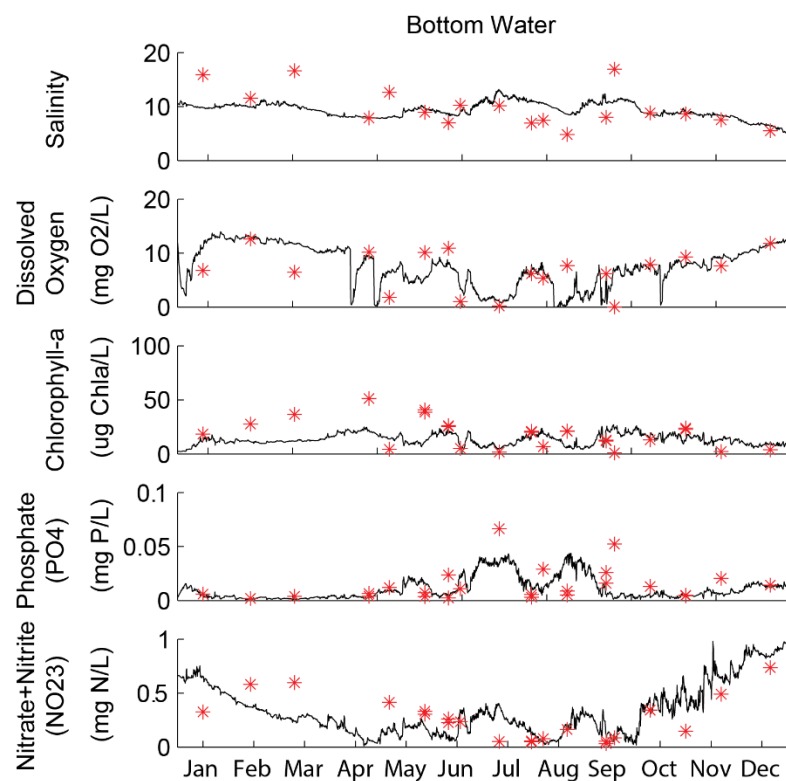
A**B**

Figure 2.5. Comparison of water column (a) surface and (b) bottom-water observation data at CBP station ET4.2 (Figure 2.3b) and the no change scenario model output.

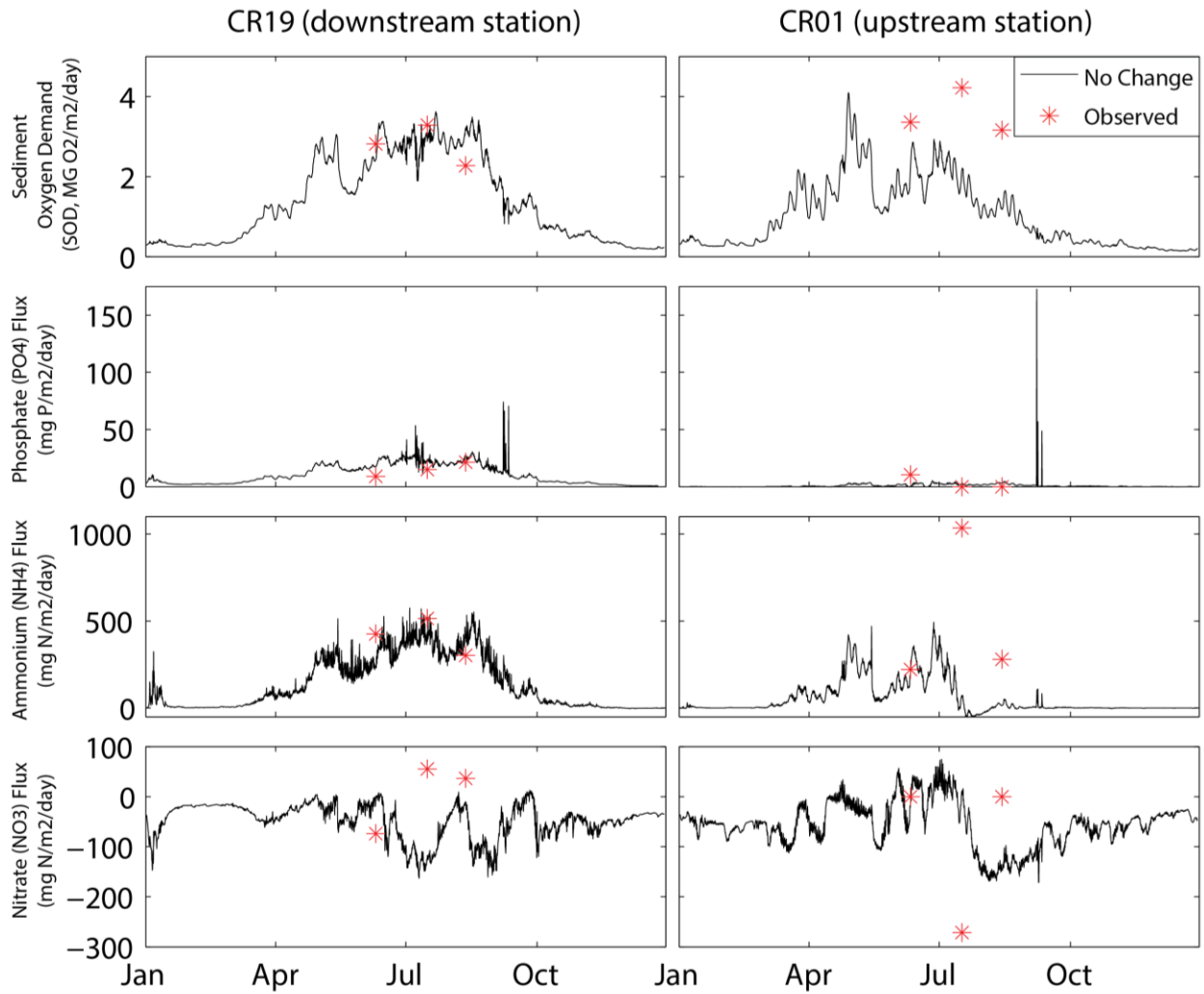


Figure 2.6. Comparison of observed sediment-water fluxes at SONE stations CR01 and CR19 (Figure 2.3b) and the no change scenario model output.

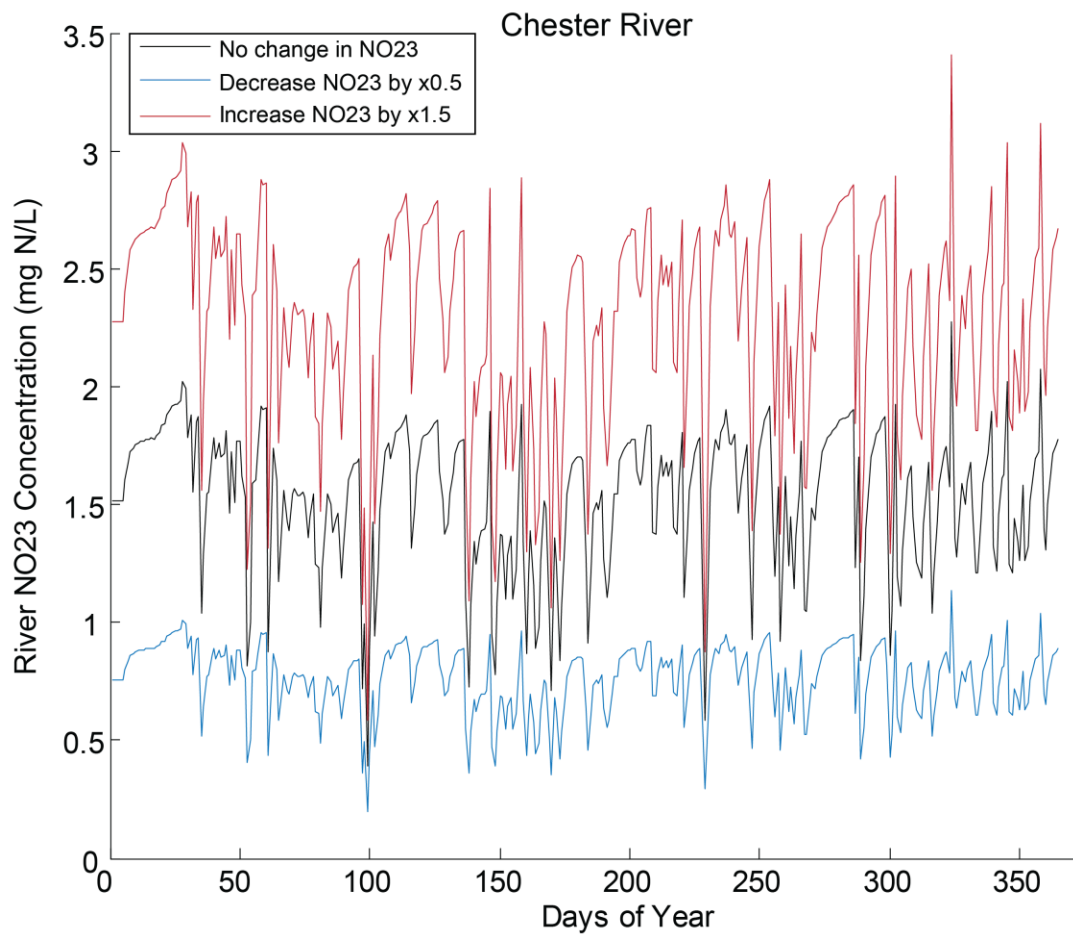


Figure 2.7. Example of nitrogen (NO₂₃) concentration increase and decrease scenarios setup for one Chester River estuary tributary. This process was repeated for the phosphorus (PO₄) concentration increase and decrease scenarios.

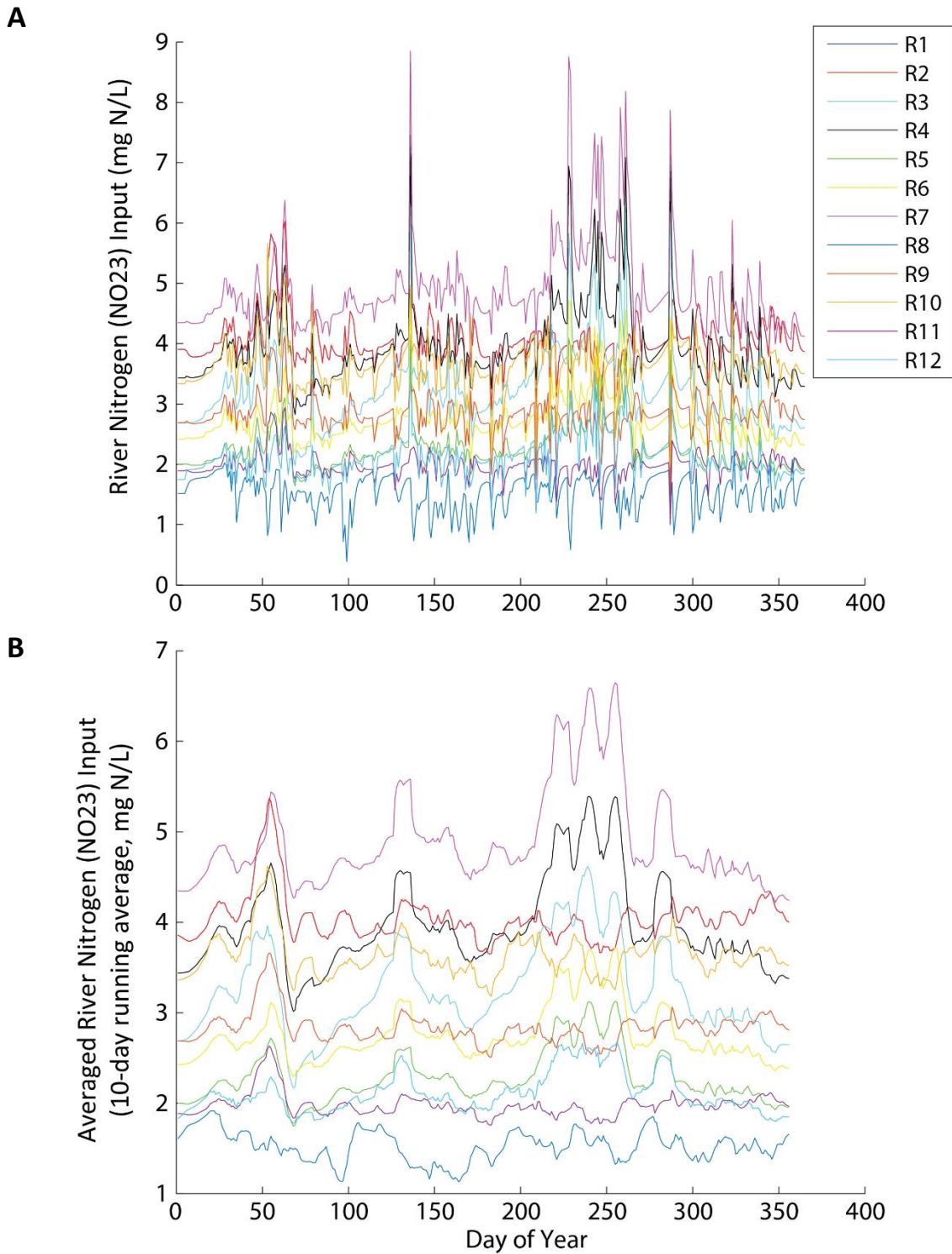


Figure 2.8. (a) Original nitrogen concentration in the 12 boundary rivers in the Chester River estuary. (b) 10-day running average of river NO₂₃ inputs used for nutrient shift scenarios. The location of river inputs to model grid can be found in Figure 2.3a.

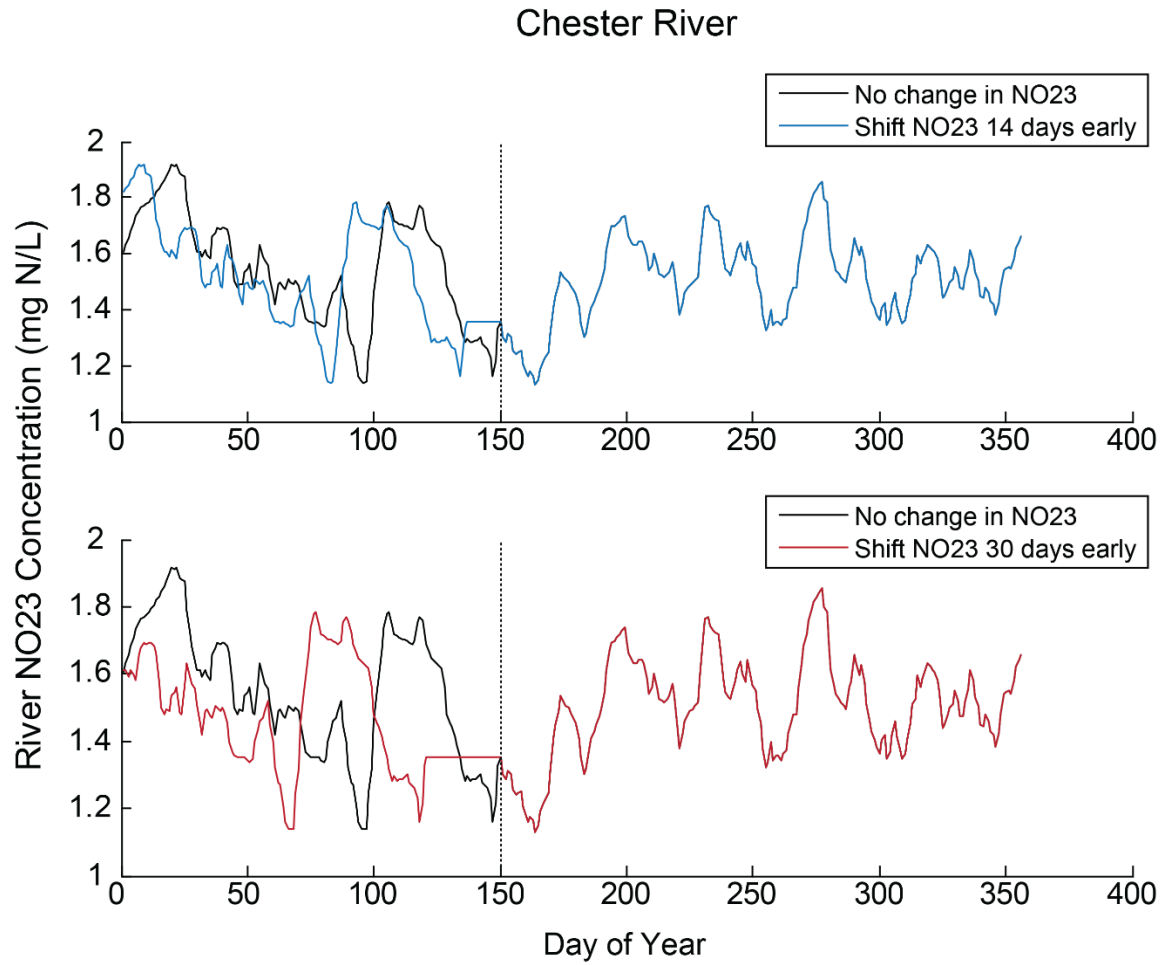


Figure 2.9. Example of shifts in tributary nitrogen concentration by 14 days (top) and 30 days (bottom). Day 150 was used as a reference point (dashed line).

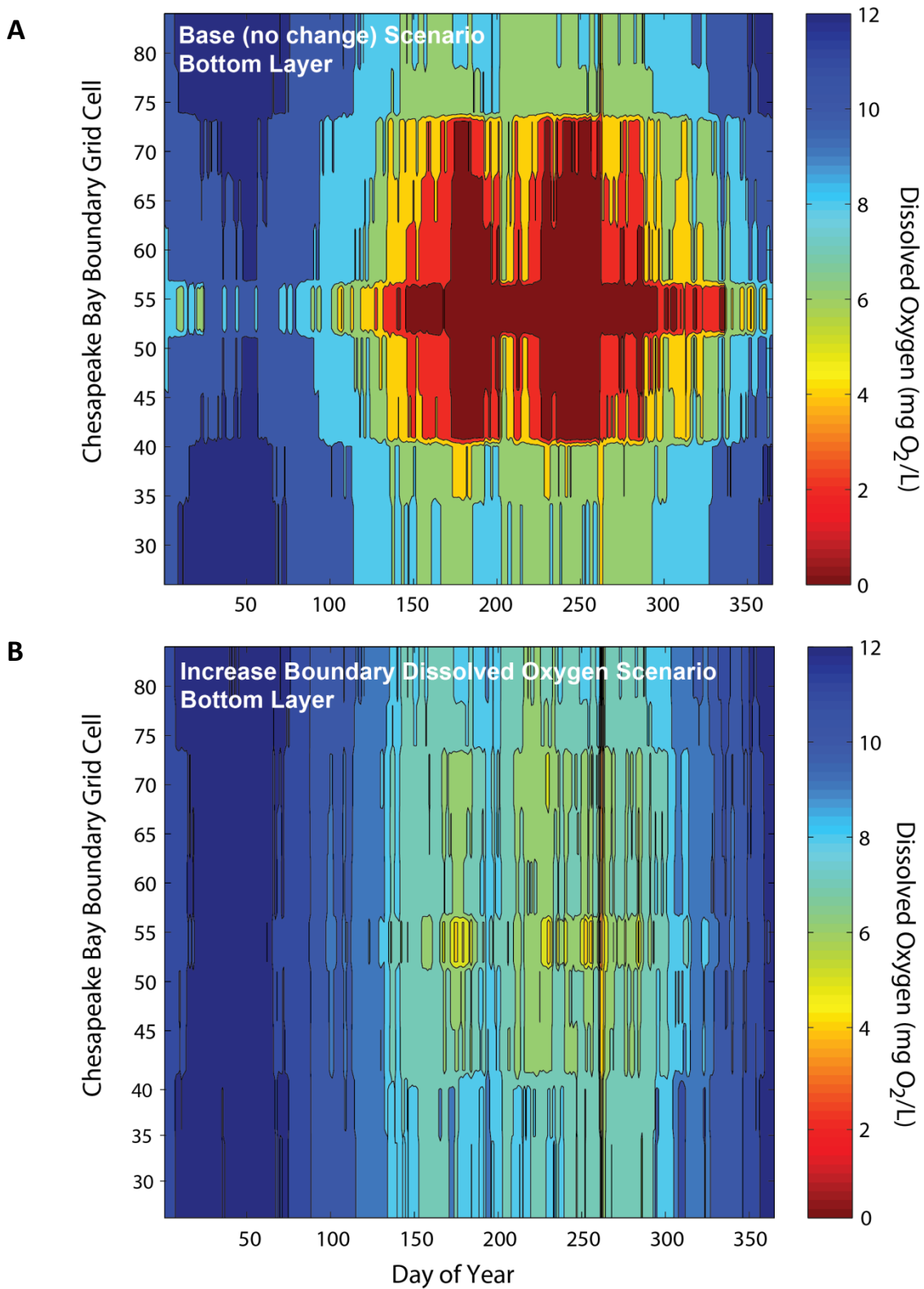


Figure 2.10. Example of bottom water layer of Chester model comparison between the (a) Base (no change) scenario and (b) setup of scenario for increased dissolved oxygen in the lower layers of the boundary condition.

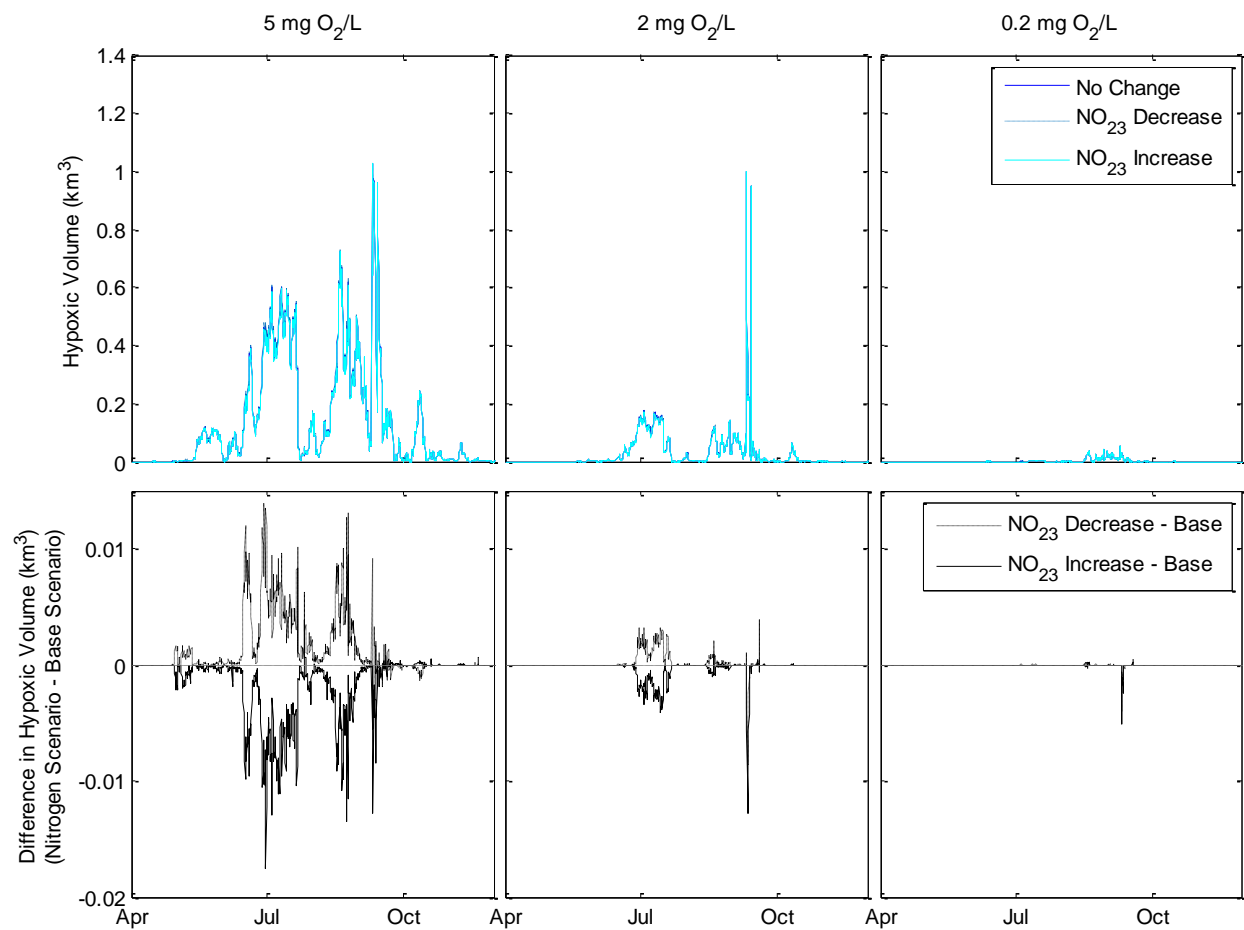


Figure 2.11. Comparison of the hypoxic volume (top) of NO₂₃ nutrient increase and decrease scenarios to the Base (no change) scenario and the difference between them (bottom) at different dissolved oxygen thresholds.

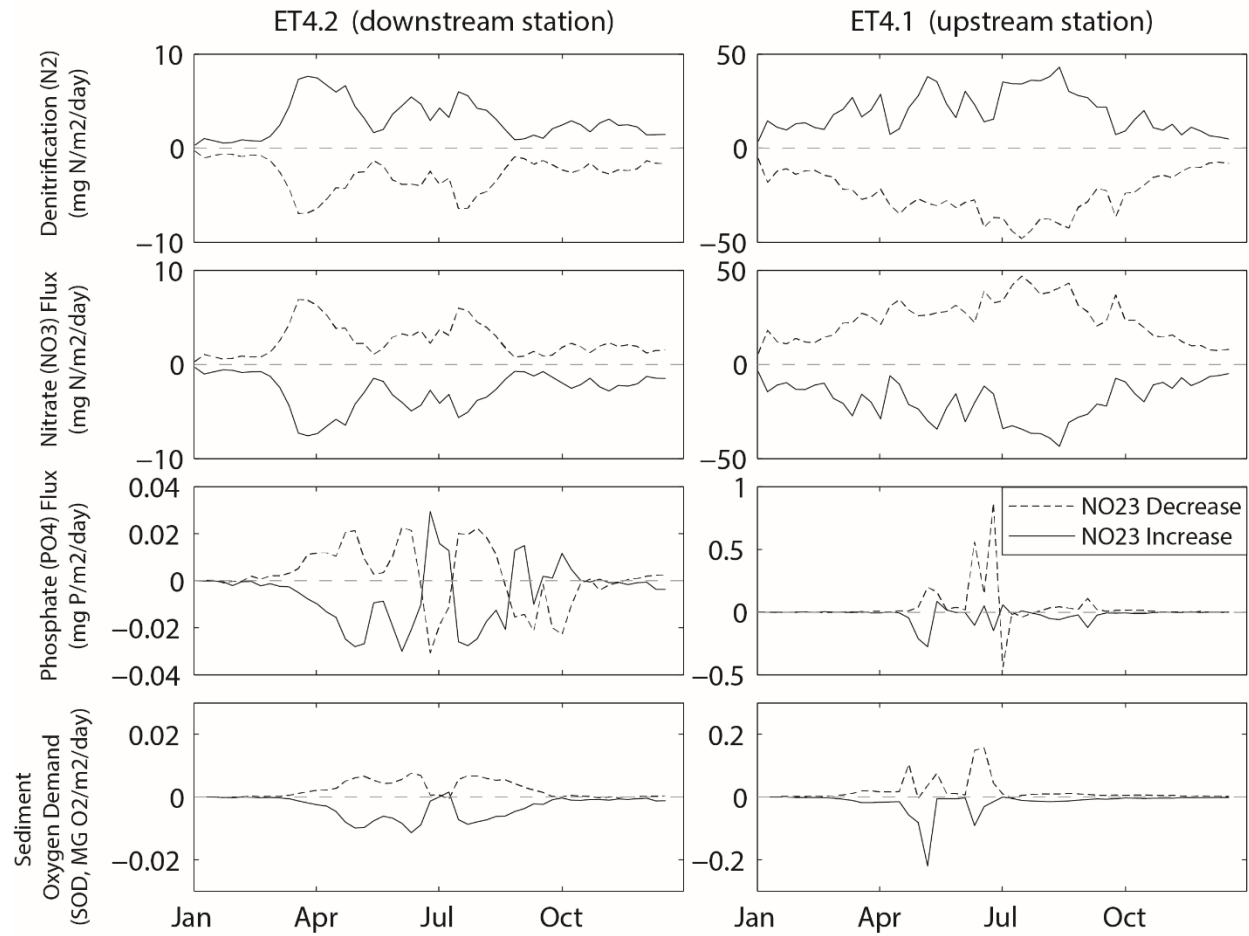


Figure 2.12. Difference in sediment-water fluxes between NO₂₃ load change (increase/decrease) scenarios and the Base scenario at two CBP stations (ET4.1 and ET4.2).

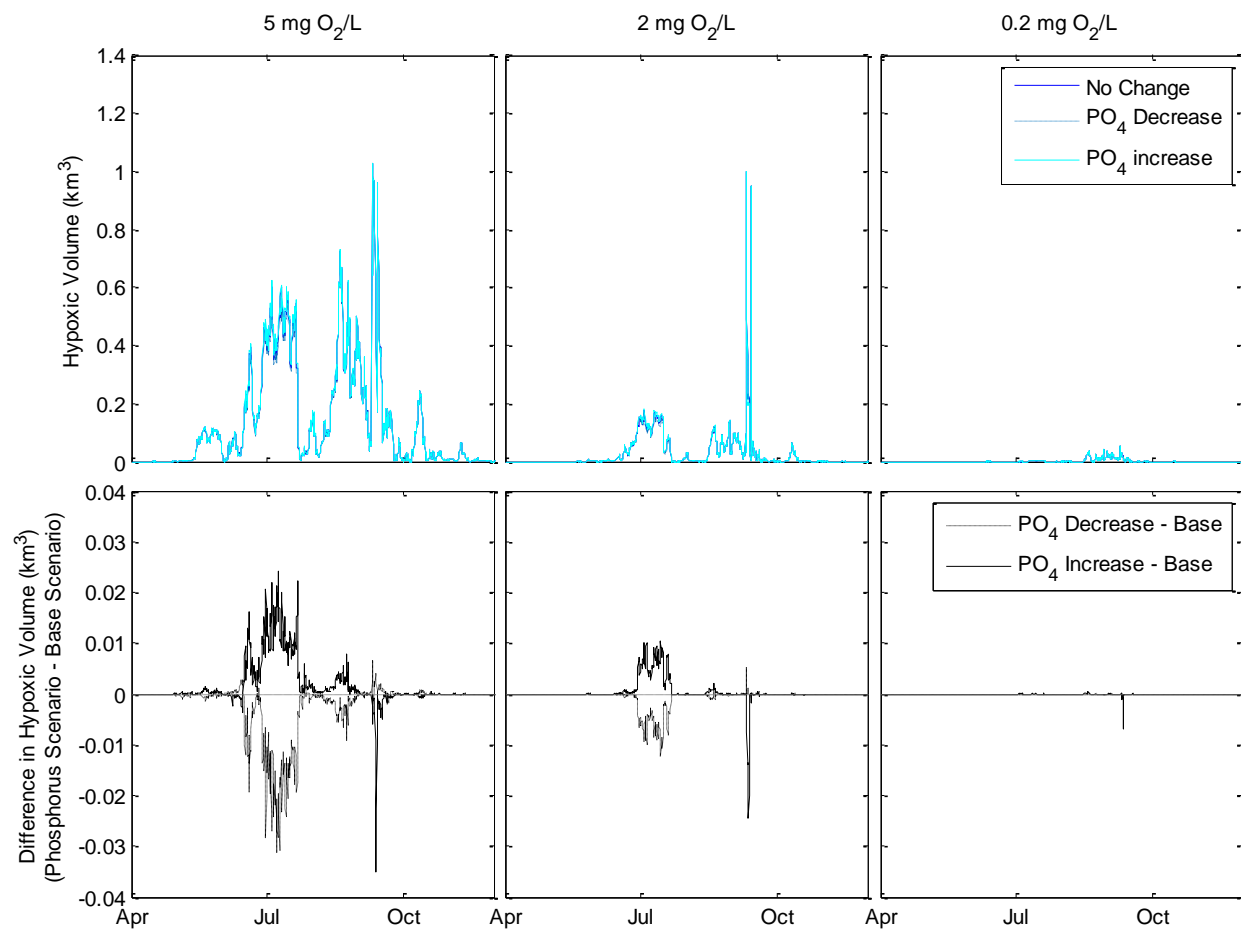


Figure 2.13. Comparison of the hypoxic volume cycle (top) of PO₄ nutrient increase and decrease scenarios to the Base (no change) scenario and the difference between them (bottom) at different dissolved oxygen thresholds.

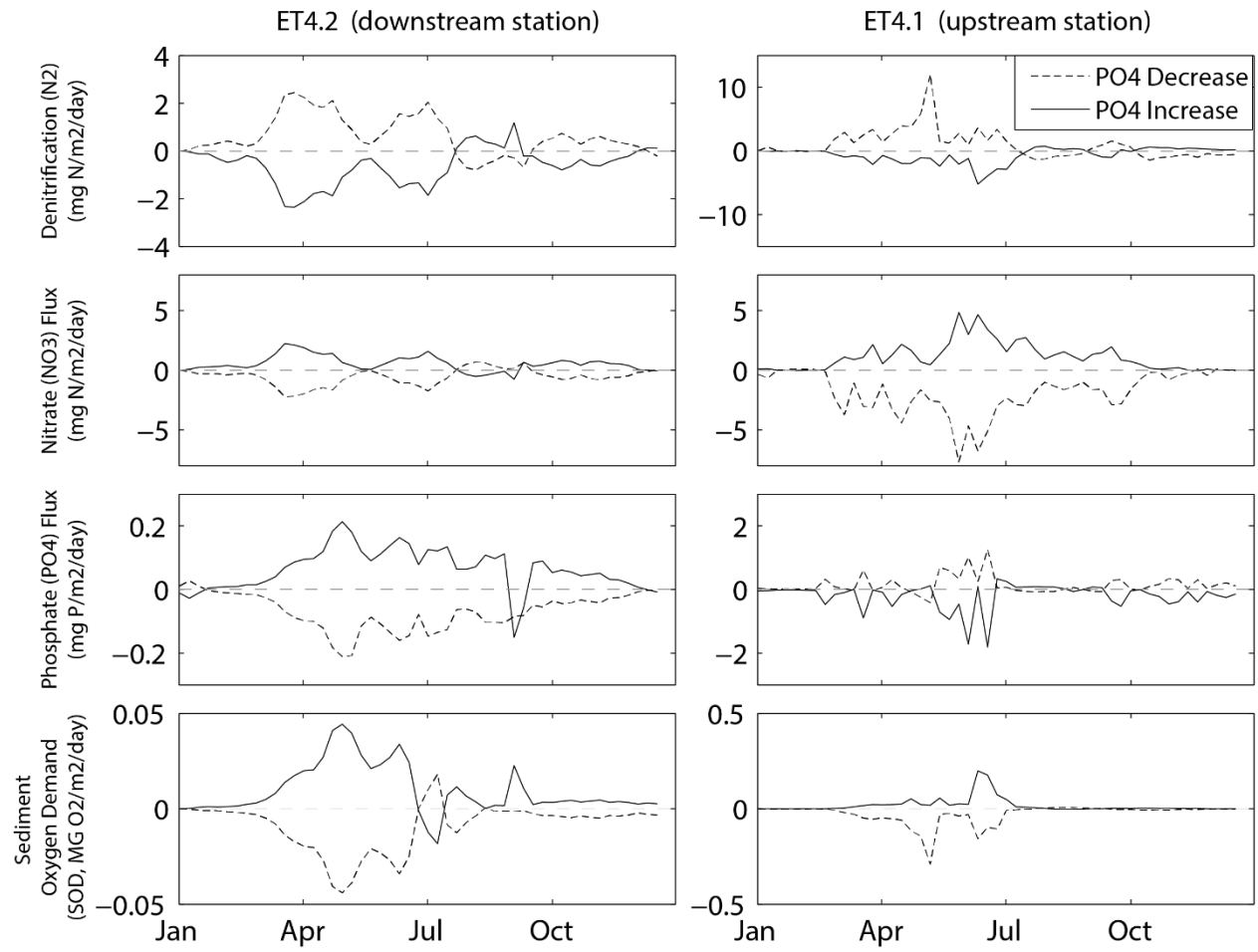


Figure 2.14. Difference in sediment-water fluxes between PO₄ load change (increase/decrease) scenarios and the Base scenario at two CBP stations (ET4.1 and ET4.2).

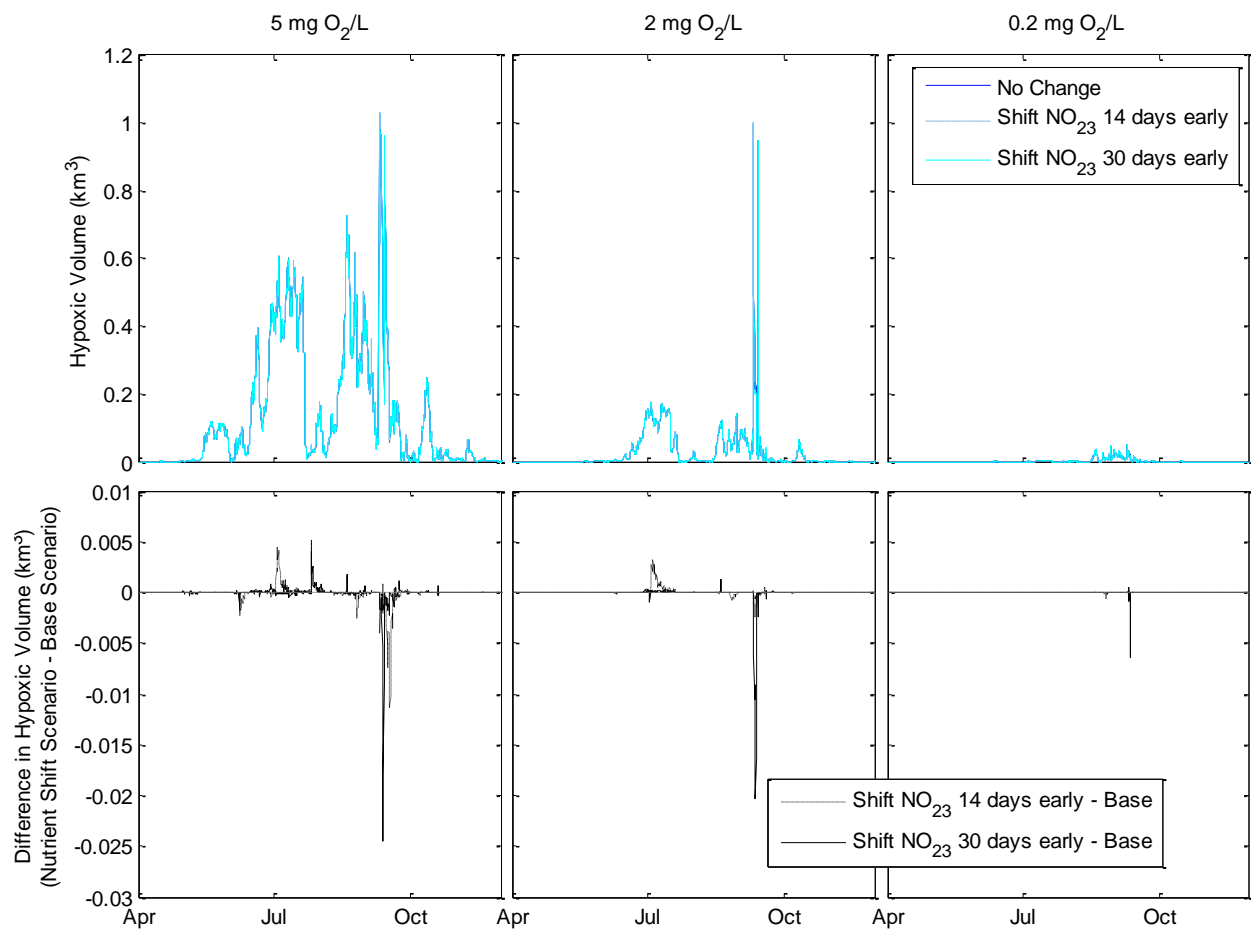


Figure 2.15. Comparison of the hypoxic volume (top) of nutrient load (NO₂₃) shift scenarios to the idealized Base (no change) scenario (bottom) at different dissolved oxygen thresholds.

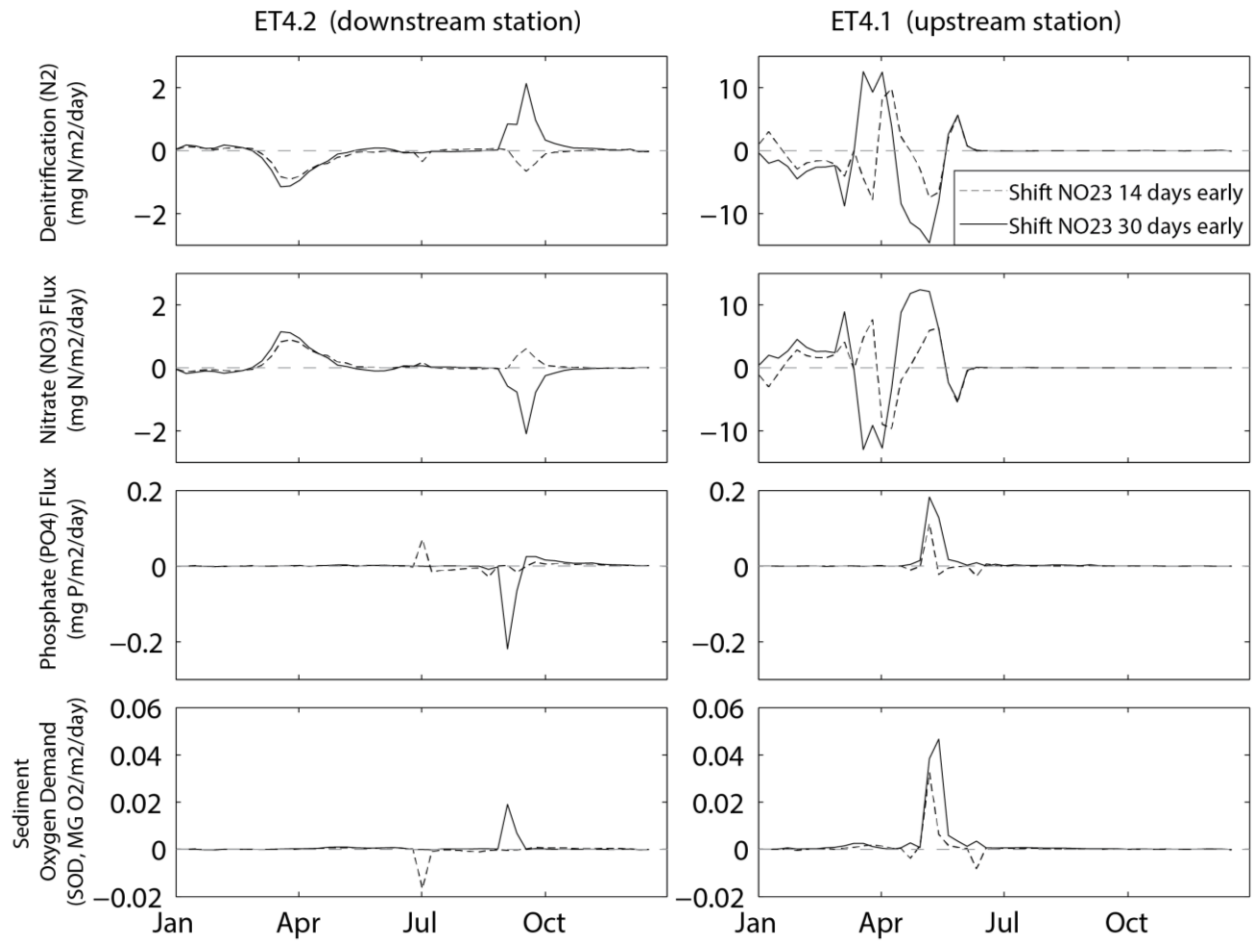


Figure 2.16. Difference in sediment-water fluxes between nutrient shift scenarios and the Base scenario, for both the 14-day (dashed line) and 30-day (solid line) shifts respectively at two CBP stations (ET4.1 and ET4.2).

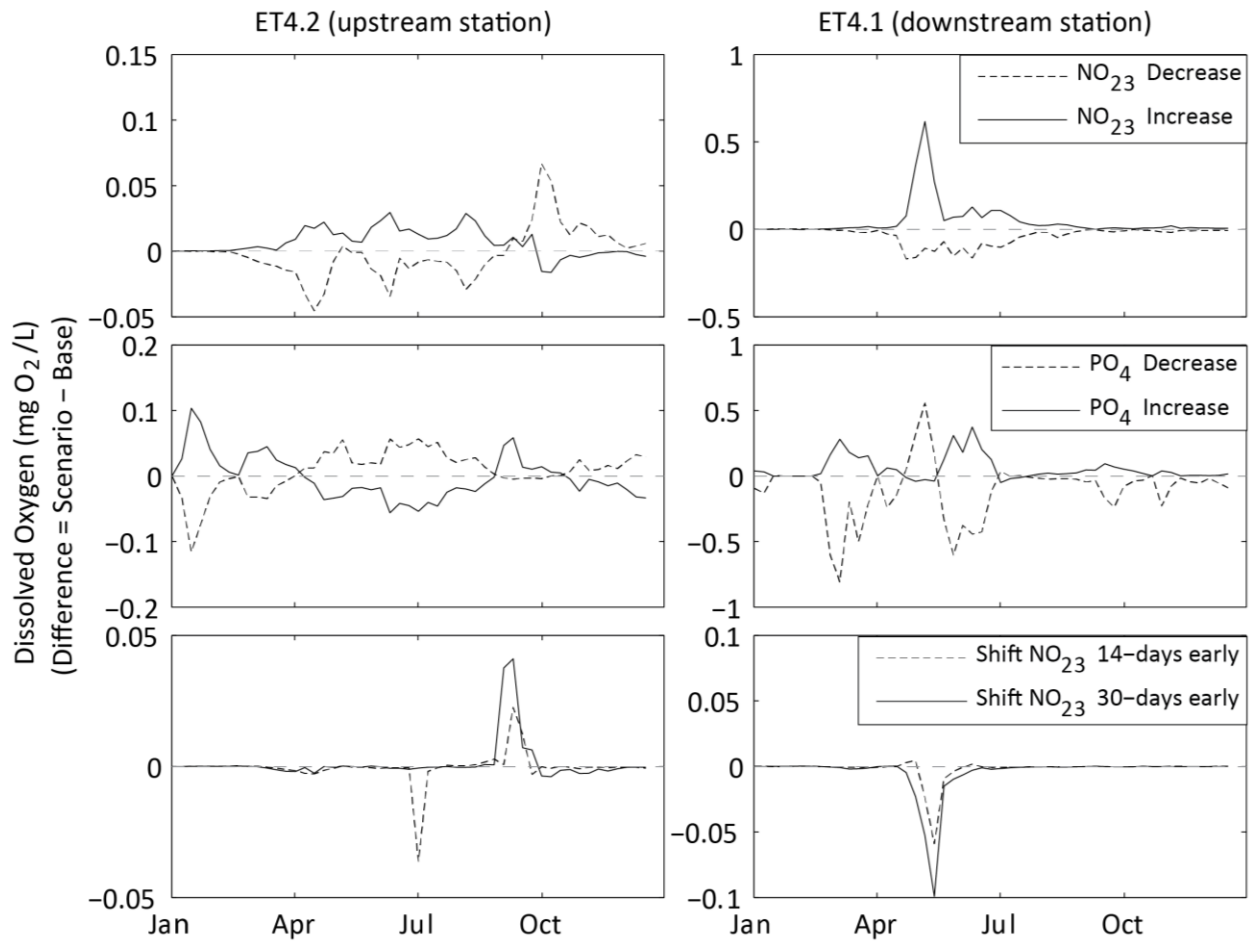


Figure 2.17. Seasonal cycle of differences between bottom water dissolved oxygen at two CBP stations (ET4.1 and ET4.2) between the base simulation and all scenarios.

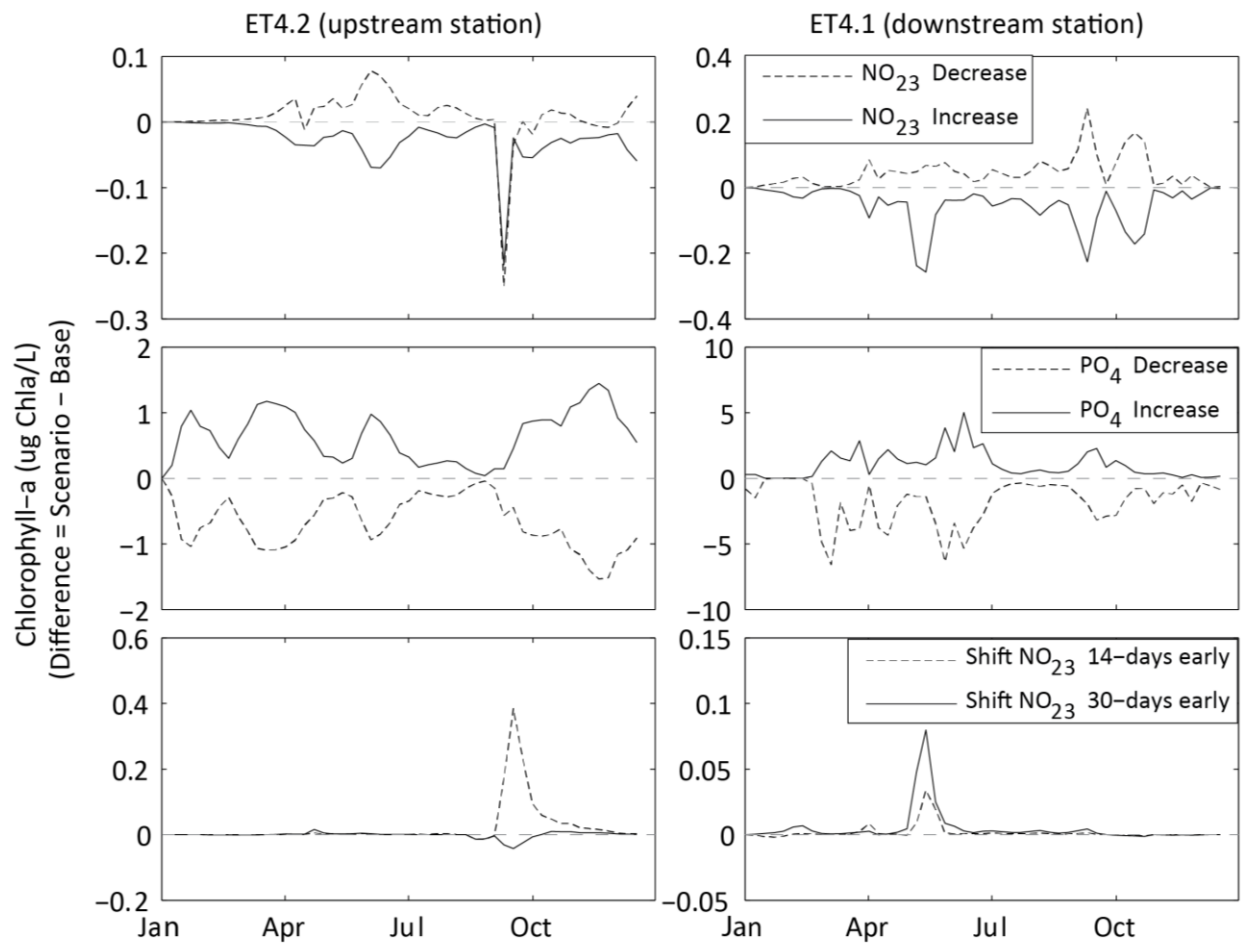


Figure 2.18. Seasonal cycle of differences between bottom water chlorophyll-a at two CBP stations (ET4.1 and ET4.2) between the base simulation and all scenarios.

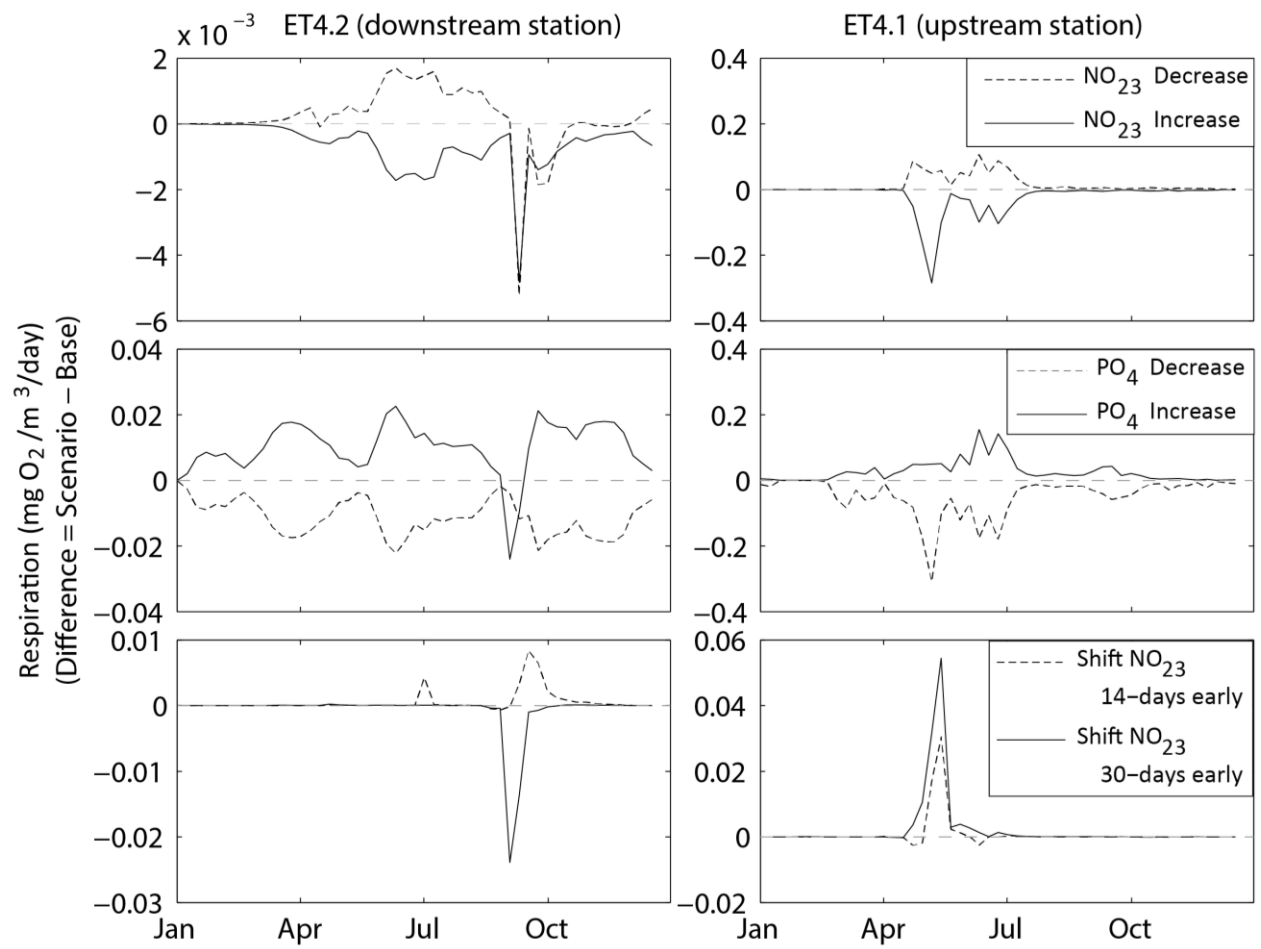


Figure 2.19. Seasonal cycle of differences between bottom water respiration at two CBP stations (ET4.1 and ET4.2) between the base simulation and all scenarios.

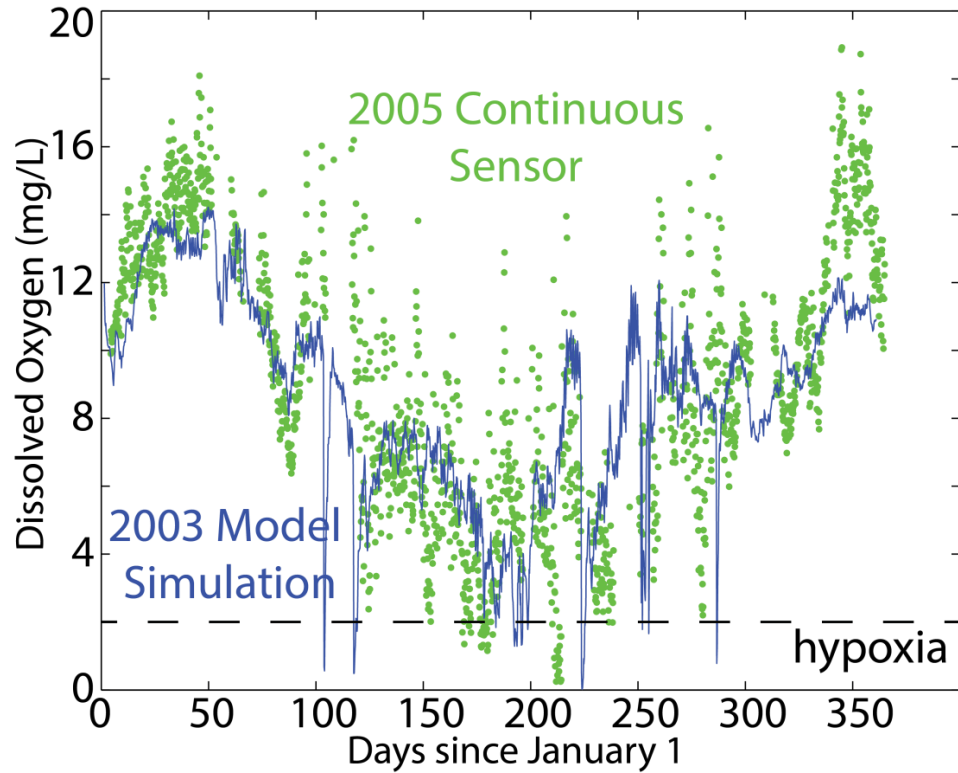
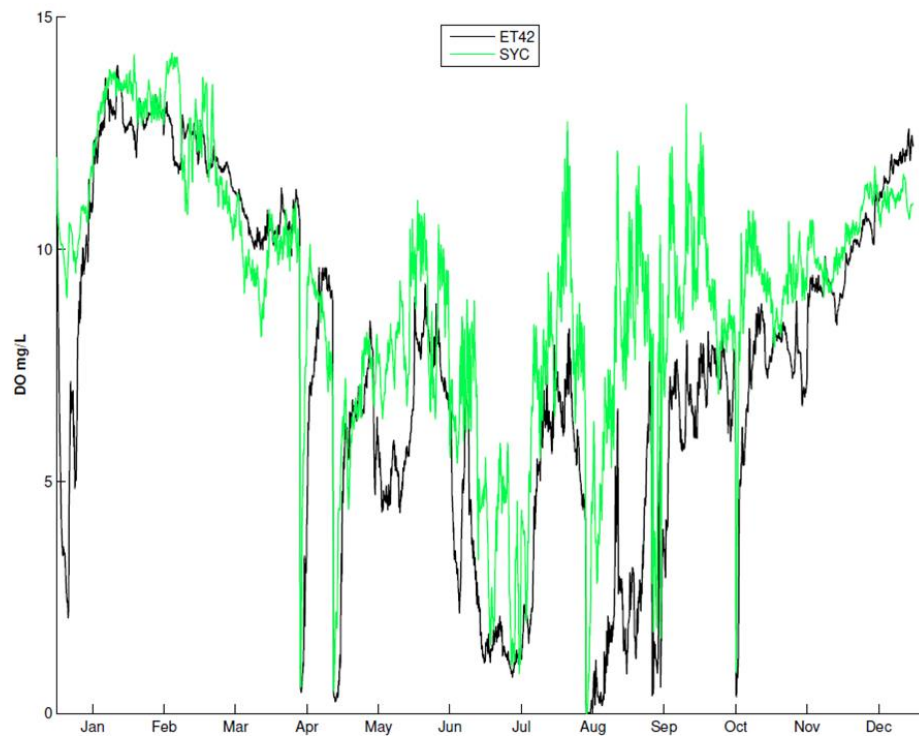
A**B**

Figure 2.20. (a) Comparison of model (blue line) versus ConMon station data (green circles) at Sycamore Point (upper Corsica River) (Walter R Boynton et al., 2009). (b) Comparison of modeled, bottom water dissolved oxygen at CBP station ET4.2 (downstream; black line) versus Sycamore Point (SYC; Corsica River; green line).

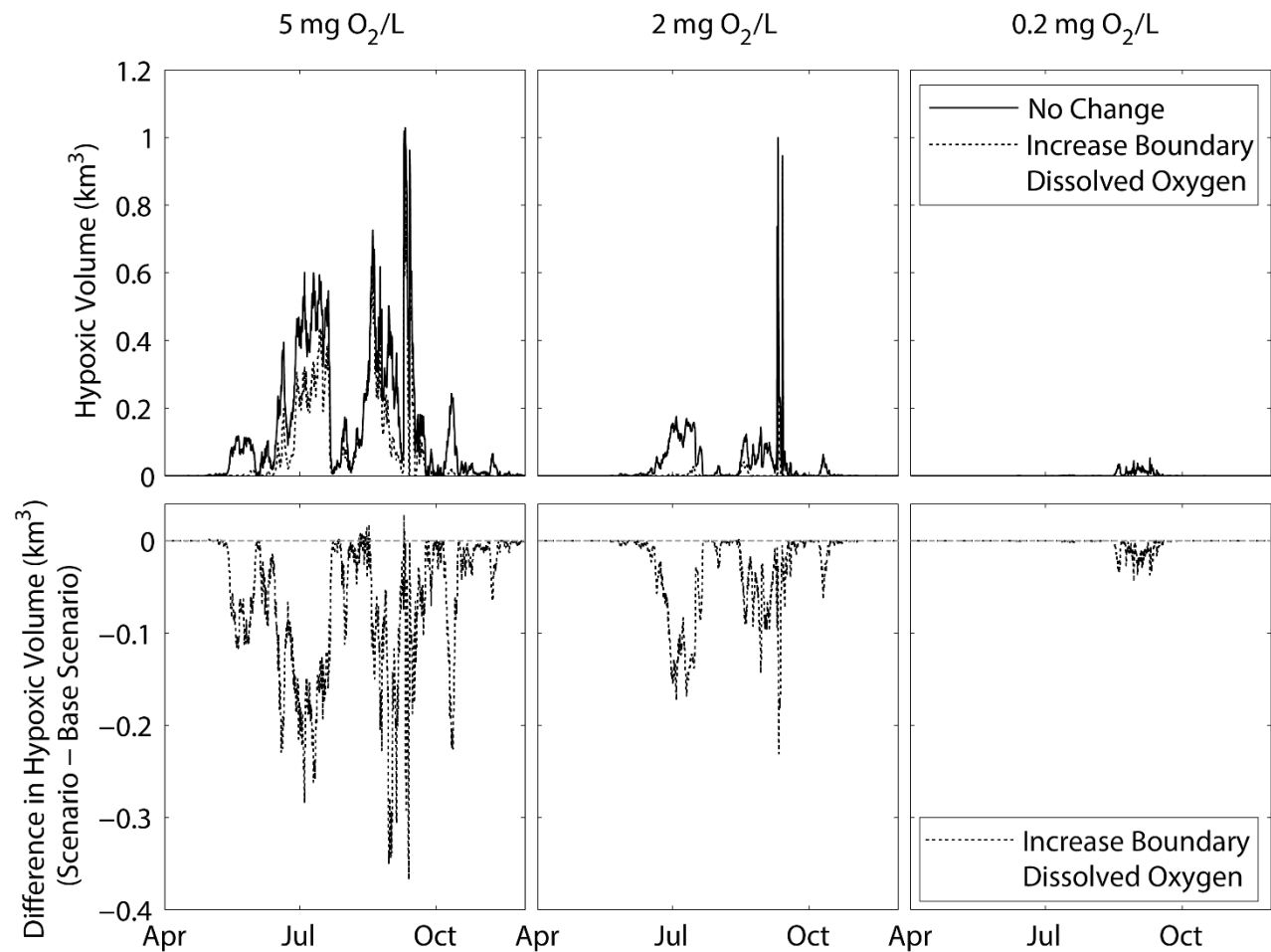


Figure 2.21. Comparison of the hypoxic volume (top) of the increase to Chesapeake Bay boundary dissolved oxygen scenario to the Base (no change) scenario and difference between them (bottom) at different dissolved oxygen thresholds.

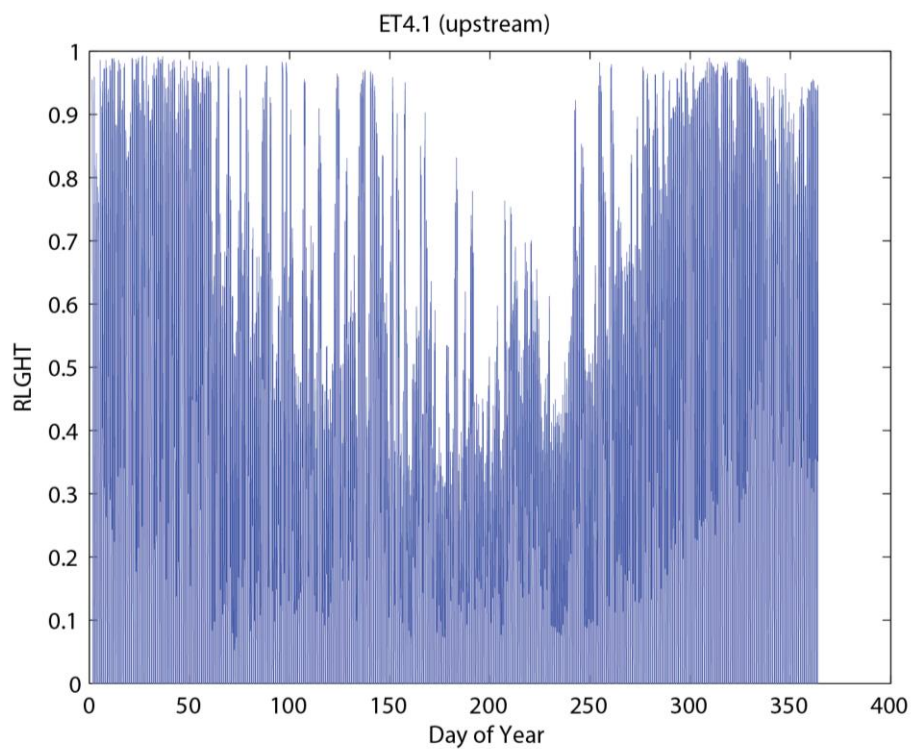
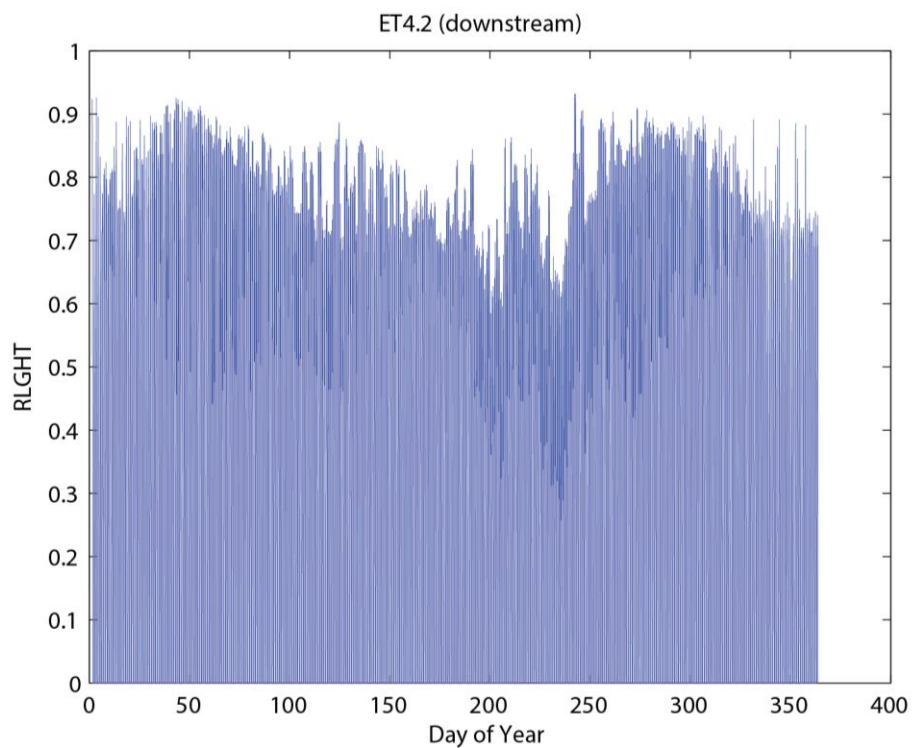
A**B**

Figure 2.22. Comparison of modeled light limitation factors (RLIGHT) in RCA at two CBP stations (a) ET4.1 and (b) ET4.2. Note: Light is not limiting when $RLIGHT > 0.9$.

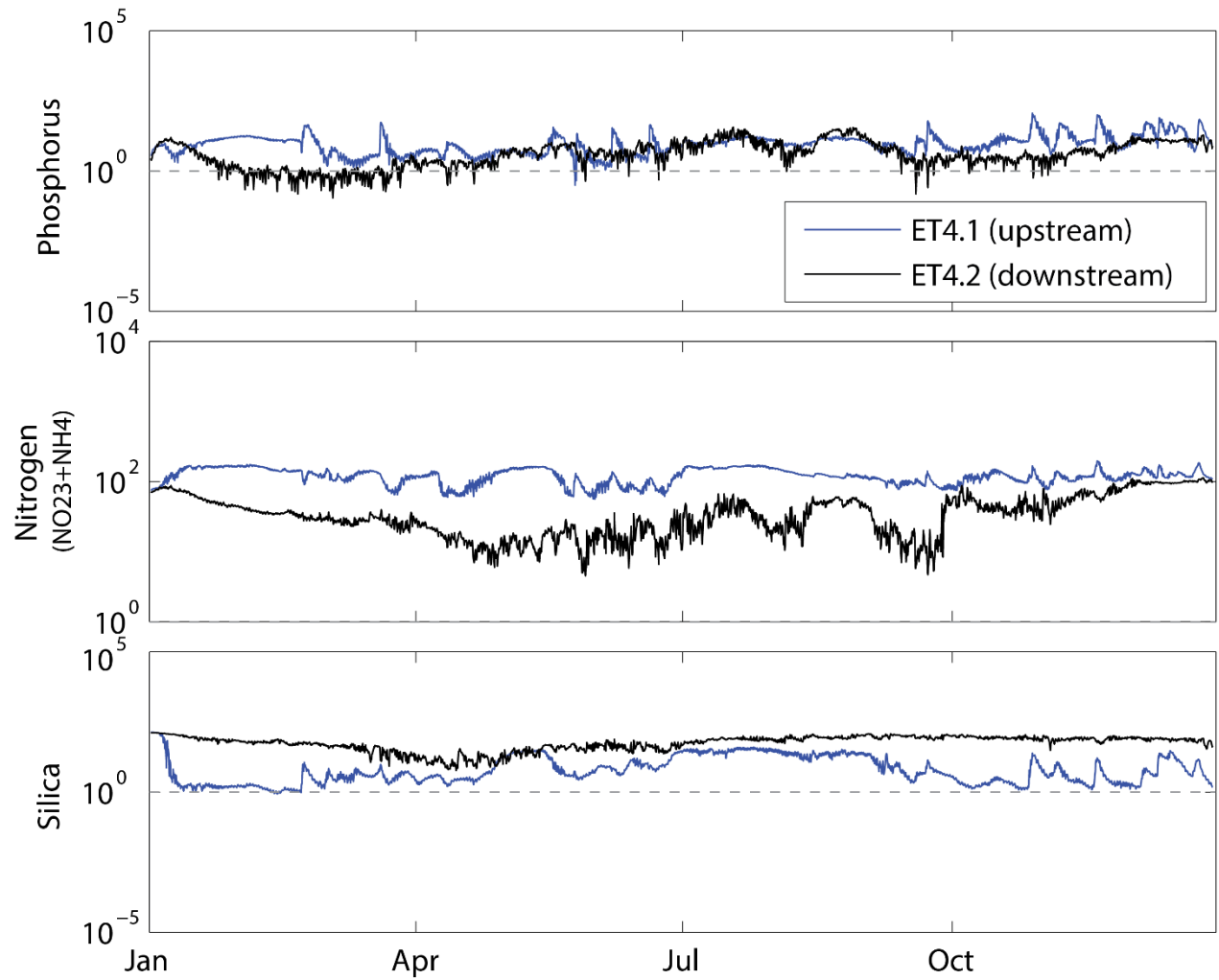


Figure 2.23. The ratio of phosphorus, nitrogen and silica concentrations to the half-saturation coefficient (k_s) 0.001 mg P/L, 0.010 mg N/L and 0.020 mg Si/L respectively for the Base (no change) scenario. Note: The lower y-axis limit for nitrogen is the ratio of 1.